MAY-AUG. 2004
Volume X Number II
ISSN 0859 144X

THE ASEAN JOURNAL OF RADIOLOGY

Published by The Radiological Society and
The Royal College of Radiologists of Thailand,
Bangkok, Thailand

MAY-AUG. 2004
Volume X Number II
ISSN 0859 144X

THE ASEAN JOURNAL OF RADIOLOGY

Published by The Radiological Society and
The Royal College of Radiologists of Thailand,
Bangkok, Thailand

Chief Editor

Professor Kawee Tungsubutra
Kaweevej Hospital, 318 Taksin Road, Dhonburi, Bangkok 10600, Thailand.

Asean Journal of Radiology.
Instructions for Authors.

1. The Asean Journal of Radiology publishes the papers on Radiological Sciences, such as research work, review articles, case reports, innovations in Medical Sciences related to all branches of Radiology, and letters to the editor. The aforementioned materials can be written in English only.

2. The authors have to submit 2 copies of the manuscript and a diskette: **to Prof. Dr. Kawee Tungsubuttra.** 318 Kaweevej Hospital, Taksin Road, Dhonburi, Bangkok 10600, Thailand.

3. The original copy to be submitted must be typed in a double space on one side of the page of 8.1/2" x 11.1/2" paper.

4. The format of the article must include :
   a. Title page and address of the author (s)
   b. Abstract
   c. Introduction (Background)
   d. Material and Method
   e. Results and discussion (Tables and Illustrations)
   f. Acknowledgement (if any)
   g. References (Follow the Vancouver style developed by ICMJE)

5. We will provide 25 copies of reprints for the author (s) who submit (s) an article for publication in the Asean Journal.

6. The illustrations and tables must be clearly prepared with legends in English as they are the art works to be reproduced.

7. The authors are reponsible for the contents of the article as to its facts and findings.

8. Ethics.

Paper reporting studies which might be interpreted as human experimentation (e.g. controlled trials) should conform to the standards of the Declaration of Helsinki (see British Medical Journal 1964:2:177) and should indicate that, approval that such studies may proceed, has been granted by the local or hospital Ethics Committee.

When reporting experiments on animals indicate whether the institution's or the National Research Council's guide for, or any national law on, the care and use of laboratory animals was followed.

THE ASEAN JOURNAL OF RADIOLOGY

Volume X Number II MAY-AUG. 2004

CONTENTS

THE ASEAN JOURNAL OF RADIOLOGY

Volume X Number II MAY-AUG. 2004

CONTENTS

RADIODIAGNOSIS OF THE DISEASES AND ABNORMALITIES IN THE BRAIN COMMONLY FOUND IN THAILAND USING CT AND MRI.

Vallop LOAPAIBUL[1] M.D.,
Kawee TUNGSUBUTRA[2] M.D., F.R.C.R. (England)

ABSTRACT

Radiodiagnosis of the diseases and abnormalities in the brain commonly found in Thailand using plain films, CT and MRI will be presented, in a series of papers according to the etiologies, caused by congenital, traumatic or diseases. It will be presented in 6 consecutive parts starting from introduction and followed by 5 main groups of abnormalities from different causes, abbreviated as "TICGO", T = trauma, I = infection, C = Congenital, G = Growth or Neoplasm, O = Obstruction and others or Miscellaneous.

Key worlds: CT and MRI. of diseases and abnormalities in the brain. General introduction and **"TICGO"**

INTRODUCTION

CT. and MRI. of the brain with or without contrast enhancement are the useful and most convenient methods to obtain the quick and accurate diagnosis of the abnormalities commonly found in the nervous system especially in the brain. The presentation will be done in 6 consecutive papers or chapters, according to the etiology, pathogenesis, diagnosis and treatment by X-ray or Ionizing radiation. The diagnosis will be done by CT and/or MRI or both modalities.

The first paper will be started by General Introduction, followed by the diagnosis of the diseases or abnormalities caused by "TICGO". We rank the priority to describe the Diagnosis of the Brain Disease or abnormalities of the brain that are commonly found in Thailand. "TICGO" means as followed; T = trauma, I = Infection, C = Congenital, G = Growth or Neoplasm, O = Obstruction and Others, miscellaneous.

1. TRAUMA

Head Injury will cause danger to the brain or CNS. The causes of injury may be devided into two main groups.

1.1 External causes e.g. accidents in the traffic, along the roads, car accidents, boat accidents, air accidents. Another major causes of injury are violative crimes, by gun, explosive or injury from weapons, sharp or blunt. Most of these patients are surgical cases.

1.2 Internal causes. The Cerebral hemorrhage occurs secondary to the pre-exsisting diseases of the patients themselves. They are medical cases and are not caused by any injury from outside or accident. They are collectively called CVA or cerebrovascular accident, as colloquially called "stroke". These patient may have pre-existing diseases such as arterio-venous malformations (AVM), congenital aneurysm, Berry Aneurysm in the Circle of Willis, arteriosclerosis of old ages, V.D., diabetes mellitus (DM), hypertension and venous thrombosis from pre-existing diabetes mellitus.

[1] Department of Radiology, Faculty of Medicine, Khon Kaen University, Khon Kaen, THAILAND.

Whatever be the causes of trauma to the brain, CT. and MRI will greatly be benificial for the doctors in making the decision what is the best way to save the life and not only the life but also to save the disability of the patients to the minimum when they recover. CT and MRI are the quick and best method to give us the quick and accurate diagnosis for planning the best management for the patients. CT. and MRI can tell us the site or sites of bleeding or brain injury and also the amount of bleeding so that the physician can make the choice of treatment. Not only to save the life, but also we have to make the patients and there relatives to lead the lives happily after survival.

2. INFECTION

Infection to the CNS including bacterial viruses, fungi or mixed infections. We may find inflammatory processes in the CNS causing abscess or abscesses and finally locally brain death. The infection may be direct infection from fracture skull and tearing of dura or direct spreading from infection of neighbouring organs or blood stream infection. The infection may directly spreading from Ca. Nasopharynx or Sinuses.

The infections commonly found are, TB., Mixed Infections, Rabies, Toxoplasmosis, cryptococcosis, HIV making the body resistance lower down and secondary infection into the CNS may be easier and wide spreading. The secondary infections, which may be found in the CSF mostly, are fungus, e.g. Toxoplasma Capsulatum or Cryptococcus Neoforman. In Thailand we may find people from the Northern part or the North-Eastern part who are fond of eating raw foods especially pork infested with parasitic larva, especially the larva of tape worm, Cysticercus cellulose which human-being is the intermediate host of Taenia Solium. In the X-ray film we may see many small round calcifications distributed around the cerebral cortex where the Cryptococcus cellulose are buried by calcification and cause convulsion or other symptoms according to the position in the brain where they are.

3. CONGENITAL

Malformation of the fetuses in Utero may the be genitical i.e. abnormal chromosomes from the maternal and paternal side, or drug intoxication from the mother during pregnancy. Sturg - Weber syndrome and congenital aneurysm of the Circle of Willis.

4. GROWTH or NEOPLASM

Intracranial tumours which may be found, are benign or malignant tumours, the same as in other organs of the body.

4.1. Meninges. The most common benign tumours found in the Meninges are Meningiomas. The common sites which may be found are at the Crista Galli, Sphenoidal ridge, Frontal, parasella and temporal region. The recommended treatment is excision with post-operative radiation therapy, at the tumours bed to prevent local recurrence. Eventhough they will not causing distant metastasis but they are notorious of local recurrence therefore local excision is indicated. It had been proved that for benign meningioma, local excision with post-operative radiation of tumour bed is the treatment of choice to prevent recurrence and repeated excision.

4.2 The brain cellular components consisted of 2 kinds of cells: one is the nerve cells and another is the glia cells. At present, we have not found tumour originated from nerve cell neither benign nor malignant. All brain tumours originated from Glia cells. There are two kinds of Glia cells namely, Astrocytoma and Oligodendroglioma. The difference between these two kinds of cells is the number of dendrites. Both Astrocyte and Oligodendroglia have only one Axon, while Astrocyte having numerous dendrites, but Oligodendroglia having only few dendrites. Both kinds of glia cells have only malignant tumours. There is no benign Glia cells tumour. Both kinds of Glia cells have 4 Grades malignancy. The most malignant Glia cell tumours is Grade 4 Astrocytoma which have a special name "Glioblastoma Multiforme" and have

been found most often among primary brain tumours. Glioblastoma Multiforme is the only malignant brain tumour which can infiltrate through the thick and tough fibrotic membrane preventing the malignant diseases spreading from one cerebral hemisphere to the opposite hemisphere. It is the "Falx Cerebri"

4.3 Tumours, which are found in the Ventricles of the brain, have the origin from the cells which are the embryonal content and anatomical contents in the Ventricles and can spread by seedling via the CSF. CSF. fill up the subdural spaces and all the ventricles acting as the shock absorber to the Central Nervous System. These tumours mostly originated from embryonic cells having all together 5 different kinds of cells. Tumours which have the origin from the Ventricular Contents are:

4.3.1. PNET or Primitive-Neuro-Ect dermal-Tumour. This kind of tumour have the origin from the cellular content of the Pineal Gland. They are composed of primitive nerve cells and ectodermal embryonal cells which were the content of the Pineal Gland and can spread by seedling through the CSF.

4.3.2. Choroid plexus tumour. Choroid plexus is a network of capillaries and blood vessels floating in the Ventricles of the brain. The embryonal cell rest which is poorly differentiatel may develop to be Choroid plexus tumour.

4.3.3. Medulloblastoma. Medulloblast are the embryonal rest cells which are at the Cerebello-Pontine they can become malignant in nature and seedling through the CSF.

4.3.4 Ependymoma. Ependymal cells are the cells lining of the ventricles, therefore they can float freely in ventricles and seedling at random in ventricles.

4.3.5 Leukaemia. Leukaemic cells which respond to a certain kind of chemotherapy at certain concentration in the blood, but the chemotherapy could not pass from the blood into the CSF. at a concentration which can eradicate the leukaemic cells, because the Blood-Barrier. After the chemotherapeutic agents have been excreted through the kidneys and/or detoxified by the liver, the leukaemic cells that survive in the CSF. can pass out from the CSF. into the blood circulation and produce the recurrent of Leukaemia. The ways to make a complete remission of Leukaemia are only either to inject chomotherapeutic agents intrathecally or to do the whole CNS irradiation with a special technique and precaution.

4.4 Brain is a special and important organ for life and daily performance so it needs high concentration of Oxygen in the blood. Brain is an organ with a specially rich in blood supply. There may be two kinds of **tumours of the blood vessels** in the brain, namely:

4.4.1 Haemangio-endothelioma- it is the tumour of the endothelial cell that form the wall of the blood vessels.

4.4.2 Haemangio-pericytoma- it is the tumour of the pericytes which make the wall of the blood vessels strong enough against the blood pressure in the lumen of vessels not to break through the wall.

4.4.3 Congenital hemangiomas.

4.5 Pituitary gland in the sella turcica. Tumours of Pituitary can be divided into 2 groups according to different functions, hormone producing and non-hormone producing. Tumour in the Pituitary can be diagnosed easily by lateral view of the skull, showing enlargement of sella turcica. **Non-hormone producing tumour;** This kind of tumour consisting of Chromophobe cells which can be seen in the microscope as pink cells, or neutrophilic. They are growing rather fast in comparison with the **hormone producing tumours,** which can be seen in the microscope as red cell, or Acidophilic and blue cells or basophilic.

The chromophobe cells cause symptoms by pressure effects with compression of the other two kinds of cells in the pituitary glands. The acidiphilic cells or the cells staining red, secrete Somatotrophin to stimulated the adrenal cortex to secrete growth hormone. If this tumour occurred before puberty and before the fusion of the epiphyses and metaphysis of long bones, the clinical symptom will be "Gigantism". But if the timing of occurrence of this tumour is after the fusion of epiphyses, the clinical symptom will be "Acromegaly".

The basophilic tumour secrete ACTH and over secreting of ACTH will cause Addison disease and Diabetes Mellitus. The hormone-producing adenomas having small size are called "microadenoma" and show clinical symptoms by producing excess of trophic hormones to affect the target organs such as the adrenal or thyroid gland. The Non-hormone producing tumours cause pressure symptoms to the neighbouring organs. The rapidly increasing number of chromophobes adenoma cells cause the pressure symptoms to the hormone producing cells with the clinical symptoms of deprivation of the trophic hormones to the adrenal, and the gonads of both sexes. In the male patients the complaint is the decrease in libido but rather please that they do not need to shave everyday. In the female, the complaint is amenorrhoca or the delay of secondary sex characteristics. If the tumour is growing very big, it will cause the pressure symptoms to the optic chiasma causing bilateral hemianopsia i.e. the lateral visual fields are narrowing or complete loss without limitation of eye movement as seen in the Ca. Nasopharynx.

In Ca. Nasopharynx, there is direct extension of the tumour into the skull and pressed on cranial Nerve IV and VI causing paresis or paralysis of lateral rectus and superior oblique muscles of the affected side causing internal squint and Ptosis of the eye of that side. In pituitary tumour, the Chromophobe adenoma, the loss of visual field are bilateral because the tumour press directly on optic nerves of both sides where the nerve fibers are crossing.

N.B.; Hints for remembering Pituitary tumours, different kinds and their effects.

1. Hormone producing tumours.

A= Acidophile, staining Red produce Somatophile, Clinical Symptoms, Acromegaly or Gigantism.

B= Basophilic, staining Blue produce ACTH, Cortisone, Cushing Syndrome

2. Non-hormone producing tumour.

C= Chromophobe, staining Pink, produce pressure symptoms. Apart from the brain tumours which have been described in 5 major groups, there may some other 5 small groups of tumours in the brain.

4.6 Optic Glioma derived from the optic nerves.

4.7 Acoustic. Swannoma derived from the nerve sheath of Acoustic N.

4.8 Craniopharyngioma derived form primitive cell around or above the sella turcica,parasella tumour.

4.9 Chordoma. Tumour of notochord which may be found at the cervical, thoracic or sacral region.

4.10 Retinoblastoma. Tumor originate from the retina cells of the eye.

Apart from Primary Tumours which have been described, there are also Metastatic tumours which have primary origin from other organs and spread to the brain by blood stream e.g. Bronchogenic Ca, Breast Cancer and Ca. Thyroid etc.

5. OBSTRUCTION

There is some obstruction of the flow of CSF. from all the causes which have been described such as Trauma. There may be either complete or partial obstruction of the flow of CSF. by blood clot, or

tumour or damaging tissues. Congenital cause of obstruction of CSF is Arnold Chiary Malformation.

DISCUSSION

In the old days before the development of CT. and MRI., the radiodiagnosis of the diseases and the abnormalities of the brain or the nervous system, can be done only by plain films and cerebral angiography using opaque media. The injection of opaque media into the carotid artery required a skillful hands and event more difficult if we want to do the vertebral artery angiograms. Anyhow after invention of CT and MRI, radiodiagnosis of the diseases, abnormalities either congenital or acquired can easily be visible, diagnosed by CT and MRI or both modalities in the diagnoses and proper treatment or management can be done. In traumatic or cerebro-vascular accidents, prompt and accurate diagnosis can be done and taking the least time by CT. or MRI. alone or both which are complimentary to each other. We can not only save the lives, but also save the deformities or sequelae affecting the patients after these unfortunate incidents.

The presentation of this subjects with be presented in a series of 6 consecutive papers in this journal. This is the introduction paper, another 5 papers will be followed.

CONCLUSION

6 consecutive papers about the radiodiagnosis of the diseases and abnormalities in the brain commonly found in Thailand using CT. and MRI. will be presented in this journals in 3 volumes, 2 in each volume.

REFERENCES

1. Bradley WG Jr. et al. Compassion of CT. and MRI. in 400 patients with suspected diseases of the brain and cervical spinal cord. Radiology 1984; 152: 695-702.
2. Harso AN, Fahmy J.L. Posterior fossa neoplasms. In: Stark DD, Bradley WG. Jr.eds. Magnetic Resonance Imaging, Chpt. 30, 2nd ed. St. Louis: Mosby-ycaebook; 1992: 963-987.
3. Brant-Zawadski M, Nosman D, Newton TH, et al. Magnetic resonance of the brain: the optimal screening technique, Radiology 1984; 152:71-77.
4. Bradley WG Jr. Fundamentals. In: Bradley WG Jr. Bydder GM, eds Magnetic resonance imaging (MRI) Alas of the Brain. London: Martin Dunitz; 1990; 1: 6.
5. Castillo M. Control enhancement in primary tumors of the brain and spinal cord.Neuroimaging Clin, Nosily Am 1994; 4: 63-80.
6. Chamberlain MC. Pedriatic aids: a longitudinal comparative MRI and CT brain imaging study, J. Child Neurol 1993; 8: 175-181.
7. Faerber E. Cranial computed tomography in infants and children. Philadelphia, PA Lippincot, 1986.
8. Flodmark O. Neuroradiology of selected disorders of meninges, Calvarium and venous sinuses. AJNR 1992; 13: 483-492.
9. Gentry LR. Imaging of closed head injury Radiology 1994; 191: 1-17.
10. Gentry LR. Godersky IC, Thompren B. MR imaging of head trauma: review of the distribution and radiopathologic features of traumatic lesions. AJNR 1988; 9: 101-110.
11. Jordan JE, Enzmann DR. Encephalitis. Neuroimaging Clinic North America 1991; 1: 1-29.
12. Laissy JP, Sawyer P, Parlicr C, et al. Persistent enhancement after treatment of cerebral toxoplasmosis in patients with AIDS: predictive value for subsequent recurrence. AJNR 1994; 15: 1773-1778.
13. Lallemand DP, Brash RC, Char DH, et al. Orbital tumors in children. Radiology 1984; 151: 85-88.
14. Lindgren A, Norrving B, Rudling O,Johansson BB. Comparison of clinical and neurological findings in first-ever stroke. A population base study. Stroke1994; 25: 1371 -1377.

15. Lipper MH, Kishose PRS, Enao GG, et al. Competed tomograplry in the prediction of outcome in head injury. AJNR 1985; 6:7-10.
16. Mashall SB. Klanber MR, et al. The diagnosis of head injury requires a classification based on computed axial tomography. J Neurotrauma 1992; 9: 5287-5292.
17. Mayton J, Bienkowski RS, Patel M, Evistas L, The value of brain imaging in children with headaches, Pediatrics 1995; 96: 413-416.
18. Pressmen BD, Tourje E J, Thompson JR. Early CT sign of ischemic infarction: increased density in a cerebral artery. AJNR 1987; 8: 645-648.
19. Savioardo M, Bacchi M, Passeri A, Visciani A. The vascular territories in the cerebellum and brain stem: CT and MRI study. AJNR 1987; 8: 199-209.
20. Snow RB, Zinnerman RD, Gandy SE, et al. Comparison of magnetic resonance imaging and computed tomography in the evaluation of head injury. Neurosurgery. 1986; 18: 45-52.
21. Taphorn MJ, Heimanas JJ, Kaiser MC, et al. Imaging of brain metastases, Comparison of CT and MR imaging. Neuroradiology 1989; 31:391-395.
22. Wolf M, Ziegengeist S, Michalik M, et al. Classification of Brain tumors by CT image Walsh spectra. Neuroradiology 1990; 32: 464-466.
23. Meyer JE, Lpke RA, Linfors KK, et al. Chosdomas: their CT appearance in the cervical, thoracic, and lumbar spine. Radiology 1984-153:693-696.

PROMPT AND ACCURATE DIAGNOSIS OF CEREBRO-VASCULAR ACCIDENTS AND DISEASES BY CT AND MRI

Vallop LOAPAIBUL[1] M.D.,
Kawee TUNGSUBUTRA[2] M.D., F.R.C.R (England)

ABSTRACT

Cerebro-vascular diseases or CVA is a condition leading to insufficiency of blood supply to the brain followed by brain anoxia with cerebral infarction ending in life or incapability. The causes may be single or multiple which may be from insufficieney of the arterial supply, venous thrombosis or embolism. Cerebral haemorrhage may be caused from hypertension, diabetes or aneurysm, Arterio-Venous Malformation (AVM) or other Cerebro-vascular diseases which may cause pathology in the brain presenting with a variety of nervous deficiency.

PRESENTATION OF CASES: PROMPT AND ACCURATE DIAGNOSIS CAN BE OBTAINED BY CT AND MRI

CASE I: Cerebral infarction: Rt. Middle Cerebral Artery.

Clinical: Female, age 61 yrs., having a history of hypertension, fell down in the bath room with paralysis of left half of the body.

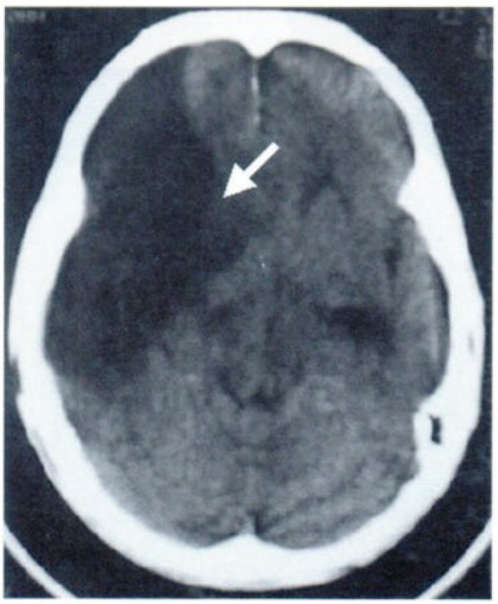

Fig.1A NC.CT.

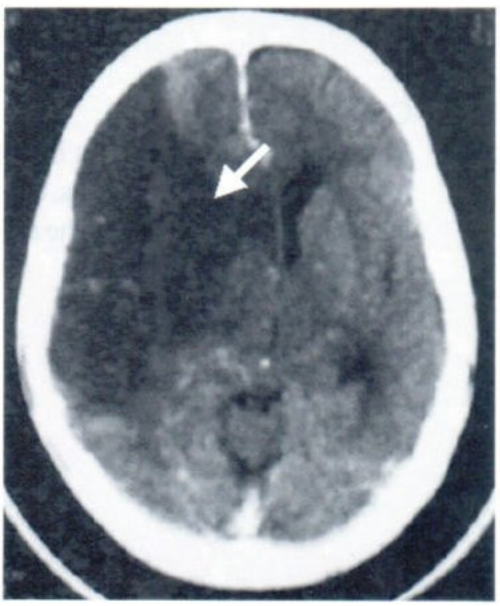

Fig.1B CE.CT.

CT. show black area of Rt. Cerebral hemisphere corresponding to the area supplied by anterior cerebral artery. There was infarction of Rt. cerebral hemisphere with paralyses of left half of the body.
NC.CT. = No Contrast CT., **CE.CT.** = Contrast Enhancement CT.

[1] Department of Radiology, Faculty of Medicine, Khon Kaen University, Khon Kaen, THAILAND.

CASE II: Cerebral infarction.
Clinical: Female, age 52 years, with a history of Diabetes and Hypertension, faint and hemi paralysis Rt. half of the body.

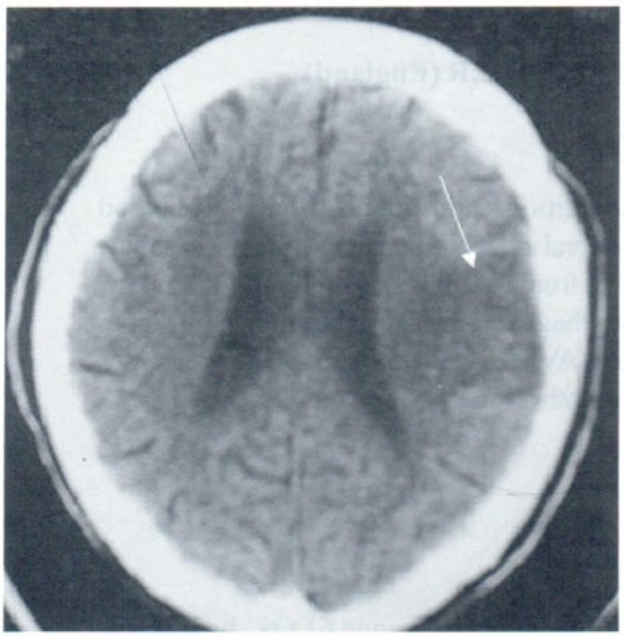

Fig. 2A

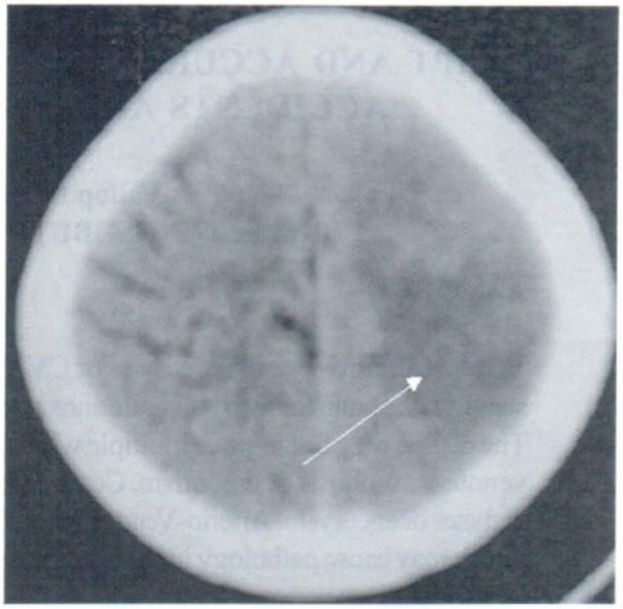

Fig. 2B

CT. show infarction of the Cerebral Cortex, black area, pointed by the white arrow at two different levels, as shown in Fig.2A and Fig.2B.

CASE III: Cerebral infarction.
Clinical: Male, age 65 years, with a history of hypertension for several years, faint and unconscious. After first aid, he recover with Lt. half paralysis.

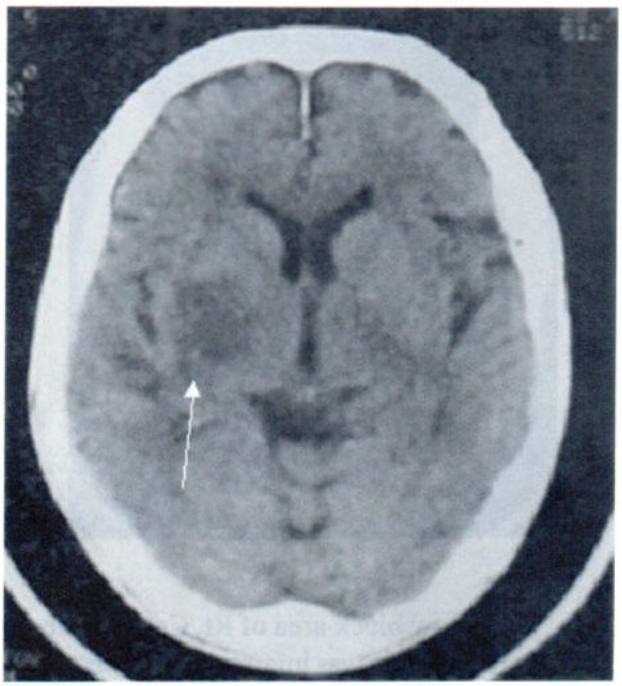

Fig. 3

Fig.3 CT. scan showed cerebral infarction at the Rt. basal ganglia, black area pointed by white arrow. Cerebral angiogram showed obstruction of lentriculostriate arteries from cerebral arterial thrombosis.

CAES IV: Cerebral infarction: Embolic, hemorrhagic infarction.
Clinical: Male, age 70 years sleeping in bed, did not wake up until late in the morning. His daughter wake him up but found him unconciously lying in bed with semi body paralysis.

CT. showed cerebral infarction of the black area pointed by white arrows, caused by cerebral embolism. Two weeks after that, another CT. was done, 3 small white areas appeared in the black area previously seen. The white areas may be the bleeding in the infarcted areas of the brain after the brain death, and the emboli are dislodged. The bleeding may come from the necrotic arteries where the obstruction of the arteries had taken place previously.

The picture shows NC.CT. taken 2 weeks after the 1st CT.

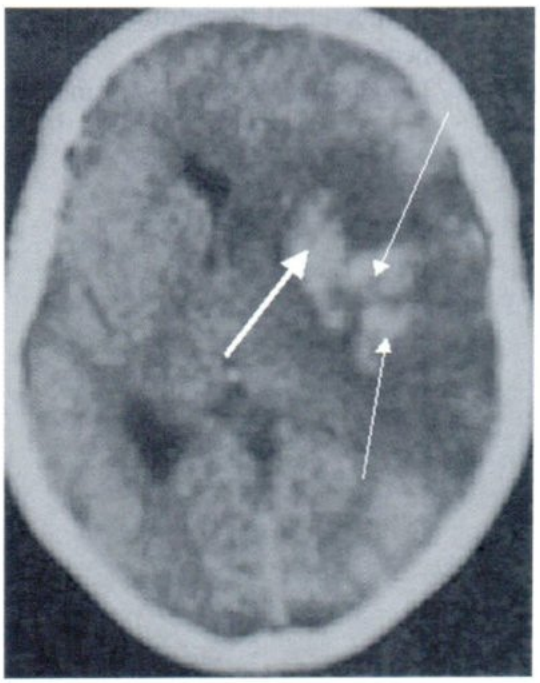

Fig. 4

CASE V: Intracerebral hematoma: basal ganglia.
Clinical: Male 68 years, with a history of hypertension, faint and unconscious with intracerebral haemorrhage and paralysis, left half of the body.

NC.CT. showed white mass indicated by the white arrow interpreted as a hematoma at the Rt. basal ganglia causing Lt. half paralysis.

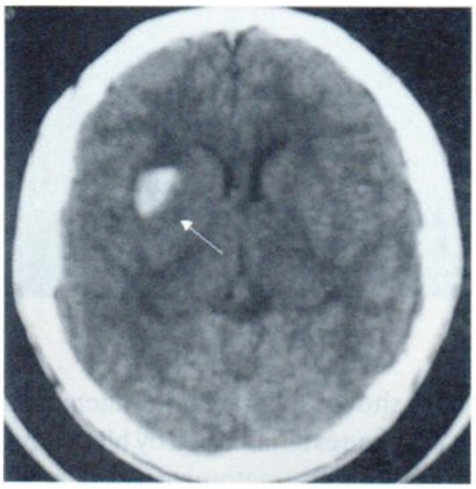

Fig. 5 NC.CT. showed white mass indicated by the white arrow interpreted as a hematoma at the Rt. basal ganglia causing Lt. half paralysis.

CASE VI: Intracerebral hematoma: Cerebellum.
Clinical: Male, age 74 years, having a history of Hypertension for several years, faint and unconscious.

NC.CT. showed cerebellar hematoma Rt. side showing by small, long white arrow. There was also hematoma filling into the 4th ventricle, pointed by short, thick white arrow.

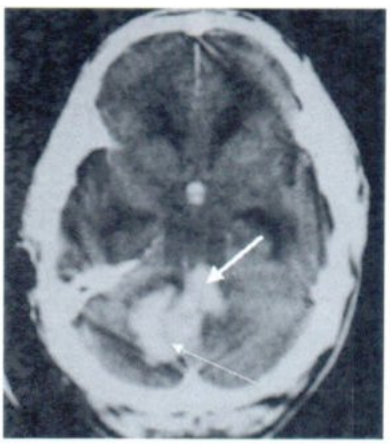

Fig. 6 NC.CT. showed cerebellar hematoma Rt. side showing by small, long white arrow. There was also hematoma filling into the 4th ventricle, pointed by short, thick white arrow.

CASE VII: Intracerebral hematoma: Brain stem hematoma.

Clinical: Female, age 78 years, faint and unconscious.

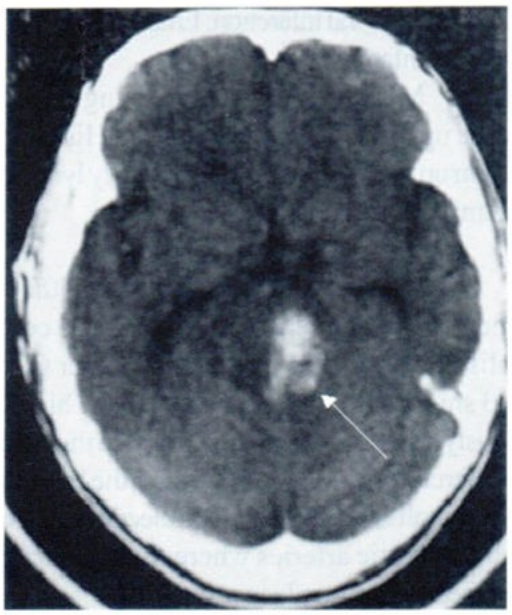

Fig. 7 CT. without contrast, a white mass of hematoma is found at the brain stem, at Pons.

CASE VIII: Subarachnoid Hemorrhage: Rupture Aneurysm.

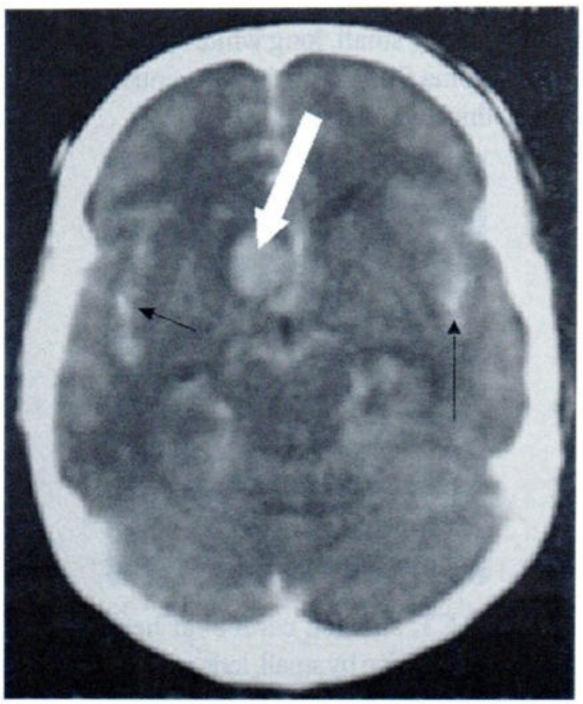

Fig. 8A CT.

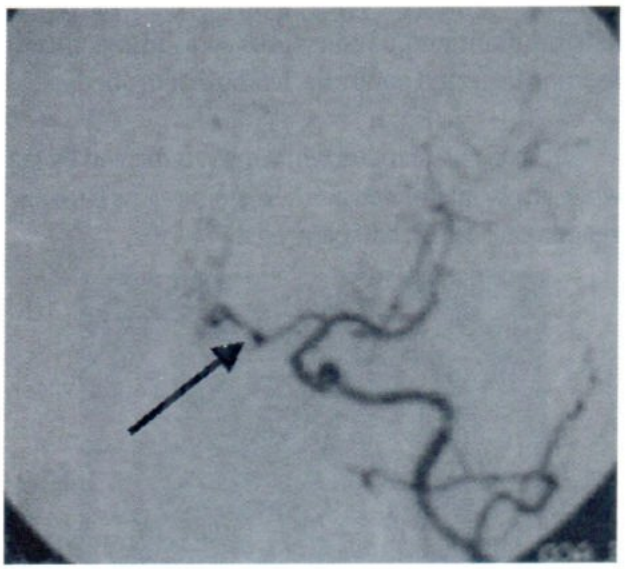

Fig. 8B DSA.

CT. shows subarachnoid haemorrhage at both sylvian fissures as indicated by black arrows and also intracerebral haematoma near the position of aneurysm, white arrow. Picture from digital subtraction angiography show the position of ruptured aneurysm as pointed by the black arrow.

CASE IX

Clinical: Patient, old ages and debilitated, has venous thrombosis in the brain because of bed ridden.

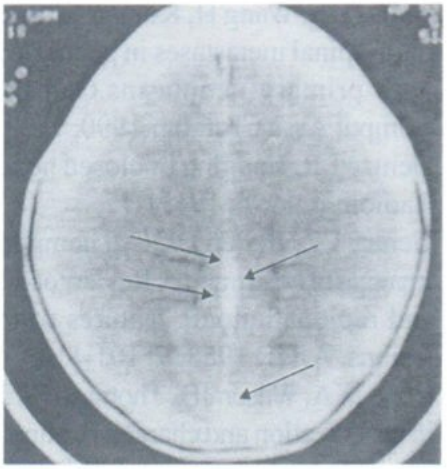

Fig. 9 NC.CT. shows venous thrombosis as pointed by black arrows.

CASE XI: Arterio-Venous Malformation.

CT. showing congenital mal-formation having AVM in the brain, making nervous deficit of the brain functions in the areas replaced by AVM.

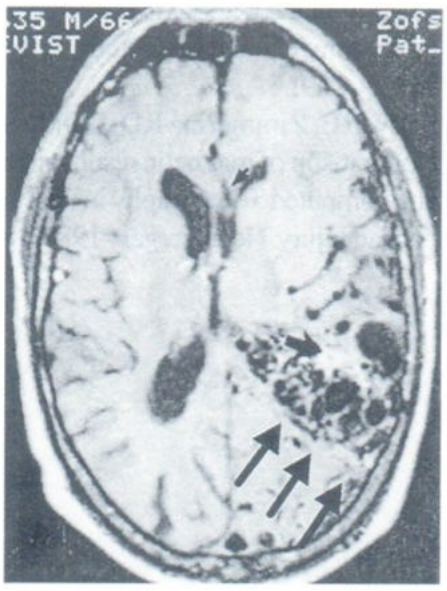

Fig.11A NC.CT. showed Arterio-Venous Malformation (AVM) at left side of the brain (black arrows).

CASE X: Cerebral venous thombosis.

Clinical: Female taking birth control pills., age 40 years. She took sleeping pills by mistake and never wake up.

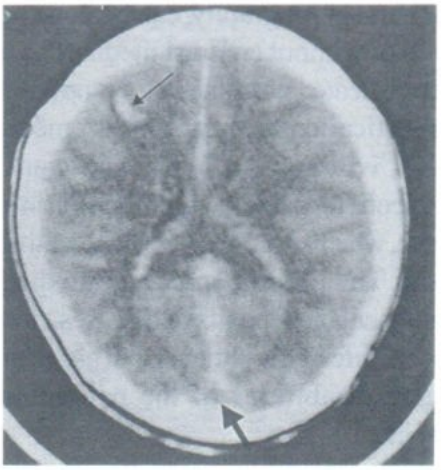

Fig.10 CT. show petichial hemorrhage at frontal lobe as indicated by small black arrow. There is also thrombus in the superior sagittal sinus as indicated by thick, short arrow called delta sign or empty triangular sign. "delta sign" is a special name for superior sagittal sinus thrombosis.

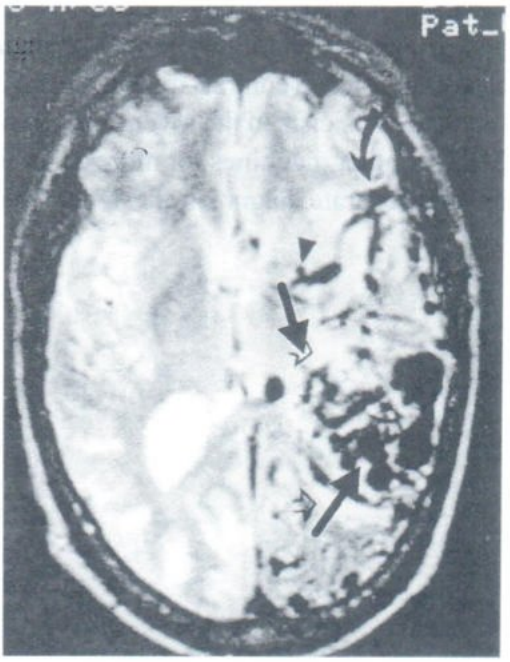

Fig.11B CE.CT. showed AVM which replaced normal brain causing nervous deficit to the patient.

DISCUSSION

Prompt and accurate diagnosis of cerebro -vascular accidents or diseases, now-a-day, apart from cerebral angiography, can be done by CT and MRI with or without contrast media. The more and more sophisticated machine of CT. and MRI. and the more investications of new contrast media for CT. and MRI., will help both the physicians and the neurosurgeons to make the right decision in giving the treatments, whether, surgical or conservative medical treatment. The prompt and accurate diagnosis of cerebro-vascular accidents or diseases, not only, we can save the life of the patients, but also can save the permanent disabilities of the patients in future surviving life.

11 cases

CONCLUSION

Further progresses of Roentgen Diagnosis using CT. and MRI. needs more attentions and co-operation of multidisciplinary scientists, not only the medical professions, neurologists, neurosurgeons, and neuro-radiologists, but also the pharmacists specially interested in contrast media, the engineers and medical physicists in the invention of new CT. and MRI. or other machines for more economical, prompt and accurate diagnosis of CVA or diseases.

REFERENCES

1. Barkovich AJ. Pediatric neuroimaging, New York: Raven press, 1995.
2. Blews DE, Wang H, Kumar AJ, et al. Intra-dural spinal metastases in pediatric patients with primary neoplasms.Gad-DTPA. J. Comput Assist Tomogr 1990; 14: 730-735.
3. Gentry LR. Imaging of closed head Injury. Radiology 1994; 191: 1-17.
4. Gentry LR. Godersky JC, Thompon B. MR Imaging of head trauma: Review of ditribution and rapiopathologic features of traumaic lesions. AJNR 1988; 9: 101-110.
5. Hope JKA, Wilson JL., Thomson FJ. 3D CTA in the detection and characterization of intra-cranial berry aneurysm. AJNR 1966; 17: 439-445.
6. Lipper MH, Kishore PRS, Enass GG. et al. CT. In the prediction of outcome in head injury.
7. Pressman BD, Tourje EJ, Thompson JR. early CT sign of ischemic Infarction: Increased density in a Cerebral artery. A JNR 1987; 8: 645-648.
8. Savoirdo M, Bacchi M, passerini A, Visciani A. The vascular territories in the cerebellum and brain stem: CT and MRI study. AJNR 1987; 8: 199-209.
9. Snow RB, Zimmerma RD, Gandy SE, et al. Compatison of magnetic resonance imaging and computed Tomography in the evaluation of head Injury. Neurosurgery 1986; 18: 45-52.

TRAUMATIC LESIONS AND HEMORRHAGES OR HEMATOMA IN THE BRAIN, DIAGNOSED BY CT. AND MRI.

Vallop LOAPAIBUL[1] M.D.,
Kawee TUNGSUBUTRA[2] M.D., F.R.C.R (England)

ABSTRACT

CT and MRI with or without contrast media, are the most convenient and quickest way of investigation to diagnose and demonstrate to the surgeons or physicians, to visualize the lesions in the brain after having traumatic lesions or cerebrovascular accidents.

Hemorrhages and Hematomas may occur in different layers of the skull and brain are:

1. **Epidural hematoma:** The bleeding or the hematoma is outside the dura, which is thick and tough layer of fibrous tissue sheath covering the brain tissues. The inner outline of the mass or hematoma pressing on the brain will be smooth.
2. **Subdural:** The bleeding is inside the dura, the pia and arachnoid may be or may be not intact. The outer layer of the lesion will be smooth but the inner layer will be undulating, but not scattering into the brain tissues, if the pia and the arachnoid are intact.
3. **Subarachnoid:** The bleeding and hematoma will be scattering freely inside the brain tissues, more on the side with direct trauma. The opposite side will be damaged by **"contra coup".**
4. **Diffuse axonal injury (DAI):** The bleeding go inside the brain along the nerve sheath of the axon.
5. **Cortical Contusion** or **Haemorrhagic Contusion:** The hemorrhages are spreading and confined in the cerebral cortex.

SYMPTOMS FROM CLOSED BRAIN INJURY MAY BE CLASSIFIED INTO 3 DIFFERENT LEVELS ACCORDING TO RESIDUAL DAMAGES.

1. CEREBRAL CONCUSSION. The symptoms of brain injury may persist for few days and having remission without residual deficit of brain functions and complete recovery. The organic lesions cannot be detected by any means but the symptoms and signs can be detected only by physical examinations.

2. CEREBRAL CONTUSION. The organic lesions can be detected by CT and /or MRI.

3. CEREBRAL LACERATION. The victims may die or alive with residual deficit or deficits of the brain functions the patients.

[1] Department of Radiology, Faculty of Medicine, Khon Kaen University, Khon Kaen, THAILAND.

1.1.1. EPIDURAL HEMATOMA

Clinical: Male, age 28 years. Car accident with head injury.
CT. shows Epidural Hematoma at Lt. Frontal region, lentiform or biconvex shape. The density of hematoma is hyperdense, pressing on the frontal lobe of brain, right side.

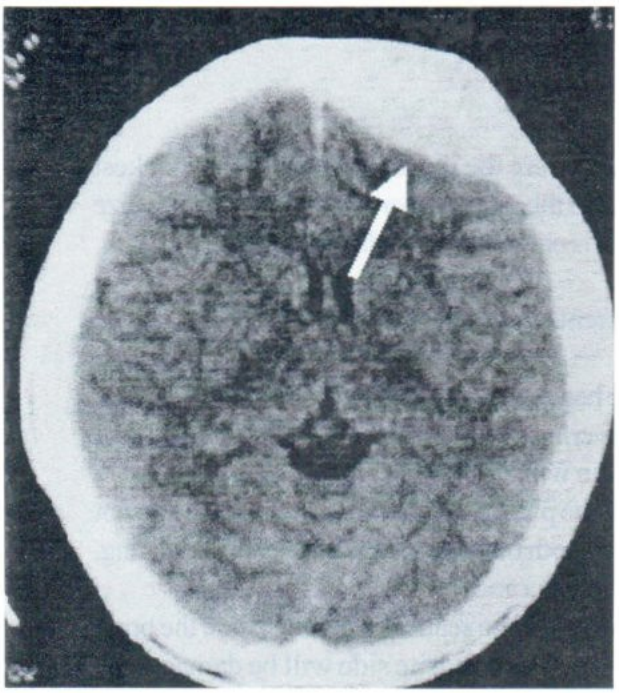

Fig. A Epidural Hematoma, Lentiform or biconvex shape.

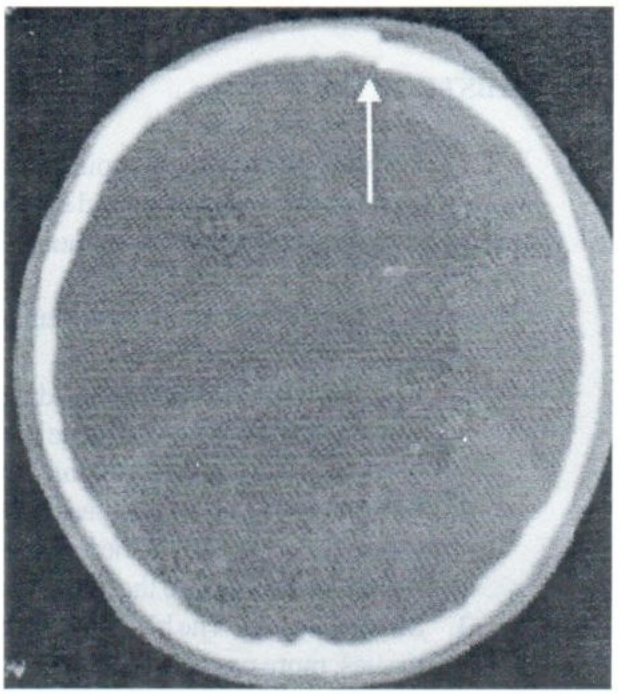

Fig. B Frecture skull, with extracranium hemorrhage around the peri-cranium spaces both side.

1.1.2. Male, age 21 years, car accident.
Epidural Hematoma, lentiform shape or biconvex shape. (White arrows)

Density: Hyperdense temporal region, Lt.
Hematoma outside skull,
Rt. from direct trauma.
Lt. from "contra coup"
Hematoma outside skull
Irregular shape, and thickness
(Black arrows)

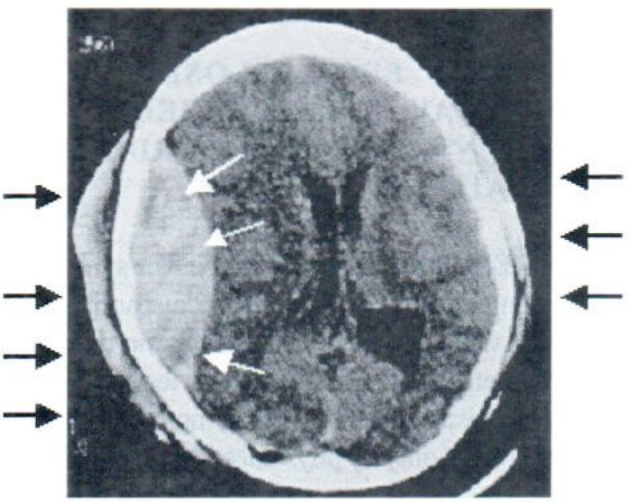

1.1.3. EPIDURAL HEMATOMA, The blood could not pass through the dura into the brain.

Clinical: Male, 48 years, car accident, not fasten the seat belt, forehead and wind shield collision.

MRI; T_1W_1 and T_2W_1 show both frontal epidural hematomas.

Signal intensity shows hyperintensity, which can be seen, whiter than, the brain showing that

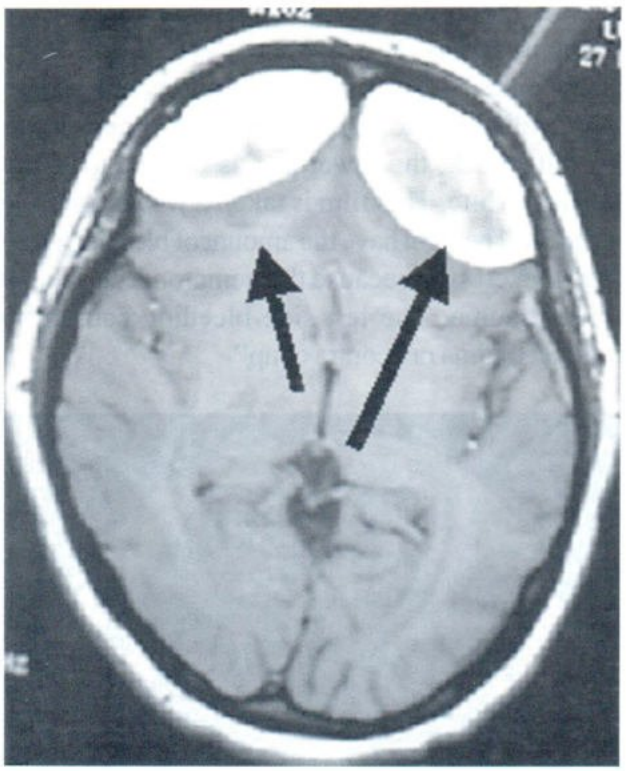

Fig. A MRI T_1W_1

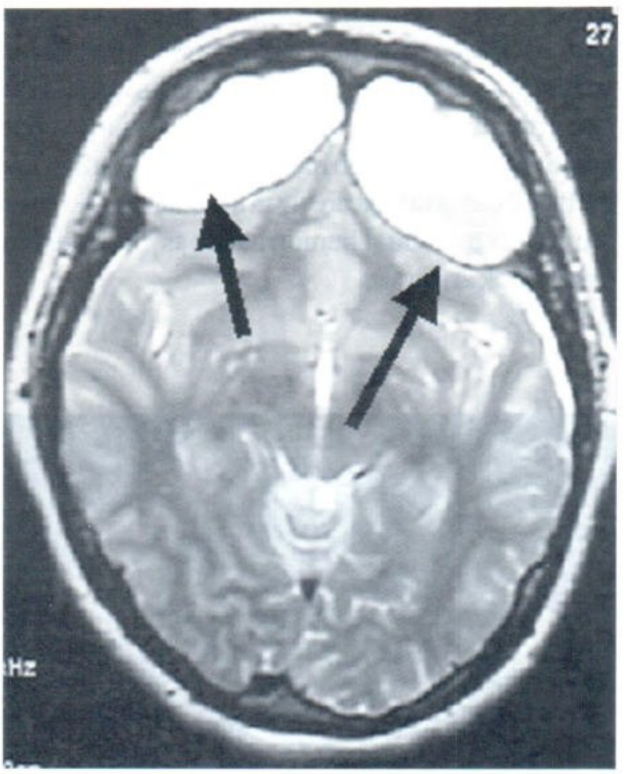

Hematoma is in the subacute stage.

Fig. B MRI T_2W_1. The inner edge of the Epidural Hematoma is smooth. It is clearly sharp and distinct because the dura is tough and thick. The blood can not passed into the brain tissue.

1.1.4. SUBDURAL HEMATOMA

Clinical: Male, age 45 years, car accident, head on collision.

CT. shows subdural hematoma Rt. Frontal Region, and subdural hematoma, small size in the Lt. fronto-temporal region. Intracerebral hematoma, small amounts also seen in the temporal region, posterior part, as pointed by small white arrow. The edge of subdural and intracerebral hematoma is not smooth and irregular because the blood can pass into brain tissue without any tough membrane as the barrier, and the blood can distribute freely in the brain tissue. There are also extracranial hemorrhages as indicated by small black arrows.

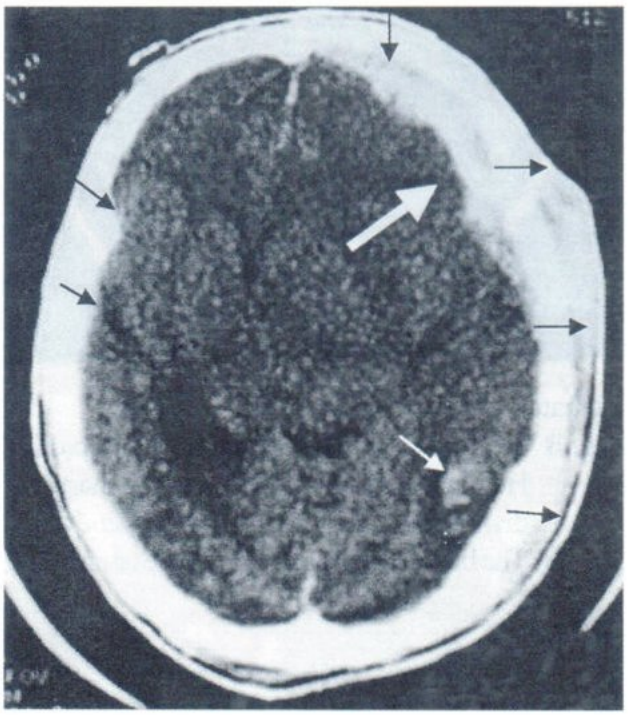

1.1.5. SUBDURAL HEMATOMA

Clinical: Male, age 31 years car accident 2 weeks ago.

CT. shows bilateral hemorrhages. The brain material is separated from the inner wall of the skull both sides by black areas indicated by small black arrows. The lower parts, of the black areas are white triangular areas. This is due to the liquidify of the Hematomas. The patient lying on his back on bed, so the liquidify hematoma is sedimenting. The upper part become black, the lower part is opaque to X-ray become white. This film is taken 2 weeks after the accident. The right have the amount of bleeding more than the left side because the hematoma caused by direct trauma. The left side bleeding caused by indirect trauma or "contra coup"

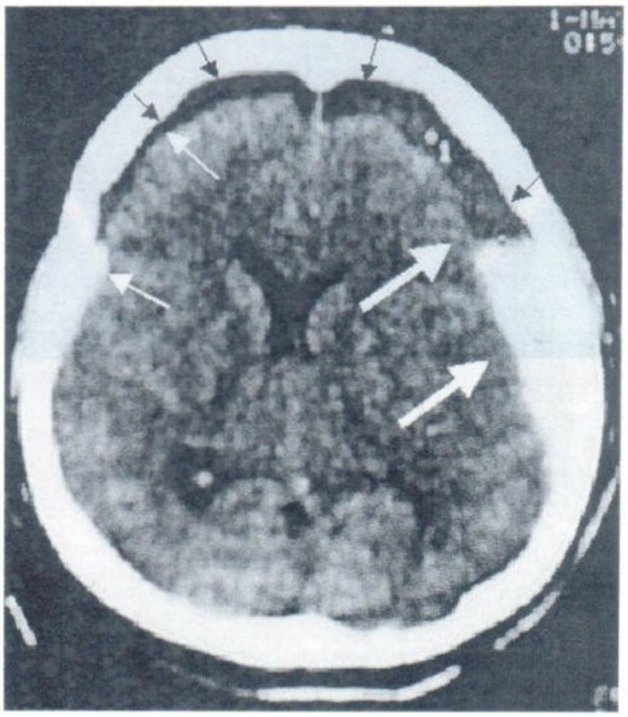

1.1.6. SUBDURAL HEMATOMA

Clinical: Male, age 23 years, car accident.

CT. of this case shows subdural hematoma. The white area of the left frontal lobe is not regularly white and uniform may indicate that the bleeding is still active. The brain was compressed, so only the lateral ventricle of the right side is clearly seen.

In this case there are, epidural, subdural, intracerebral and extracranial hematoma.

The newly formed hematoma will appear as hyperdense.

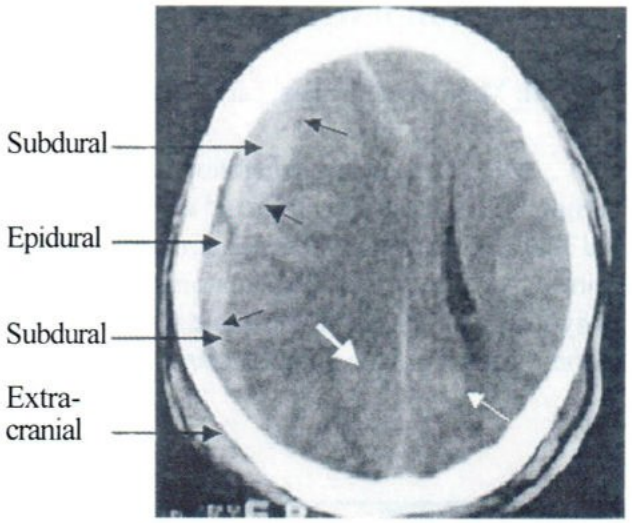

Intracerebral white arrows

1.1.7. SUBDURAL HEMATOMA

Clinical: Male, age 58 years, car accident 2.5 months ago.

(A.) CT. without contrast **(B)** contrast enhancement CT. Subdural hematoma presented as cresent shape density and will liquidify after one week and sediment to the lower part of the hematoma. The upper part will become hypodense when the times pass by. The Subdural hematoma presses on the lateral ventricle right side, as seen in the CT, the right ventricle is narrowing and small. The whole brain is shifting to the left.

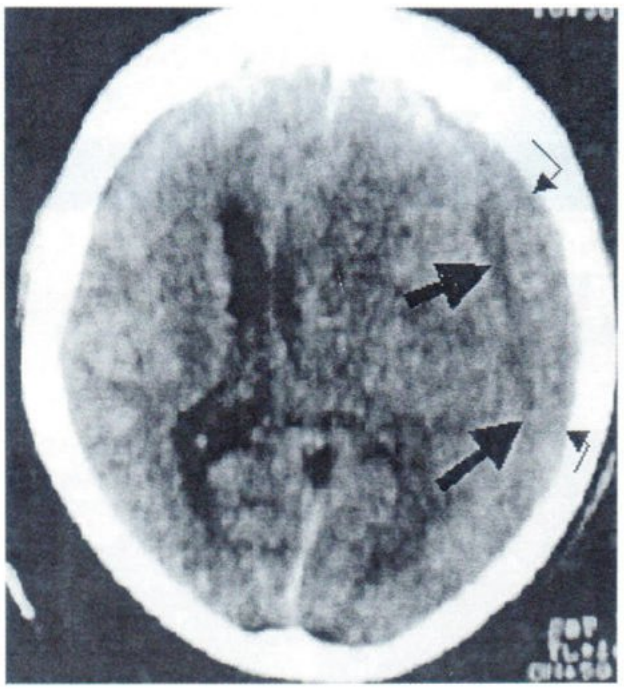

Fig. A Non-contrast CT

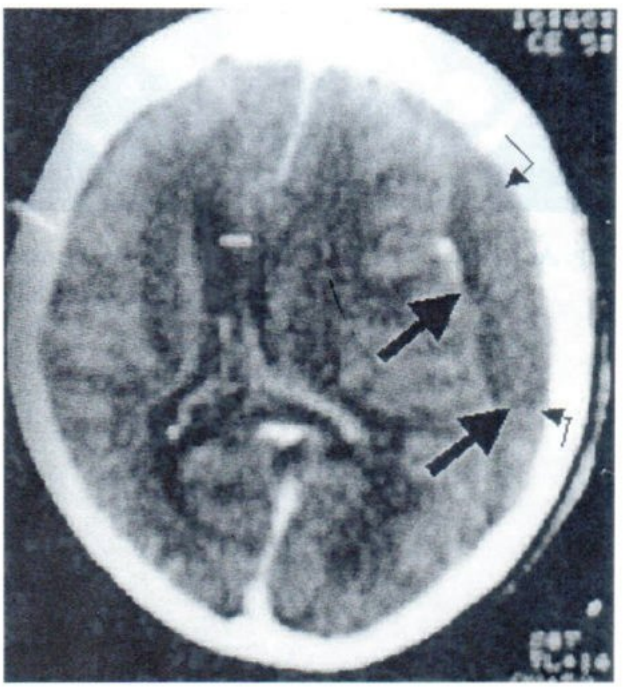

Fig. B Contrast enhanced CT.

1.1.8. SUBDURAL HEMATOMA

Clinical: Male, age 60 years, car accident.

MRI. The patient having subdural hematoma Lt. side with brain atrophy from old age. MRI, T_1W_1 and T_2W_1 show subdural hematoma, crescent shape, pointed by white arrow. The hematoma will present as hypersignal density in the acute stage and will become isosignal in the subacute stage.

The outer edge of the white crescent shadow separated the brain and the skull and is smooth because is being covered by the dura which is thick and tough. The inner edge is undulated because it is covered by thin arachnoid and pie mater, indicative that it is the subdural hematoma. The left lateral ventricle is obliterated indicative there in also intracerebral hemorrhage.

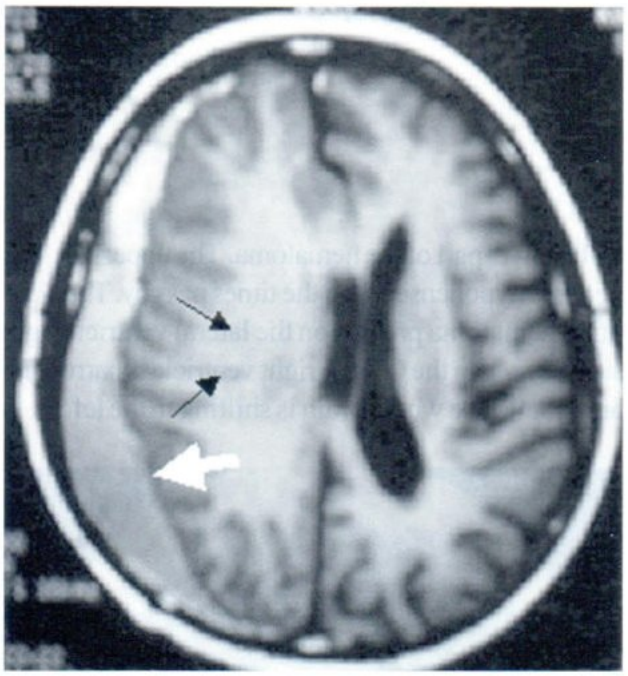

Fig. A MRI, T_1W_1 Black arrows indicating intracerebral hematoma filling up the left ventricle.

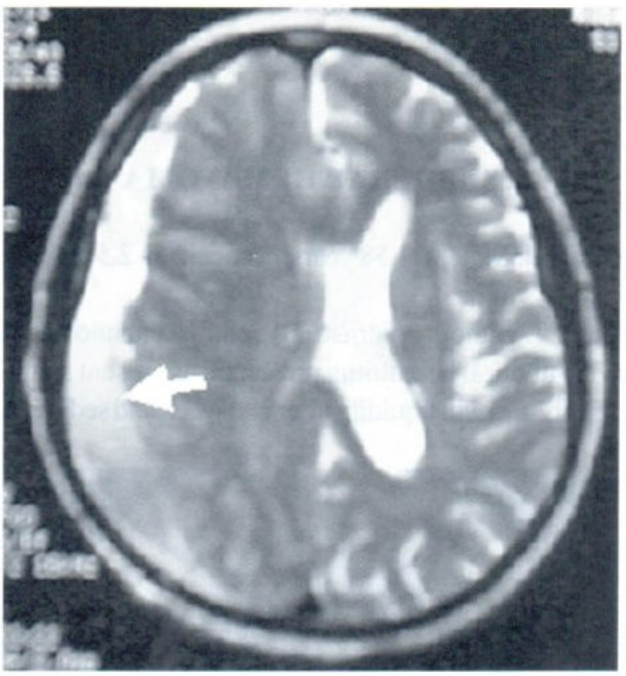

Fig. B MRI, T_2W_1

1.1.9. SUBDURAL HEMATOMA

Clinical: Female, age 54 years, hemiparalysis, drowsiness and progressive loss of coniousness for 1 week with a history of head injury from accident in the bath room for 1 month.

CT. (A.) before opaque media injection (B.) after opaque media injection. The pictures in the CT. films showed crescent shape density in the left side of the cerebral cortex displacing the lateral ventricles to the right side. There is also a smaller crescent shape abnormal shadow in the frontal region of cerebral hemisphere, right side. The upper parts of the abnormal shadow in both sides are black, the lower parts are white suggestive of subdural hematoma, in both frontal lobes, more marked on the left side. The left side hematoma caused by direct brain injury, right side by "contra coup"

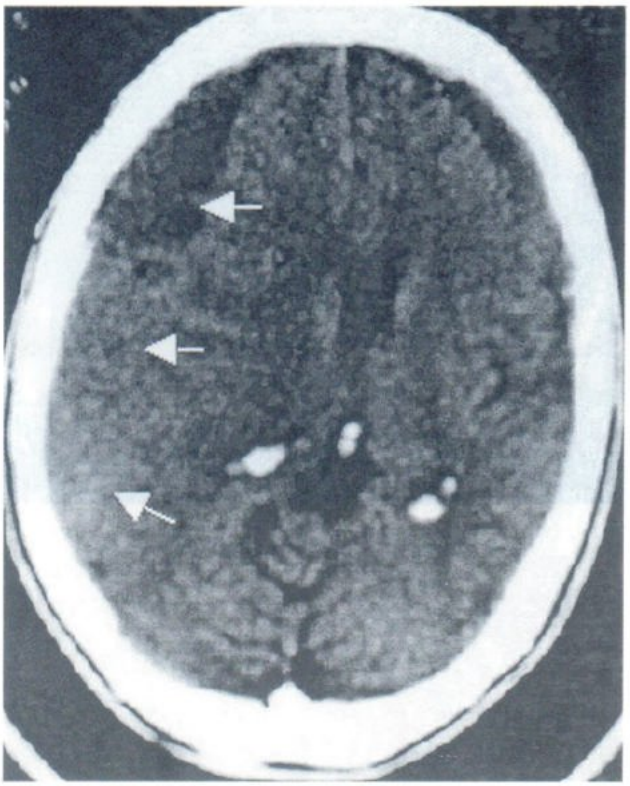

Fig. A Subdural hematoma CT before contrast media injection.

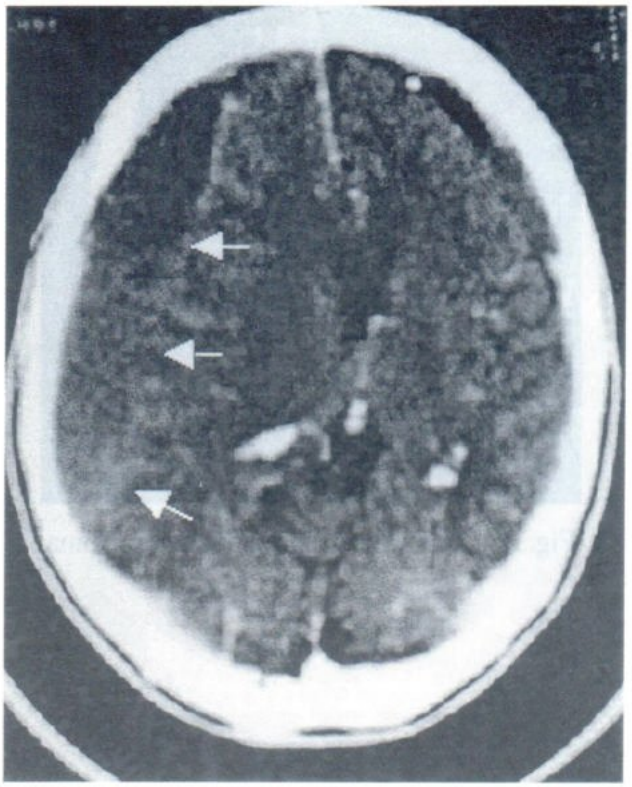

Fig. B Contrast Enhancement CT of the same patient.

1.1.10. SUBDURAL HEMATOMA

Clinical: Male, age 80 years, brain atrophy and head injury in the bathroom.

A. Axial projection T_1W_1 MRI., black space between skull and brain showed brain atrophy.

B. Coronal projection T_1W_1 MRI., hematoma in both projection shown in white areas. Hematoma will show hyper signal intensity in acute and subacute phases.

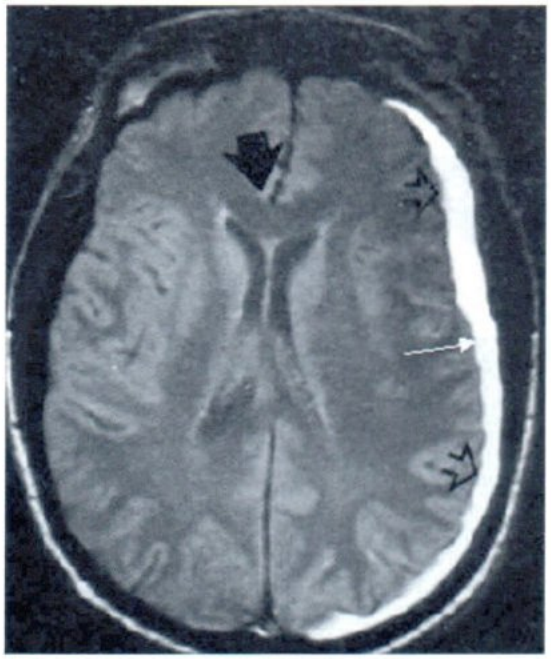

Fig. A Coronal section subdural hematoma.

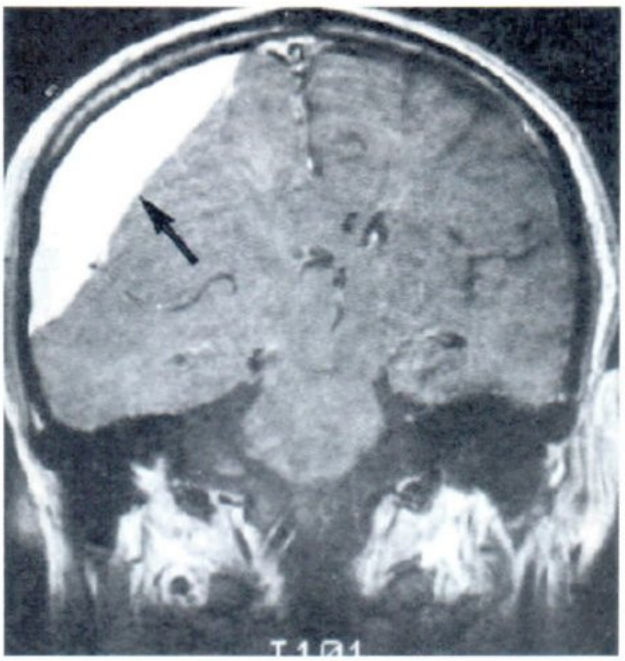

Fig. B Sagital section.

1.1.11. SUBDURAL HEMATOMA

Clinical: Male, age 18 years, car accident with hematoma at the tentorial area. The shape of hematoma needs not be crescent as in the pervious examples. Fig. A. Film taken in axial projection, MRI. T_1W_1. Fig B. Coronal projection CT. Coronal projection MRI T_1W_1 thin black arrow showed hematoma at the tentorial area left side, thick black arrow showed extracranial hematoma.

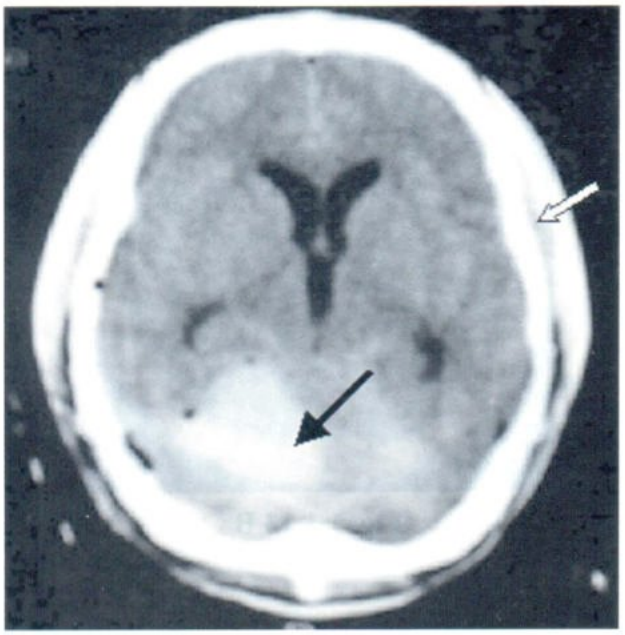

Fig. A MRI, T_1W_1 Coronal projection

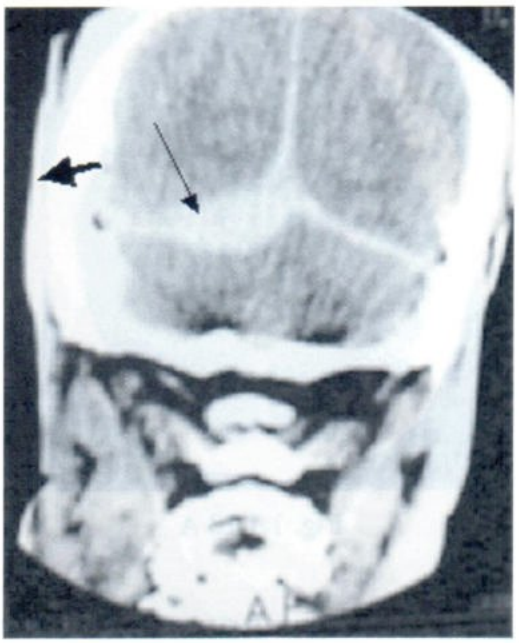

Fig. B MRI, T_1W_1 Sagital projection

1.1.12. SUBARACHNOID HEMORRHAGE

Clinical: Male, age 43 years, car accident and unconscious.

CT. Scan showed bleeding in the subarachonid space. In the film, white area as pointed by the black arrow, were the subarachnoid hemorrhage which was seen in the suprasellar cistern, in normal individual, black area of CSF will be visualized.

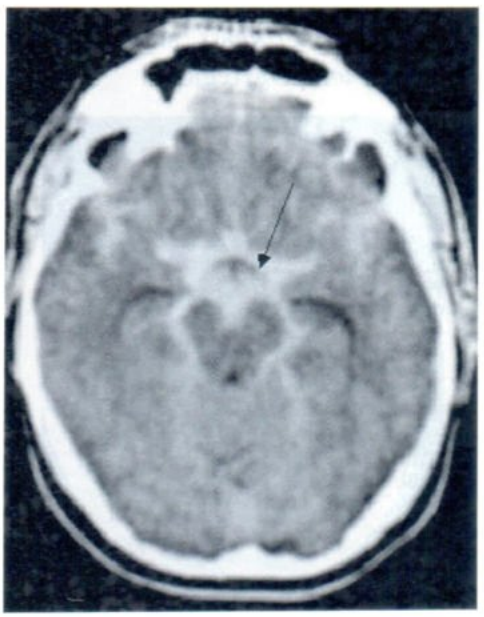

Fig.1.1.12 Subarachnoid hemorrhage at the basal cistern

1.1.13. HEAD INJURY, DIFFUSE AXONAL INJURY (DAI)

CT. showed hemorrhagic diffuse axonal injury showing general brain edema and hemorrhagic spots at basal ganglia. The patient was in coma stage. The bleeding diffused along the axon of nerve cells showing small white spots surrounding the axon of nerve cells.

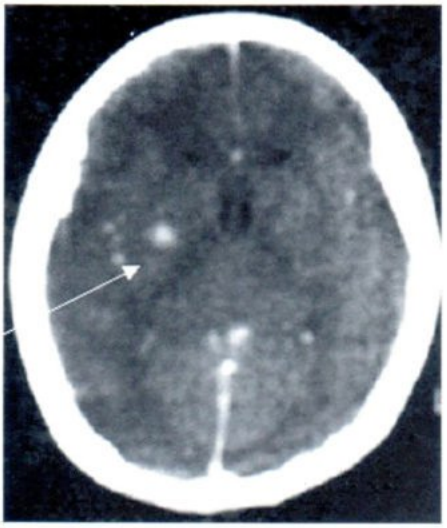

Fig. 1.1.13 A

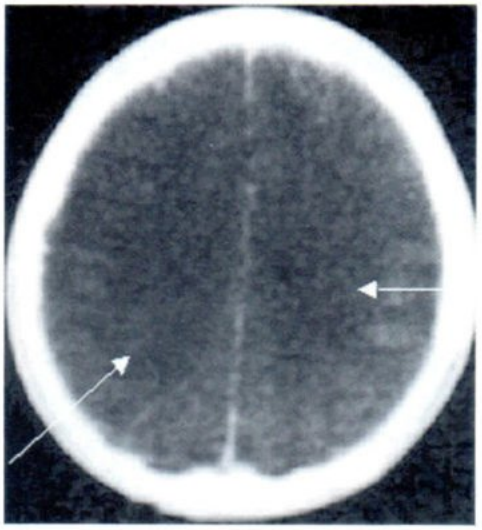

Fig. 1.1.13 B

1.1.14. FOREIGN BODY, BROKEN END OF THE STABBING KNIFE.

Clinical: Male age 27 years, stabbed by knife at fronto-temporal region.

Fig. A Showing the broken end of the stabbing knife (black arrow).
Fig .B Showing bones window after removing the broken end of the knife (white arrow).

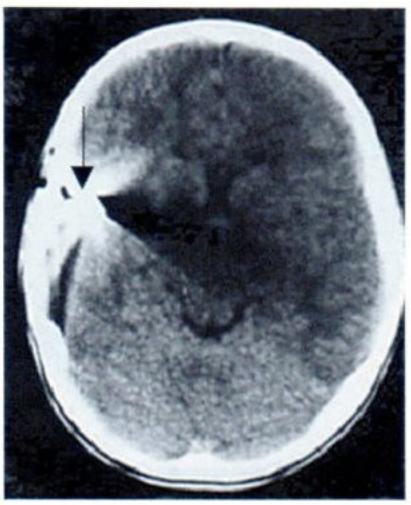

(A)

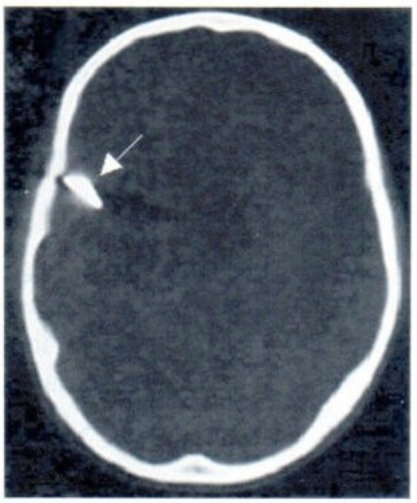

(B)

CT. skull Fig. 1.1.14 A and B

1.1.15. CORTICAL CONTUSION

Clinical: Male, age 21 years, head on collision car accident, semi-conscious,

Non-contrast CT. shows hemorrhagic cortical contusion at Lt. Frontal lobe.

NC.CT. Haemorrhagic area is black at Lt. frontal lobe.
CE.CT. Haemorrhagic area is white at the area of contusion.

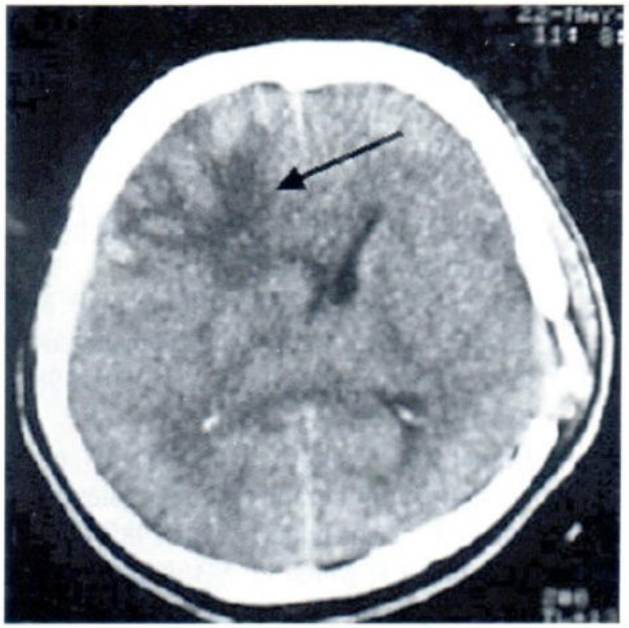

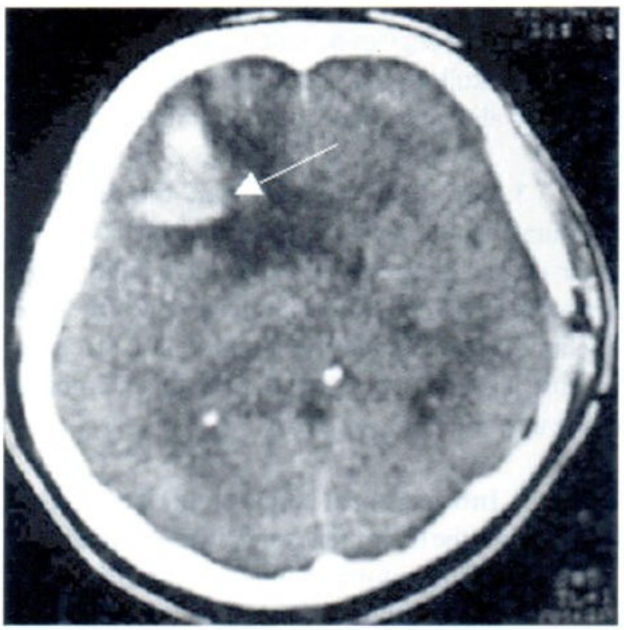

DISCUSSION

Traumatic lesions and hemorrhage or hematoma in the brain, prompt and accurate diagnosis about the position, the number of the lesions, the extent of the hemorrhage or hematoma, are the primary important data for the doctor in charge of the Accident and Emergency Department of a hospital in deciding to give the appropriate management, not only to save the life of the patient but also to preserve the brain functions both the sensory and motor, as much as possible. It is useless to be alive with unconsciousness and become to be the burden of the family. It is very critical to choose or to make a prompt decision to use surgical or medical treatment. Only CT. and MRI with or without the contrast enhancement can help the expert team in making the decision to give the right management at the right time. There should be a team which should be composed of experts in different specialties, or subspecialties, namely, neurologists, neurosurgeons, neuro-radiologist, anesthetist, experts in ICU or Intensive care unit, etc.

CONCLUSION

The roentgen diagnosis in this paper, we have shown the few examples of extra, and intracranial hemorrhages, which we can show the site or sites of the lesions, the number of lesions, the extent of the lesions in order to give the right treatment at the right time. By CT and MRI with or without contrast we can devide the lesions, hemorrhage or hematoma into 6 different levels, namely as

1. Extra-or peri-cranium. We can see the shadow of hematoma outside the skull bone shadow,

with irregular shape and thickness. The site of direct trauma may also has fracture of the skull. We can see the hemorrhagic shadows in both sides of the skull, more marked at the site of trauma, the opposite side also had a thinner shadow of hemorrhage or hematoma caused by **"Contra coup"**

2. Epidural hematoma: the shape is lentiform, the outer edge of hematoma is along the inner table of the skull, the inner edge of hematoma is smooth and sharp along the thick and tough fibers of dura.

3. Subdural hematoma: the shape of Subdural hematoma is characterized by having the inner edge irregular, but the outer edge of the hematoma will be merged with the shadow of the skull. The inner edge of subdural hematoma is irregular because it is covered by the softened thin membrane of Pie and arachnoid and CSF.

4. Intracerebral hematoma: There may be bleeding into the brain tissues and fill up the ventricles. The shape of hematoma is indefinite the blood can distribute freely in the brain tissues.

5. Diffused axonal injury (DAI): Intracerebral hemorrhage may be found in the form of diffused axonal injury showing general brain edema and hemorrhagic spots at the basal ganglion. The patient will be in the coma stage. The bleeding diffused along the axon of nerve cells showing small white spots surrounding the axon of nerve cells.

6. Foreign body remaining in skull or brain tissue such as the part of the knife or the bullet may be shown and located by CT.

7. Cerebral concussion can be detected only by physical examination. Only cerebral contusion and cerebral laceration can be detected by CT. and MRI or both with or without contrast. The contusion and lacerated lesion will be hypotense and appeared as black area with plain CT. without contrast. The contusion and the lacerated areas will be shown by CT. or MRI with contrast enhancement as the white areas by the enhancement of the contrast, the same as the hemorrhagic area.

REFERENCE

1. Gentry LR, Imaging of closed head injury. Radiology 1994; 191: 1-17.
2. Gentry LR. Godersky JC. Thompson B. MR Imaging of head trauma; and radiopathologic features of traumatic lesions. AJNR. 1988; 9: 101-110.
3. Lipper MH, Kishore PRS, Enas GG, et al. Computed tomography in the prediction of outcome in head injury. AJNR 1985; 6.7-10.
4. Marshall LF, Marshall SB, Klauber MR, et al.The diagnosis of head injury requires a classification based on computed axial tomography. J Neurotrauma 1992; 9: 5287-5292.
5. Maytal J. Bienkowski RS, Patel M, Eviatar L. The value of brain imaging in children with headaches. Pediatrics 1995; 96: 413-416.
6. Snow RB, Zimmerman RD, Gandy SE, et.al. Comparison of magnetic resonance imaging and computed tomography in the evaluation of head injury. Neurosurgery 1986; 18:45-52.

ADULT INTUSSUSCEPTION : A CASE REPORT

Rutchanee PAISUWAN, MD.[1]

Intussusception is mostly often found in infants and children. Adult intussusception is rare and the underlying cause can be identified in most cases, while the etiology in children is mostly idiopathic.The symptom and sign are often chronic and relapsing, presenting as recurrent episodes of subacute obstruction and variable abdominal signs. Ultrasound and CT studies play an important role in establishing the diagnosis. Therefore I would like to report one case of adult intussusception with the literatures reviewed.

CASE REPORT

A 42-year-old woman presented with a 6-month history of chronic abdominal pain, predominantly at the mid-abdomen, with a weight loss of 10 Kgs. in 6 months. Previously she had been healthy and had had no history of operation. Physical examination revealed a pale, cachectic patient without a palpable mass. Acute abdomen series showed colonic contents in right-sided colon and dilated mid-transverse colon suggestive of obstruction at mid-transverse colon (Fig.1 A,B). Ultrasound shows bowel mass, measuring about 3.8x3.4 cm. in size, and the various layers, concentric rings may represent mesentery and bowel wall that has been drawn into the intussusception (Fig.2). CT findings are compatible with intussusception at mid-transverse colon (Fig.3). Exploratomy laparotomy was performed and found similar findings on CT scan. Transverse colon resection with end to end anastomosis was performed.

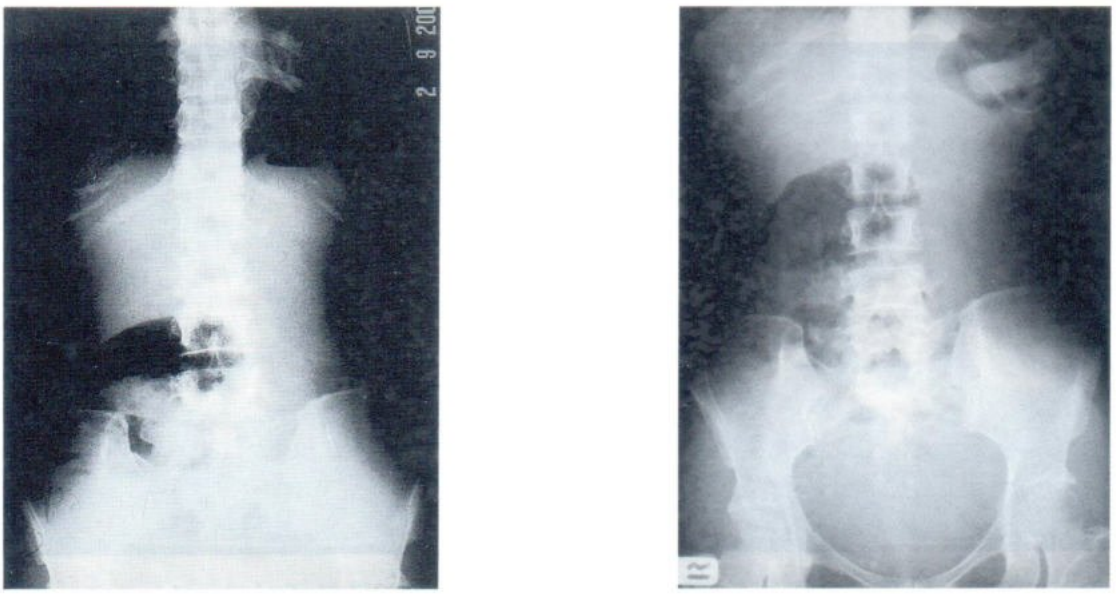

A B

Fig.1 a,b. Plain film abdomen supine and upright view revealed dilated right part of transverse colon with much colonic contents contained (arrows) and absent contents in left sided colon suggestive of colonic obstruction at mid-transverse colon.

[1] Department of Radiology, Vachira Phuket Hospital, Phuket, THAILAND 83000

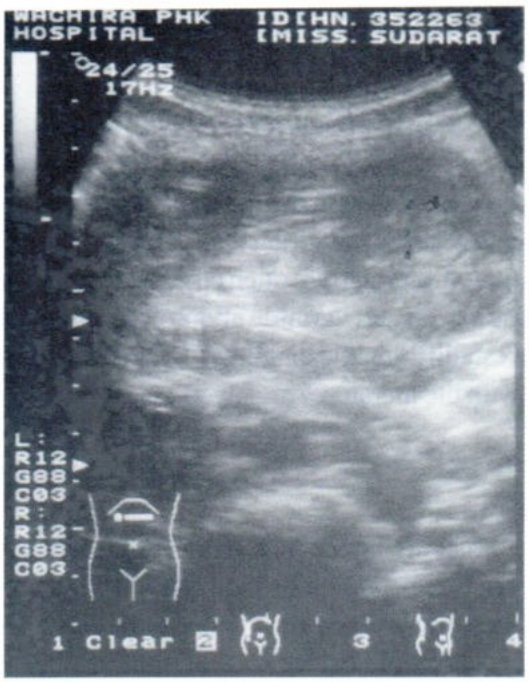

Fig. 2 Longitudinal scan shows bowel mass (arrows) and multifocal echogenic center and sonolucent periphery represent edematous wall.

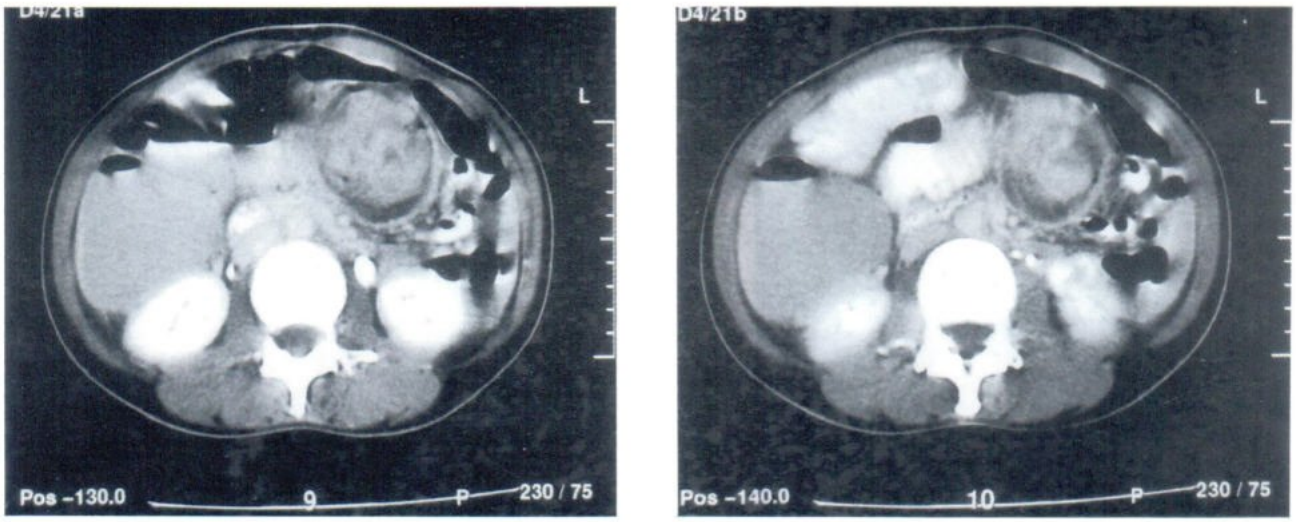

Fig. 3 Axial CT scan shows bowel in bowel appearance with mesenteric fat being drawn into the intussusception.

DISCUSSION AND REVIEW OF LITERATURE.

Intussusception is defined as prolapse of proximal segment of bowel (intussusceptum) into an adjacent distal segment (intussuscipiens), is a rare condition in adults and differs substantially from the much more common intussusception in infants (only about 5 % of intussusceptions occur in adults, while 95 % in infants). Intussusception causes 1% of all bowel obstruction.[1] In contrast to childhood intussusception, which is idiopathic in 90% of cases, adult intussusception has an underlying cause in about 90%.[1-8] Neoplasm is the most common cause in these series and was found in approximately 65% of the adult cases. Non-neoplastic processes constitute 15-25% of the cases, and idiopathic or primary intussusception about 10%.[8] In the majority of cases, (about 65%) intussusception arises in the small bowel. The etiology can be classified broadly into the major headings of

1) neoplastic diseases
2) post-surgical complication (e.g. adhesion, bowel wall edema)
3) miscellaneous pathology (e.g. Meckel's diverticulum, coeliac disease, AIDS related gastrointestinal disorder) and
4) idiopathic

Intussusception in the large bowel is more likely to have a malignant etiology, with primary malignant lesions, adenocarcinoma and lymphoma occurring in 50-60% of the cases.[8,9]

Clinical presentation of adult intussusception is variable, most often chronic intermittent abdominal pain. Other symptoms include nausea/vomiting, melena, weight loss, fever and constipation.[2,10-11] Symptoms are in most cases of long duration, lasting several weeks to several months. Physical examination is often unremarkable. Intussusception in adults therefore difficult to be diagnosed clinically and necessitates imaging.[2] The role of plain abdominal radiograph is limited in adult intussusception where findings are usually non-specific. There might or might not be signs of bowel obstruction with an associated soft tissue mass.

The sonographic appearance of intussusception presents as an oval, pseudokidney mass with central echoes on longitudinal imaging and a sonolucent donut or target configuration on crosssectional imaging.[12-14] The central echoies are apparently compressed mucosa of the intussusception head, and the central echoes are apparently compressed mucosa of the intussusception head, and the various layers and concentric rings may represent mesentery and bowel wall has been drawn into the intussusception. The sonolucent periphery is apparently the edematous wall of the intussuscepted intestinal head. Adult intussusception often found a leading point. The CT appearance of intussusception is characteristic and allows confident diagnosis to be made. The cardinal features are:

1) Thickening of the affected bowel loop due to telescoping of two bowel segments. This procedures a "target" or " sausage" shaped mass-like lesion depending on the orientation of the intussusception.
2) Eccentrically located fat attenuation areas and mesenteric vessels within the intussusception representing invaginated mesentery.
3) Demonstration of the leading mass of intus susception surrounded by air or contrast.

Further management following the diagnosis of intussusception in adult is almost invariably surgery. Given the high rate of malignancy, surgical resection of the affected bowel segment without reduction is usually undertaken.

CONCLUSION

Adult intussusceptions are rare. Most causes of them are neoplasm. Clinical symptom is nonspecific. With the wide spread use of ultrasound and CT in the evaluation of non-specific abdominal pain, the diagnosis of intussusception is nowadays most often made by the radiologist since the ultrasound and CT features described here are virtually pathognomonic.

REFERENCES

1. Agha FP. Intussusception in adults. AJR 19786; 146: 527-31.
2. Azar T, Berger DL. Adult intussception. Ann Surg 1997; 226: 134-138.
3. Nagorney DM, Sarr MG, McIlrath DC. Surgical management of intussusception in the adult. Ann Surg 1981: 193: 230-236.
4. Coleman MJ, Hough TB, May RE, Jensen MJ. Intussusception in the adult. Aust N Z Jsurg 1981; 51: 179-180.
5. Carter CR, Morton AL. Adult intussusception in Gladgow, UK. Br J surg 1989; 76: 727.
6. Reijnen Ha, Joosten HJ, de Boer HH. Diagnosis and treatment of adult intussusception. Am J Surg 1989; 158: 25-28.
7. Hamaloglu E, Yavuz B. Intussusception in adults. Panminerra Med 1990; 32: 118-121.
8. Begos DG, Sandor A, Modlin IM. The diagnosis and management of adult intussusception. Am J Surg 1997; 173: 88-94.
9. Felix EL, cohen MH, Bernstein AD. Schwartz JH. Adult intussusception, case report of recurrent intussusception and review of the literature, Am J Surg 1976; 131: 758-61.
10. Warshauer DM,Lee JKT. Adult intussusception detected at CT or MR imaging : clinical -imaging correlation. Radiology 1999; 212: 853-60
11. Gayer G, Apter S, Hofmann C, et al. Intussusception in adults: CT diagnosis. Clin Radiol 1998; 53: 53-57.
12. Swischuk LE, Hayden CK Jr, Boulden T: Intussusception: indications of ultrasonography and an explanation of the donut and pseudokidney sign. Pediatr Radiol 1985; 15:388-391.
13. Holt S, Samuel E: Multiple concentric ring sign in the ultrasonographic diagnosis of intussusception. Gastrointest Raduiol 1978; 3:307-309.
14. Montali G, Croce F, DePra L, et al: Intussusception of the bowel: a new sonographic pattern. Br J Radiol 1983; 56:621-623.

IMAGING OF PERSISTENT BRAIN DAMAGE FROM HYPERTENSIVE ENCEPHALOPATHY IN A CHILD WITH NEUROPSYCHIATRIC SYSTEMIC LUPUS ERYTHEMATOSUS (NPSLE) AND ALFA THALASSEMIA TRAIT, A CASE REPORT.

Siriporn HIRUNPAT,[1] Prayong VACHVANICHSANONG,[2]

Chakree HIRUNPAT.[3]

ABSTRACTS

An unusual case of a neuropsychiatric systemic lupus erythematosus (NPSLE) child with hypertensive encephalopathy is presented. Despite the rare presentation of hypertensive encephalopathy in children, characteristic lesions in the brain should be recognized as possible manifestation of this condition. In contrast to other reports in which the brain damage was almost always reversible, we present a serial follow up images which demonstrate both reversible and irreversible brain damages. Brain lesions associated with hemorrhage, which are seldom described in most reports, have less likelihood reversibility.

Keywords: Encephalopathy, Hypertension, NPSLE, Child, Thalassemia

INTRODUCTION

Hypertensive encephalopathy (reversible posterior leukoencephalopathy) is an important clinical entity to be recognized because of the clinical and imaging findings, as the name implies, are usually reversible.

The clinical signs and MRI findings are characteristic. The condition is rarely reported in children and is usually seen in association with other systemic diseases.[1,2] Its true prevalence may be underestimated. We add a case report of a boy who had typical imaging of hypertensive encephalopathy in the serial imaging follow up from the first attack of the disease until recovery. Both reversible and irreversible changes in the brain were seen in this patient.

CASE REPORT

This 11 year old boy with SLE and Alfa Thalassemia trait had acute cortical blindness and drowsiness during admission for cholecystectomy. His blood pressure was 160/110 mmHg. SLE is diagnosed on the basis of thrombocytopenia, positive ANA (1: 640), nephritis (biopsy = lupus nephritis) and CNS involvement.

His CT scan at 1 day after the onset of acute cortical blindness showed low density areas in the subcortical white matter of both the occipital and parieto-occipital regions, more prominent at the right side, without significant enhancement. Minimal hypodensity at the subcortical white matter of the left frontal lobe was also noted. (Fig 1 A&B)

[1] Department of Radiology,
[2] Department of Pediatric,
3 Department of Ophthalmology Faculty of Medicine, Prince of Songkla University, Hat-Yai, Songkhla, Thailand
Correspondence: S. Hirunpat, Department of Radiology, Faculty of Medicine, Prince of Songkla University, Hat-Yai, Songkhla, Thailand 90110 Fax:66-74-429927. E-mail:Hirsirip@ratree.psu.ac.th

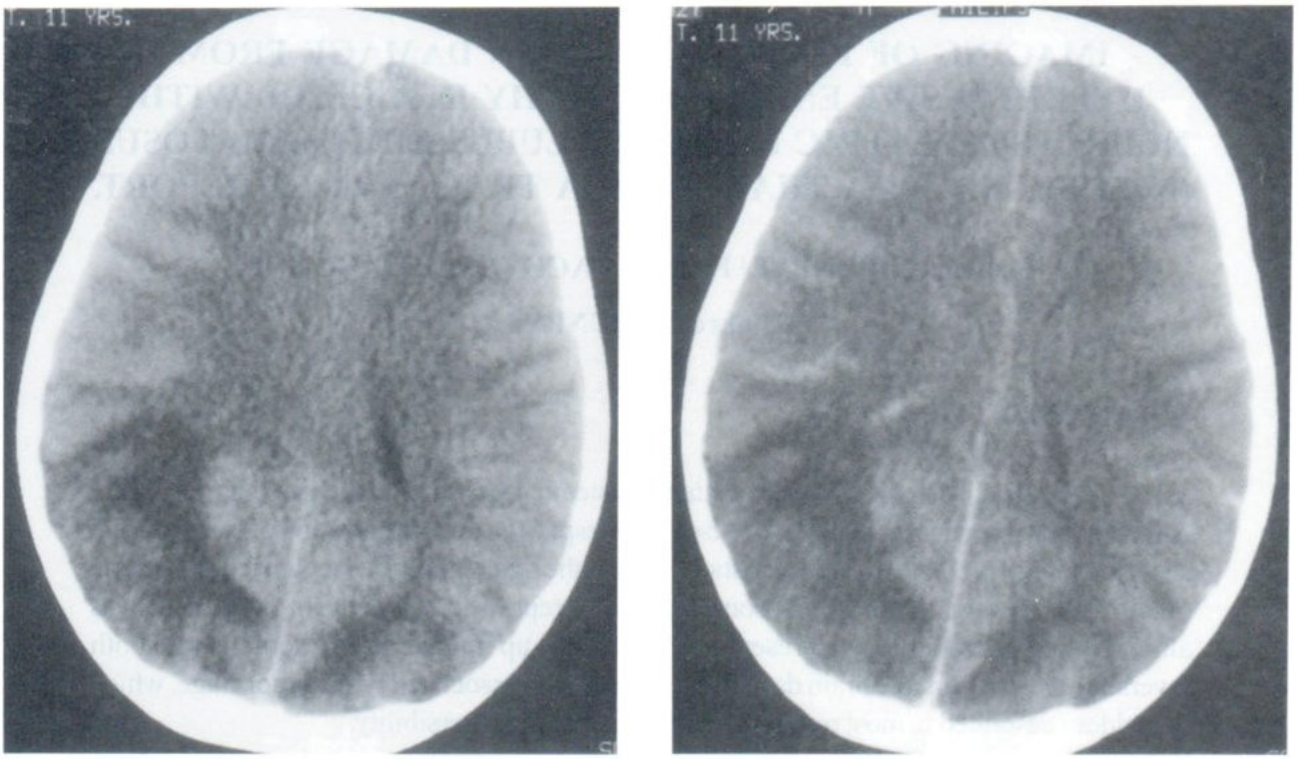

1a 1b

Fig.1 **a.** Plain axial CT and, **b.** Post contrast axial CT scan reveal low density areas in the subcortical white matter of both the occipital and parieto-occipital regions, more prominent at the right side, without significant enhancement. Minimal hypodensity at the subcortical white matter of the left frontal lobe was also noted.

Two days later, an MRI revealed abnormally low signal intensity on T1W and high signal intensity on T2W in both occipital and parieto-occipital subcortical white matter and at the left frontal subcortical white matter. Edematous adjacent cortical gyri were also seen, with multiple small hemorrhagic foci seen as high signal intensity on T1W and low signal intensity on T2W along both parieto-occipital and occipital gyri indicating more severe damaging brainauese from hypertensive encephalopathy. (Fig 2A &B)

The patient was treated with high doses of corticosteroids and anti-hypertensive drugs. His clinical signs rapidly improved. Visual acuity returned to normal (VA 20/20) within a few days and follow-up MR imaging 2 weeks after the first scan also showed marked resolution of the abnormal findings. However, small hemorrhagic foci along both occipital and parieto-occipital cortical gyri persisted. (Fig 3A&B)

Finally, the patient's neurologic symptoms were all resolved. A follow up MRI at 6 months after the first scan revealed an almost completely normal brain except for small gliotic areas at right parieto-occipital and right occipital cortex which indicated the more severe and irreversible brain damaged areas.

The MRI study showed no residual brain edema, but a small area of gliotic change at the previous hemorrhage sites at the right parieto-occipital cortex. (Fig. 4A& B) The smaller areas of previous hemorrhage at the left occipital and parieto-occipital cortex showed no residual abnormality.

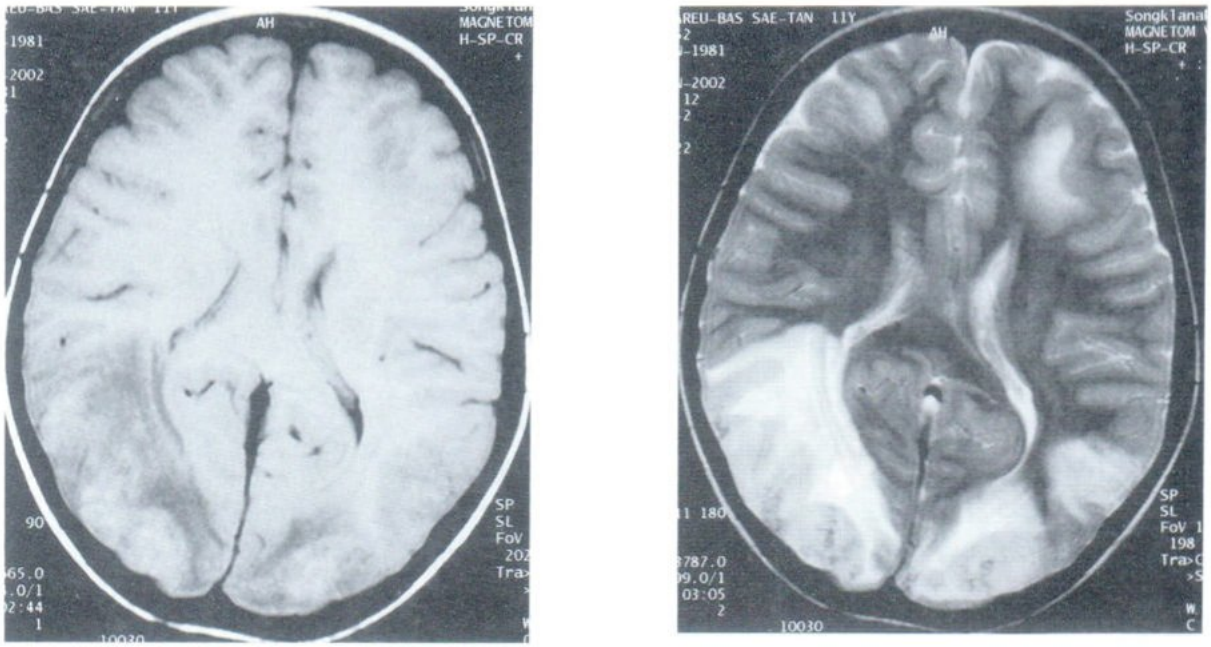

2a 2b

Fig.2 **a.** Axial SE T1W and, **b.** axial SE T2W images reveal low signal intensity on T1W and high signal intensity on T2W in both occipital and parieto-occipital subcortical white matter and at the left frontal subcortical white matter. Edematous adjacent cortical gyri were also seen, with multiple small hemorrhagic foci seen as high signal intensity on T1W and low signal intensity on T2W along both parieto-occipital and occipital gyri indicating more severe damaging brain areas

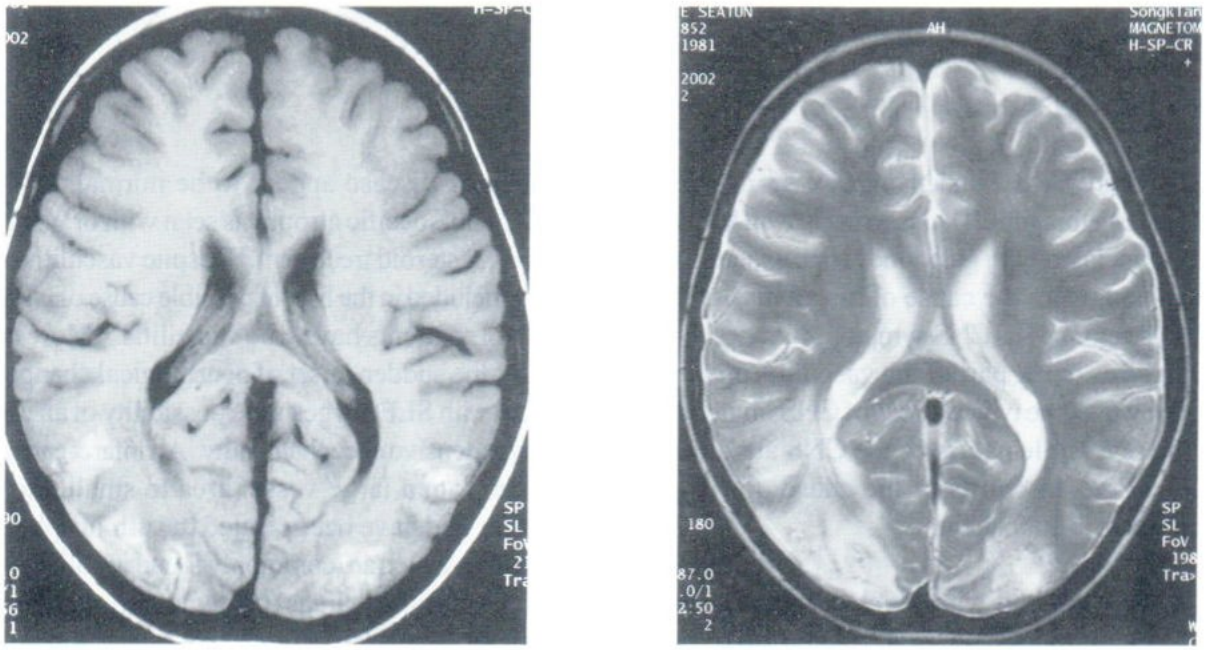

3a 3b

Fig.3 **a.** Axial SE T1W and, **b.** axial SE T2W images reveal marked resolution of the abnormal findings. However, small hemorrhagic foci along both occipital and parieto-occipital cortical gyri persisted.

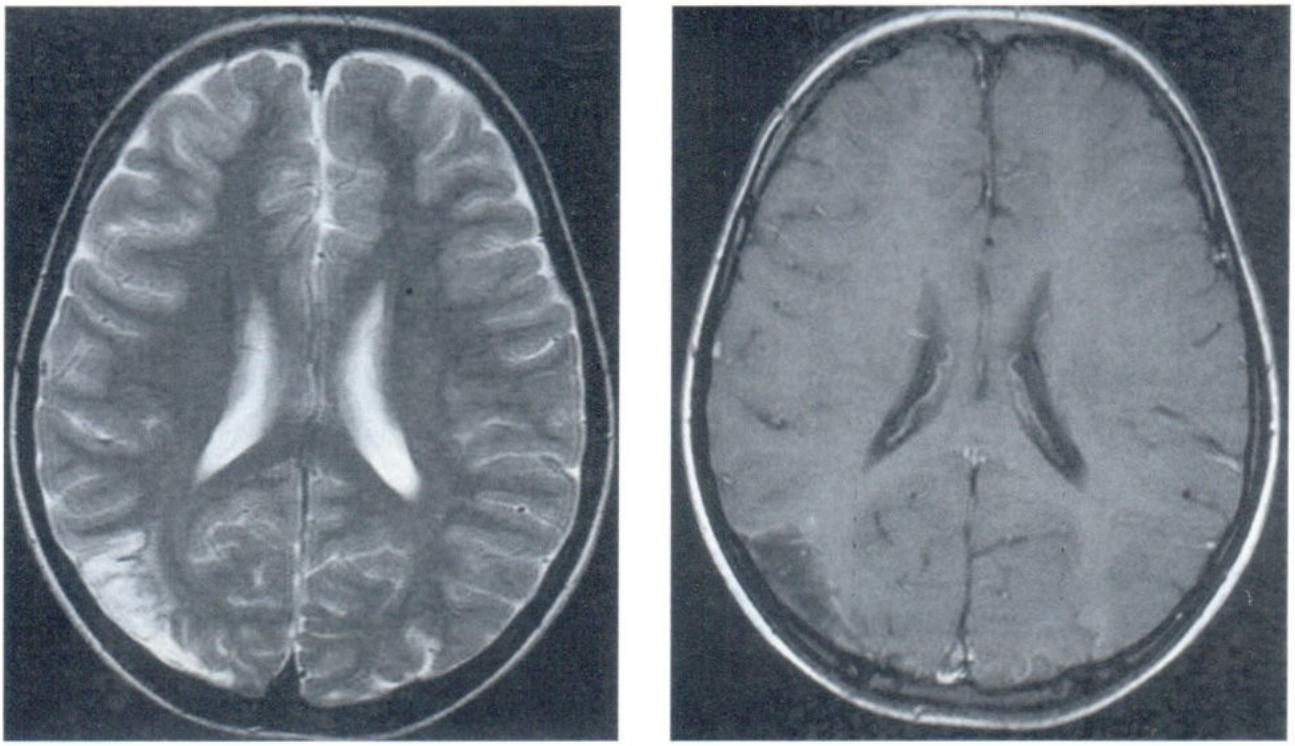

4a 4b

Fig.4 **a.** Axial SE T1w and, **b.** axial SE T2W images reveal no residual brain edema, but a few small areas of gliotic changes at the previous hemorrhage sites at the right parieto-occipital cortex.

DISCUSSION

This child had underlying diseases of SLE and alfa Thalassemia trait. Thalassemia is well known as being associated with gallstones such as seen in this patient and, were the cause of his admission for a cholecystectomy. His CNS symptoms were originally explained as being part of the vasculitis process in SLE. However the typical areas of CNS involvement and the reversible nature of the CNS abnormality excluded the vasculitis as the cause of the CNS involvement in this patient.

SLE patients who develop symptoms in the CNS system have been called Neuropsychiatric Systemic Lupus Erythematosus (NPSLE). The underlying pathological basis of brain damage is not yet clear. MRI scans in many patients with clinically confirmed disease appear to be normal. In other cases, non-specific atrophy is seen with or without a history of steroid treatment.[3] Despite vasculitis often being included in the lists of possible cause of NPSLE, few SLE patients have true vasculitis.[4] More commonly, the sudden onset of neurological change in a patient with SLE suggests the possibility of an infarct or hypertensive encephalopathy. An infarct can range in size from a large vessel area to small, lacunar infarcts, and have been related to antiphospholipid antibodies which are commonly found in patients with SLE.[4] Multifocal areas of edema, especially in the posterior cerebral hemispheres, are the result of hypertensive encephalopathy which is common in SLE due to associated renal disease. Imaging findings are similar to other conditions such as eclampsia.

CT and MRI images of this patients were typical for hypertensive encephalopathy and also correlated well with his high blood pressure (160/110 mmHg). The cause of hypertension was thought to be his renal disease (lupus nephritis). Areas of low density on the CT, and abnormal signal intensity on the MRI, were thought to be due to elevated blood pressure exceeding the autoregulatory capacity of the brain vasculature, typically seen in bilateral subcortical white matter of regions supplied by posterior circulation (occipital, parietal, posterior temporal).

However, it may also have involved the frontal lobes and corpus callosum. Although hemorrhagic foci are commonly encountered in autopsy studies,[5] they are infrequently seen in imaging except in patient with chronic hypertension[6-7] or thrombocytopenia[2] as in this patient. Contrast enhancement may also be seen in the region of signal abnormality in a small number of cases. Typically the clinical and imaging findings are reversible after control of blood pressure, and these imaging findings can establish a diagnosis without the need for a biopsy. Most of the brain lesions in this patient reversed to normal, except for a few small areas at the right parieto-occipital and occipital lobe, which showed a more severe degree of cortical hemorrhage than the other parts of the brain. Hemorrhagic foci seen in the image, to our knowledge, may have been the indicators of more severely brain damaged regions which were less likely to fully recover.

Diffusion weighted image may be normal supporting the concept of increased interstitial fluid in the white matter and not ischemia.[8-9] However, in cases of prolonged seizures or hypertension, frank ischemia or infarction may result.[4] Preliminary reports of perfusion MR images have shown preserved or increased perfusion in affected regions of the brain, where acute ischemia is associated with decreased perfusion.[10] Because a history of hypertension or seizure may not always present, the characteristic imaging findings should allow the radiologist to suggest the diagnosis and subsequent clinical management should be focused on the treatment of the hypertension and its underlying causes.[1] Follow up imaging in 1-2 weeks will usually show improvement.[2]

ACKNOWLEDGMENTS

We thank Dr. Wiwatana Tanomkiat for his kind suggestions during the preparation of this manuscript.

REFERENCES

1. Jones BV, Egelhoff JC, Patterson RJ(1997) Hypertensive encephalopathy in children. AJNR,18:101-106.
2. Nusbaum AO, Fung KM, Atlas SW (2002) White matter disease and inherited metabolic disorders. In: Atlas SW (eds) Magnetic Resonace Imaging of the brain and the spine. 3rd edn. Vol. 1 Lippincott Williams&Wilkins, Philadelphia, pp510-511
3. York DH Jr (2002) Magnetic resonance imaging of CNS disease, A teaching file. 2nd edn. Mosby, Missouri
4. Hart B, Sibbitt W, Kornfeld M, Schmidt P, Brooks W (2002) Neuropsychiatric Manifestations of lupus: Radiologic findings and pathological correlates; presented as a scientific exhibit at the 40 th Annual Meeting of the ASNR, Vancouver, Canada, May 13-17.
5. Richards A, Graham D, Bullock R (1998) Clinicopathological study of neurological complications due to hypertensive disorders of pregnancy. J Neurol Neurosurg Psychiatry, 51:416-421.
6. Sanders TG, Clayman DA, Samchez-Ramos L, Vines FS, Russo L(1991) Brain in eclampsia: MR imaging with clinical correlation. Radiology, 80:475-478.
7. Schwartz RB, Jones KM, Kalina P, et al (1992) Hypertensive encephalopathy: findings on CT, MR imaging, and SPECT imaging in 14 cases. AJR,159:379-383.

8. Schwartz RB, Mulkern RV, Gudbjartsson H, et al (1998) Diffusion weighted MR imaging in hypertensive encephalopathy: clues to pathogenesis. AJNR,19:859-862.
9. Coley SC, Poter DA, Calamante F, et al (1999) Quantitative MR diffusion mapping and cyclosporine-induced neurotoxicity. AJNR, 20:1507-1510.
10. Engelter SR, Petrella JR, Albert MJ, et al (1999) Assessment of cerebral microcirculation in patient with hypertensive encephalopathy using MR perfusion imaging. AJR, 173: 1491-1493.

ISOLATED NONCOMPACTION OF THE VENTRICULAR MYOCARDIUM

M. Puvaneswary[1] MB,BS ., F.R.C.R.

A.J. Hickey[2] M.D., F.R.A.C.P., M.R.C.P(UK)., D.D.U

SUMMARY

A case of isolated noncompaction of the ventricular myocardium with MRI findings is presented. MRI features and a review of published reports of noncompaction of the ventricular myocardium are briefly discussed.

Key words: magnetic resonance imaging: isolated noncompaction ventricular myocardium

CASE REPORT

A 59-year-old-female had a cardiac arrest in July 2002 and was resuscitated. She was admitted to the hospital for further investigation which revealed increased creatinine kinase(CK) and a raised Troponin. An electrocardiogram performed demonstrated T-wave changes in the anterolateral leads suggestive of an infarct.

The patient initially presented in 1994 with a history of palpitation of 12 months duration. Electrocardiogram (ECG) showed evidence of atrial fibrillation and the patient was commenced on Warfarin. She had a past history of hypertension for a period of 10 years. In June 2002, one month prior to her cardiac arrest , the patient presented with chest pain and had a stress test which was normal. There was no evidence of ischaemic changes and her ECG showed atrial fibrillation with normal complexes.

The left ventriculogram demonstrated sponge -like appearance of the non-compacted ventricular wall and diverticular configuration of the anterolateral wall (Fig1). There was mild hypokinesia of the noncompacted ventricular wall and there was apical akinesia. Coronary arteriogram demonstrated normal left main coronary artery, left anterior descending artery and circumflex artery. There was minor irregularities of the dominant right coronary artery with a 30% stenosis of the proximal third of the vessel. A probable diagnosis of noncompaction of the left ventricle with apical akinesia and diverticulae of the anterolateral wall and mild coronary artery disease was made.

Magnetic resonance imaging (MRI) was performed to confirm the diagnosis. Electrocardiography gated half fourier single shot turbo spin-echo (HASTE) sequences in the axial, coronal and sagittal planes, and T1-weighted fast spin-echo(FSE) and T2-weighted fast spin-echo (FSE) in the short-axis view and axial T2-weighted fast spin-echo and cine gradient-echo (GRE) sequences in the short-axis and four chamber view were performed.

Cine MRI demonstrated a thickened inner endocardial myocardium of prominent trabeculation

1 Department of Medical Imaging and
2 Cardiovascular Medicine John Hunter Hospital, N.S.W AUSTRALIA
Correspondence: Puvaneswary Dept.of Radiology Hunter Health Imaging Service John Hunter Hospital Locked Bag No1 Hunter Region Mail Centre N.S.W 2310 AUSTRALIA Ph: (02) 49213430 Fax: (02) 49213949

with deep intertrabecular recesses and a thin compacted epicardial myocardium.(Fig2A,B,C) IVNC involved the anterior, lateral and inferior segments from mid-ventricular level to the apex of the left ventricle. The largest trabeculation measured 2.6cm from the epicardial surface to the peak of the trabeculation, and 0.8 cm between the epicardial surface and trough of the trabecular recess. The ratio of the noncompacted/compacted myocardium was >2 which confirmed the diagnosis of IVNC. Cine gradient-echo sequences demonstrated hypokinesia of the left ventricular wall and there was a small focal area of thinned myocardium with akinesia of the apical lateral segment (segment16).

The T2-weighted sequences demonstrated a focal area of high signal intensity within the left ventricular cavity at the apex which was probably related to slow flow adjacent to a akinetic segment.

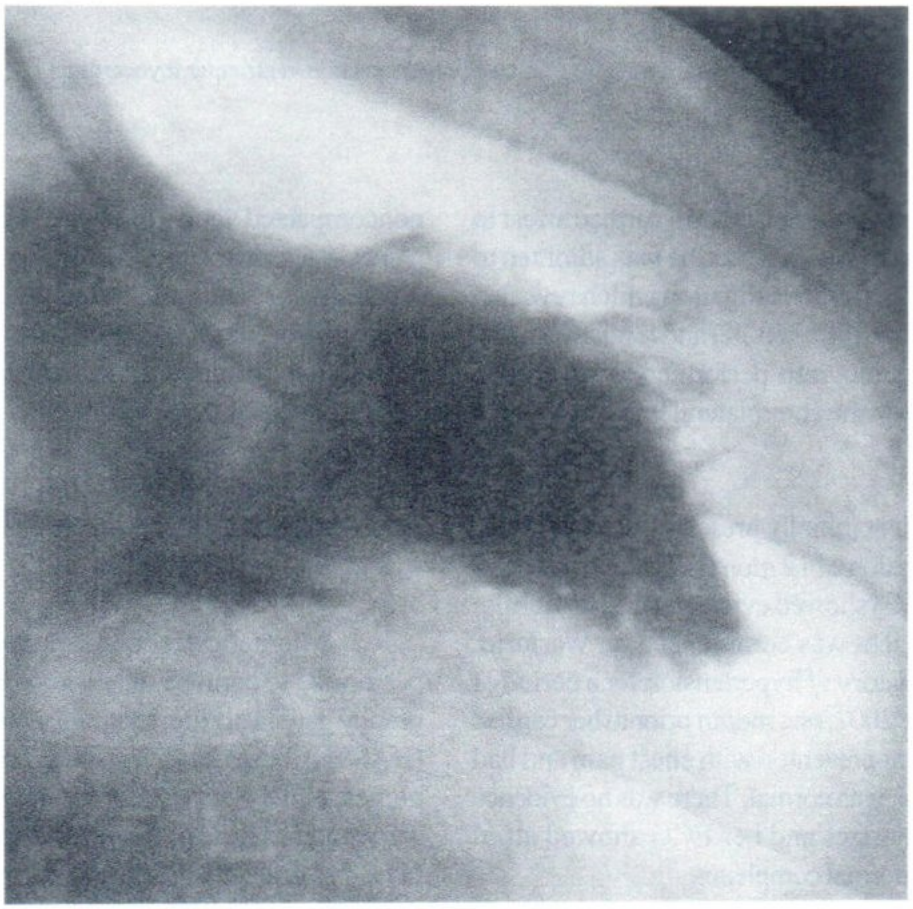

Fig.1 Left ventriculogram demonstrates sponge-like appearance of the non-compacted ventricular wall and diverticular configuration of the anterolateral wall.

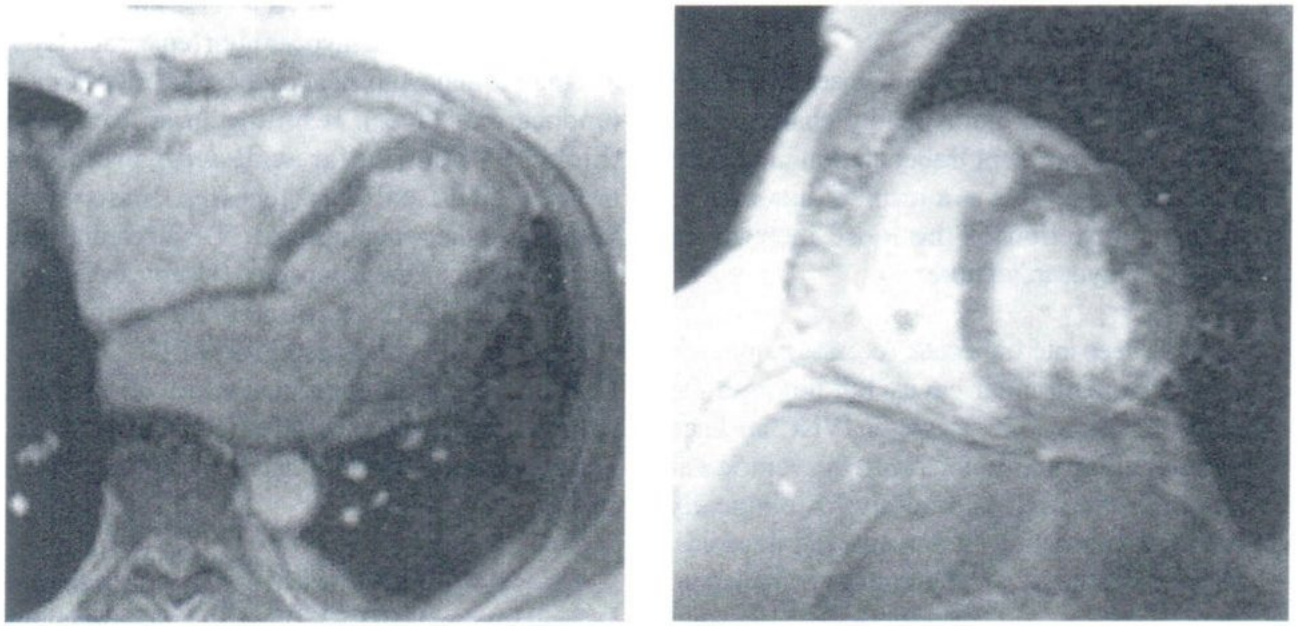

A B

Fig.2 **A)** axial GRE –image at the level of the mitral valve **B)** mid-ventricular short-axis view

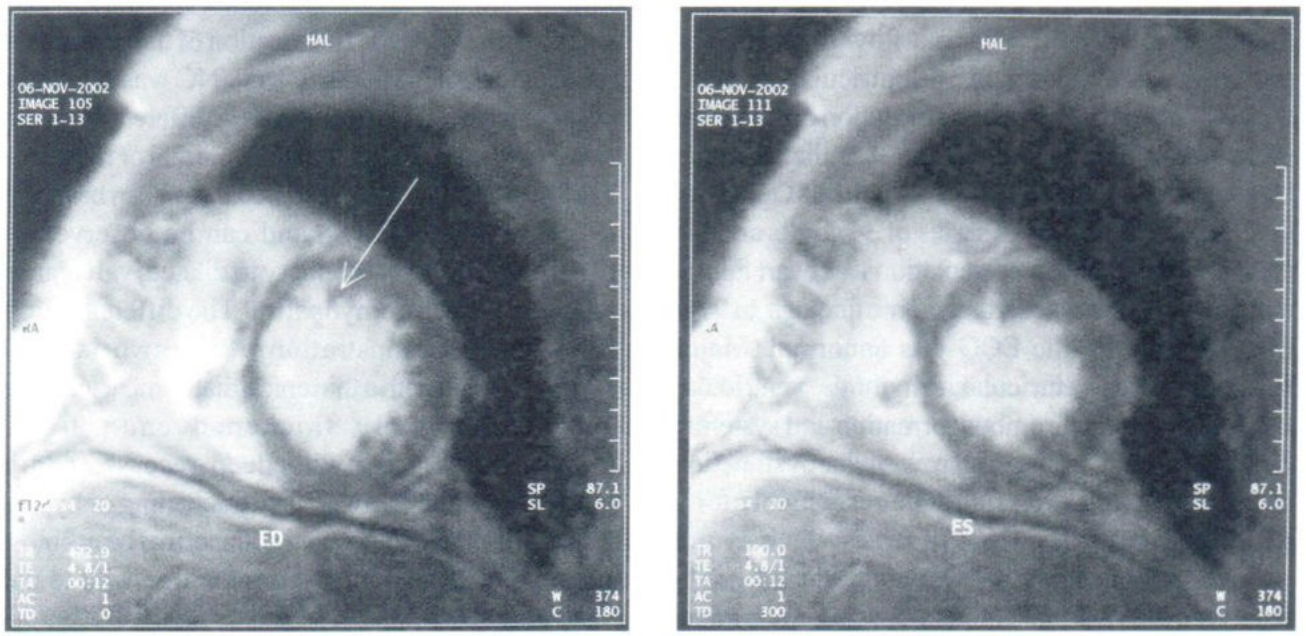

(a) (b)

Fig.2 **C)** short-axis view at the ventricular apex **(a)** end-diastolic **(b)** and end-systolic image demonstrates prominent trabeculations on the endo cardial surface of the left ventricle with deep intertrabecular recess filled with blood from the ventricular cavity.

DISCUSSION

Isolated ventricular noncompaction (IVNC) is a rare congenital cardiomyopathy characterised by numerous, prominent trabeculation and deep intertrabecular recesses as a result of intrauterine arrest of compaction of the loose interwoven meshwork of myocardial fibres.

The deep intertrabecular recesses communicate with the ventricular cavity but not with the coronary circulation. The recesses in IVNC are lined with endothelium continuous with the ventricular endocardial endothelium and are histologically different from persisting intramyocardial sinusoids, which are in continuity with the coronary circulation.

The ventricular noncompaction may occur in the left, right or both ventricles[1] and may be associated with other congenital cardiac malformation., including anomalous origin of the left coronary artery from the pulmonary trunk[2] and obstructive lesions of the left or right ventricular out flow tract, such as pulmonary atresia with intact ventricular septum.[3] Isolated left ventricular noncompaction occurs even more rarely.[4] The disorder may be familial and may be associated with facial dysmorphism.[4] Oechslin[5] et al reported the largest series of 34 adults and the most common clinical presentation was heart failure and characteristic echocardiographic findings. In 94% of their patients, the ECG was abnormal. Major cardiac risks are ventricular arrhythmia, ventricular hypokinesia with thrombus formation and systemic embolization. Coronary microvascular dysfunction associated with IVNC might be responsible for a decreased coronary flow reserve which is not confined to noncompacted segments, but extends to most segments with wall motion dysfuction and mural thrombus formation within the deep intertrabecular recesses abnormalities.[6]

The typical echocardiographic findings of noncompacted myocardium in IVNC is characterised by myocardium with extremely thickened, hypokinetic segments consisting of two layers. There is thin, compacted epicardial myocardium (epicardial layer) and thicker noncompacted endocardial myocardium (endocardial layer), resulting in an extremely thickened ventricular wall with prominent trabeculations and deep recesses. End-systolic thickness of the noncompacted (N) endocardial layer was thicker than the compacted (C) epicardial layer (ratio of $N/C \geq 2$). A ratio of noncompacted/ compacted ≥ 2 is diagnostic for IVNC. On colour Doppler imaging the trabeculation are both increased in prominence and excessive in number and deep recesses are filled with blood from the ventricular cavity.

IVNC is observed in one or more ventricular wall segments. In79% three and more segments were involved.[5] Most commonly, the apical and midventricular segments of both the inferior and lateral wall were affected in more than 80% of the patients and the midventricular anterior wall and septum and the basal segments was much less frequently involved.[5] The location of the prominent trabeculation in patients with IVNC was typically apical, inferior and lateral which is different from the prominent trabeculation found in normal or hypertrophied heart. Prominent LV trabeculation can be found in healthy hearts (68%) and can be observed in hypertrophic hearts secondary to dilated, valvular or hypertensive cardiomyopathy. The differentiation depends on demonstration of the two layered myocardial wall with a thin epicardial compacted zone and an extremely thickened endocardial noncompacted zone with deep recesses and a segmental rather than a diffuse thickening or hypertrophy. Prominent trabeculation in normal hearts most frequently (85%) course from the free wall to the ventricular septum.[7]

All noncompacted segments were hypokinetic. The normally compacted segments were occasionally hypokinetic despite normal wall thickness which was reflected by the impaired fractional shortening in 82%.[5] Oechlin et al[5] demonstrated

an enlarged left ventricular end-diastolic diameter (≥60 mm) in (67%), and reduced fractional shortening (<29%) and reduced left ventricular ejection fraction < 50% in 86% of their cases.

Cardiac catheterisation demonstrates normal left ventricular volume and increased left ventricular end-diastolic pressure, consistent with restrictive hemodynamic.[8] Hook et al[9] reported a case of IVNC presenting as restrictive cardiomyopathy. In contrast Chin et al found in their study decreased left ventricular systolic function similar to that of dilated cardiomyopathy. Discrepancy in the hemodynamic characteristic may represent the different stages of the disease process. The abundant trabecular network may limit distensibility of the left ventricle and cause restrictive hemodynamics.[8] Symptomatic patients with rapidly progressive clinical course may show hemodynamic properties similar to dilated cardiomyopathy, whereas asymptomatic patients may follow a slowly progressive course of restrictive hemodynamic physiology.

On left ventriculography Ichida et al[8] demonstrated the sponge-like appearance of the non-compacted ventricular wall during the diastolic phase and marked retention of the contrast material in the intertrabecular recesses during the systolic phase. In most of their cases, there was hypokinesia of the noncompacted ventricular wall and in one case diverticular configuration of the noncompacted ventricular wall was present.

Thallium-201 myocardial imaging[8] in 14 patients at rest demonstrated a hypoperfusion area in the left ventricle corresponding to the zones where noncompacted ventricular myocardium was localised.

Magnetic resonance imaging was able to distinguish inner zones of noncompacted myocardium from the thin outer zones of compacted myocardium. T2-weighted sequences revealed high signal intensity areas at the apex of the left ventricles in two cases, which thought to be due to disturbed microcirculation due to fibrosis, thrombus formation and hypokinesis of this area.[8]

Soler et al[10] reported the first case of first-pass MR perfusion imaging demonstration of subendocardial perfusion deficit at rest in the noncompacted myocardium of the anterior and septal walls and in the normal myocardium of the inferolateral wall.

ECG –gated spin-echo echo-planar images showed thickened myocardium and heterogeneous signal due to flow void areas. Fast gradient echo sequences demonstrated prominent trabeculations and typical blood-filled deep recesses.[10]

Compared to echocardiography MRI is less operator dependent and might be superior to echocardiography in case of impaired acoustic window and thrombus hidden in the sponge like myocardium of IVNC might not be detected.

Ichida et al[8] reported in computed tomography early defects and delayed enhancement of the noncompacted ventricular myocardium, implying fibrosis in this area. Endomyocardial biopsy demonstrated a wide range, interstitial fibrosis, endomyocardial thickening, subendocardial fibroelastosis, myocyte hypertrophy and intramural thrombosis.

Reported CT findings includes markedly thickened myocardium of the left ventricular wall with two zones of different attenuation. The thin outer portion of compacted myocardium consisted of uniform tissue attenuation iso-intense to that of muscle and an inner thicker layer composed of soft tissue attenuation of trabecular myocardium and contrast-enhanced ventricular blood filling the deep intertrabecular recesses.[11]

CONCLUSION

Isolated noncompaction of the ventricular

myocardium (IVNC) is a rare congenital cardiomyopathy with characteristic imaging findings and can be recognised on CT imaging. However it is suggested that MRI should be the modality of choice for diagnosis and follow-up of patients with IVNC.

REFERENCES

1. Junga G, Kneifel S, Smekal A.V, Steinert H, Bauersfeld U. Myocardial ischaemia in children with isolated ventricular non-compaction. European Heart Journal 1999; 20 : 910-916.
2. Dusek J, Ostadal B, Duskova M. Postnatal persistence of spongy myocardium with embryonic blood supply. Arch Pathol 1975; 99:312-317.
3. Feldt RH, Rahimtoola SH, Davis GD, Swan HJC, Titus JL. Anomalous ventricular myocardial pattern in a child with complex congenital heart disease. Am J Cardiol 1969; 23: 732-734.
4. Chin TK, Perloff JK, Williams RG, Jue K, Mohrmann R. Isolated noncompaction of left ventricular myocardium : a study of eight cases. Circulation 1990;82:507-513.
5. Oechslin EN, Attenhofer Jost CH, Rojas JR, Kaufmann PA, Jenni R. Long-term follow-up of 34 adults with isolated left ventricular noncompaction: A distinct cardiomyopathy with poor prognosis. J Am Coll Cardiol 2000;36: 493-500
6. Jenni R, Wyss CA , Oechlin EN. Isolated ventricular noncompaction is associated with coronary microcirculatory dysfunction. J Am Coll Cardiol 2002; 39:450-454.
7. Boyd MT, Seward JB, Tajik AJ, Edwards WD. Frequency and location of prominent left ventricular trabeculation at autopsy in 474 normal human hearts: implication for evaluation of mural thrombi by two-dimensional echocardiography. J Am Coll Cardiol 1987; 9:323-326
8. Ichida F, Hamamichi Y, Miyawaki T, Ono Y, Kamiya T, AkagiT, Hamada H et al. Clinical features of isolated noncompaction of the ventricular myocardium. J Am Coll Cardiol 1999;34:233-240
9. Hook S, Ratliff NB, Rosenkranz E, Sterba R. Isolated noncompaction of the ventricular myocardium. Pediatr Cardiol 1996;17:43-45.
10. Soler R, Rodriguez E, Monserrat L, and Alvarez N. MRI of subendocardial perfusion deficits in isolated left ventricular noncompaction. J of Computed Assisted Tomography 2002;26 :373-375.
11. Conces DJ, Ryan T, Tarver RD. Noncompaction of ventricular myocardium:CT appearance. AJR 1991; 156:717-718.

IMAGING OF NEONATAL HYDRONEPHROSIS

Dr. M. A. Taher

ABSTRACT

We found 4 babies of age range 46 days to 6 years suffering from hydronephrosis as confirmed by ultrasonography. The older boy and the girl also had a radionuclide renogram under computerized gamma camera using technetium 99 metastable diethylenetriamine pentaacetic acid (Tc 99mm DTPA). The younger boy had a posterior urethral valve causing bilateral hydronephrosis and was improved by uro-surgical procedure as shown by clinical and sonographic follow-up.

Key words Kidney, Ultrasound, Radionuclide renogram.

INTRODUCTION

Since most neonates are dehydrated and renal function is not optimal in the neonate, early imaging may underestimate the amount of obstruction present.[1] Instead, postnatal ultrasound should be performed at the end of the first week of life. If the renal pelvis continues to measure greater than 10 mm, we refer our patients to a pediatric surgeon or urologist. Although significant congenital hydronephrosis may result from vesico ureteral reflux, the usual cause is urinary tract obstruction. The most common site of obstruction is the ureteropelvic junction, followed by the ureterovesical junction.[2] Bladder outlet obstruction is often an obvious ultrasound diagnosis since the markedly enlarged, thick walled bladder is readily seen. A variable degree of hydronephrosis is usually also seen. Bladder outlet obstruction occurs most commonly in male fetuses who are subject to the development of posterior urethral valves, and these bladders often fill the fetal abdomen. The proximal urethra is usually dilated as well, giving the bladder a pear or keyhole shape. Renal findings vary in fetuses with posterior urethral valves. In some cases, the kidneys are markedly hydronephrotic but otherwise normal in appearance. At the opposite extreme, the kidneys are small and echogenic, secondary to obstruction-induced cystic dysplasia. Complete bilateral urinary tract obstruction occuring in utero is fatal in postnatal life, and in some cases intervention in utero is attempted. Bladder drainage with urinary electrolyte analysis (for prognostic purposes), and placement of vesico-amniotic shunts (when renal function seems reasonable) have been attempted with variable success.[3] Hydronephrosis can be caused also by congenital obstruction of the ureteropelvic junction (PUJO), by ureteric stenosis or a calculus or from external pressure on the ureters by a retroperitoneal or abdominal mass.[4]

CASE REPORTS

CASE 1

A boy of age 46 days was brought to this centre with the complaints of dribbling narrow stream of urine and swelling of lower abdomen. Ultrasonography (USG) revealed distended urinary bladder and bilateral hydronephrosis. The baby was operated for removal of posterior urethral valve and was improved

Director, Centre for Nuclear Medicine & Ultrasound, Post Box No.-16, Rangpur 5400, Bangladesh

clinically as well as sonographically upto six months of age. Long-term follow-up is being done.

CASE 2

A boy of age 5 months was sent to this centre with a palpable lump in left loin. The referring physicians asked for sonogram. Findings show normal right kidney and hydronephrotic left kidney. A radionuclide renogram was requested by the uro-surgeon, which revealed normally functioning right kidney and obstructive features in left arterial and secretory phases are depressed, and clearance is very slow (Figure 1).

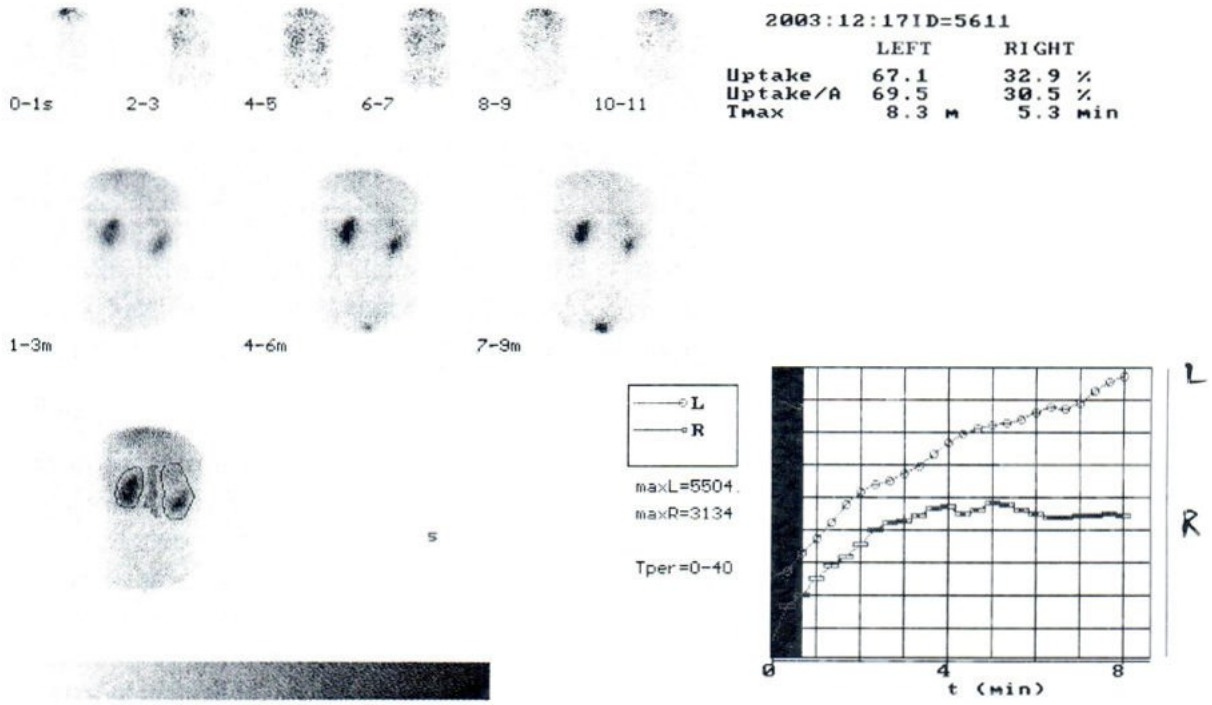

Case 2: Fig. 1 Renogram showing left renal obstruction.

CASE 3

A girl of age 6 years was sent to us by a pediatric surgeon for renogram. According to her father's statement she had a lump on right side of abdomen since birth and it was growing gradually. Ultrasonography revealed grossly obstructed right renal tract (hydronephrosis and hydroureter) without any calculus and normal-looking left kidney. Tc 99m DTPA renogram revealed a normally functioning left kidney and non-functioning right kidney (Fig. 2) all phases of renal functions are grossly depressed in the right side.

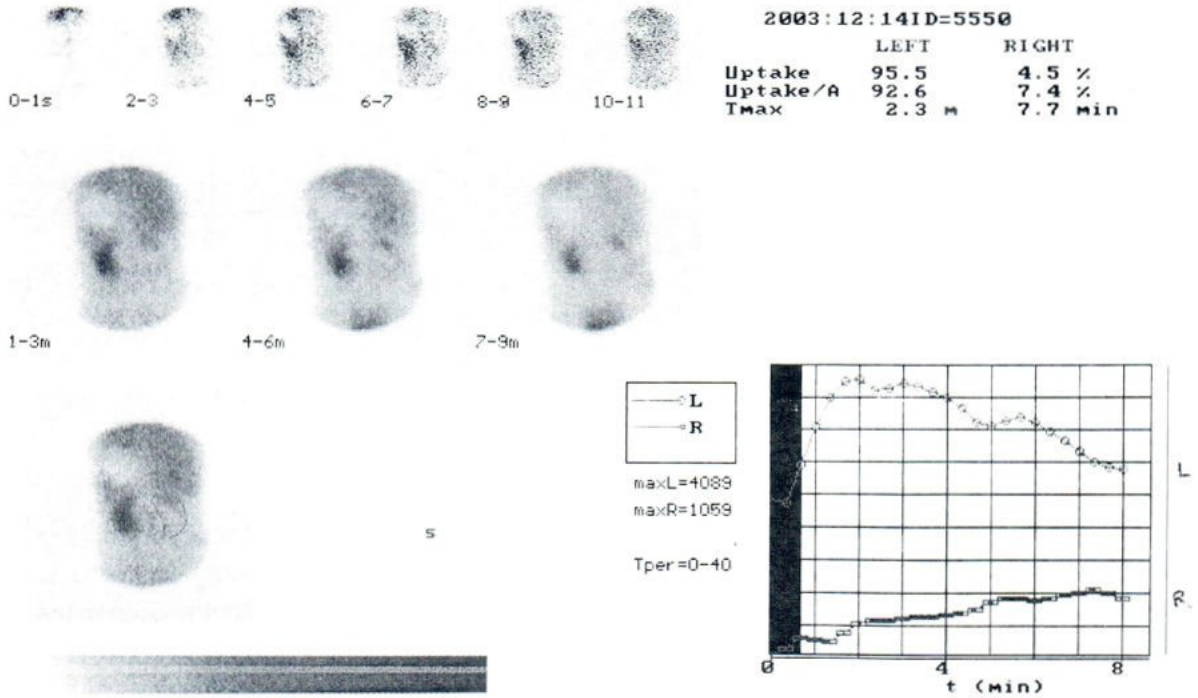

Case 3: Fig. 2 Renogram showing non functioning rt. kidney.

CASE 4

A boy of age 2 years 6 months was sent to us by a pediatric surgeon for renogram. His father had nephrectomy for hydronephrosis 3 years previously. The boy's mother noticed a lump in his abdomen since birth, and USG on 29 Oct. '03 showed congenital hydronephrosis on the left side. Tc 99m DTPA renogram showed normally functioning right kidney and a swollen faint ring in the region of left kidney suggestive of poor functioning (Figure 3). The baby could not have pyeloplasty, however, he had left-sided nephrectomy in Oct. 2004.

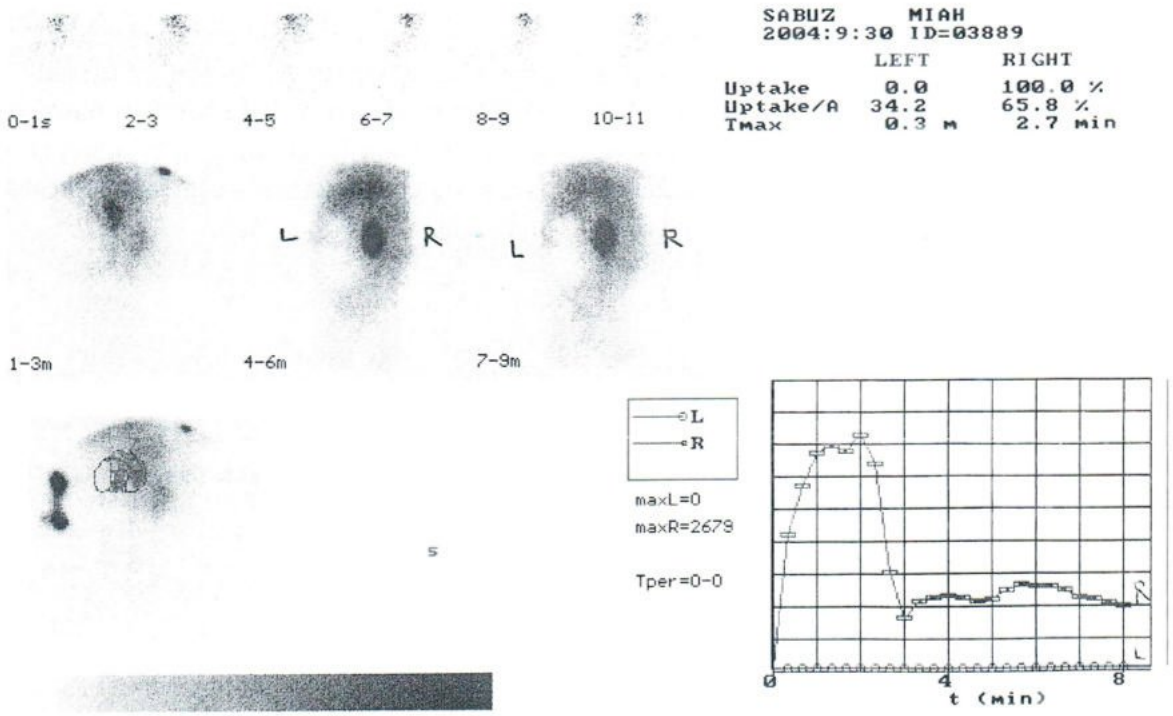

Case 4: Fig. 3 DTPA Renogram

DISCUSSIONS

Ultrasound is popular and safe imaging modality in the neonates, as it is non-invasive and non-ionizing in nature. Radionuclide renogram is much less risky than intravenous urography (IVU),however, its interpretation is sometimes difficult,--failure to visualize a kidney by Tc 99m DTPA does not preclude recoverable renal function.[5] A case of calcification of the arteries and obliterative endarteritis associated with hydronephrosis in a child aged six months was reported by Bryant and White in 1901.[6] Complications of idiopathic arterial calcification of infancy include hematuria, hypertension, congestive cardiac failure and nonimmune hydrops.[7] This condition is usually fatal,[8] although spontaneous resolution of the calcification has been reported in one survivor.[9] A good news is that sonographic mild pyelectasis is seen in 3% of normal fetuses.[10] Although anatomic severity of hydronephrosis can be detected in utero by USG, relative functional renal impairment, important for surgical planning, cannot be determined without postnatal renal radionuclide scans.[11] Serial assessment of renal function forms an important aspect of pediatric urology, particularly in children with hydronephrosis, vesicoureteral reflux and chronic pyelonephritis who may require repeated evaluation both pre and post-operative.[12] In a child under 2 years of age the injection is via a pedal vein so that we may evaluate the possibility of inferior vena cava (IVC) occlusion. The child must not perform the Valsalva during the injection or the IVC will be occluded due to increased physiological intra-abdominal pressure.[13] Homsy et al showed that diuresis renograms performed in early infancy correlated poorly with follow up examination at 3 at 6 months and suggested that the wash-out response on the initial examination should not be used to determine the need for

surgery.[14] Therapeutically Koff and Campbell concluded that most infants whose hydronephrosis was discovered by prenatal ultrasound could be managed non-operatively.[15] Gordon et al questioned the role of surgery because many neonatal hydronephrotic kidneys improved spontaneously and those that did have surgery did not show significant functional improvement.[16]

Since 85% to 90% of affected neonates may appear entirely normal on physical examination, prenatal detection of ureteropelvic junction obstruction permits early therapy of a correctable lesion that may otherwise remain unrecognized for years.[17] Obstruction frequently occurs at the ureteropelvic junction, the site of the first bifurcation of the ureteral bud. This represents the most common cause of neonatal hydronephrosis.[18] Dilatation of the fetal urinary tract is increasingly being recognized with the wide-spread uses of fetal scanning, sophistication of ultrasound equipment and greater expertises. The pediatrician is often faced with managing infants with asymptomatic hydronephrosis, which was detected in utero. In most instances, mild to moderate dilatation of renal pelvis resolves after birth. However, all such babies should be carefully investigated to exclude urinary tract obstruction and vesico-ureteric reflux. There is considerable debate regarding optimal management of patients with antenatally diagnosed hydronephrosis.

Antenatal hydronephrosis is the dilatation of the collecting system of the fetal kidney. Dilatation of the ureter may be associated. It is estimated that fetal urinary tract dilatation is identified in 1% of all pregnancies. In more than 50% cases, the antenatally detected dilatation is transient and resolves spontaneously. Antenatally detected dilatation, which persists after birth is labeled as neo-natal hydronephrosis. Pelviureteric junction (PUJ) obstruction accounts for 50-60% patients with neonatal hydronephrosis. Vesicoureteric reflux (VUR) is detected in 20-30% of such cases. It sometimes may be difficult to differentiate multicystic dysplastic kidney from hydronephrosis.

Fetal hydronephrosis of moderate degree can be detected as early as 15-18 weeks' gestation by ultrasonography. A maximum anteroposterior diameter of renal pelvis of more than 10 mm or the ratio of antero-posterior diameter of renal pelvis to kidney of more than 0.5 after 30 weeks gestation requires postnatal evaluation. Oligohydramnios indicates severe urinary flow obstruction that may be seen in fetuses with severe bilateral hydronephrosis and posterior urethral valves. A pediatric nephrologist or urologist should be consulted for such cases.

The indications for performing bio-chemical investigations on fetal urine are limited. Similarly, the criteria for fetal intervention are very few.[19]

ACKNOWLEDGEMENTS

We are grateful to Dr. Baharul Elem MBBS, FRCS and Dr. Fakhrul Islam MBBS Ph.D. (surgery) and Prof. Dr. M. Rezaul Islam MBBS, MS (Ped. surg.) for their wholehearted cooperations and valuable opinions.

REFERENCES

1. Laing FC, Burke VD, Wing VW et al: Postpartum evaluation of fetal hydronephrosis: Optimal timing for follow-up sonography. Radiology 152: 423- 424, 1984.
2. Brown T, Mandell J, Lebowitz RL: Neonatal hydronephrosis in the era of sonography. AJR Am J Roentgenol 148: 959-963, 1987.
3. Sohaey R. The fetal genitourinary system, In Zwieble WJ and Sohaey R: Introduction to Ultrasound 1998, Philadelphia,WB Saunders Co.
4. Palmer PES. Manual of diagnostic ultrasound. 2002 Geneva. WHO, & WFUMB (New Millenium Edition).

5. Taher MA. Failure to visualize a multicystic kidney with Tc99m-DTPA does not preclude recoverable function. ASEAN J Radiol IX : 77-78, 2003
6. Bryant JH, White WA. A case of calcification of the arteries and obliterative endarteritis associated with hydronephrosis in a child aged 6 months. Guys Hosp Rep 55: 17-28, 1901.
7. Nagar A M, Hanchate V, Tandon A, Thakkar H, Chaubal NG. Antenatal detection of idiopathic arterial calcification with hydrops fetalis. J Ultrasound Med 22: 653- 659, 2003.
8. Samon LM, Ash KM, Murdison KA. Aortopulmonary calcification: an unusual manifestation of idiopathic calcification of infancy evident antenatally. Obstet Gynecol 85: 863-865, 1995.
9. Marrott PK, Newcombe KD, Becroft DM, Freidlander DH. Idiopathic infantile arterial calcification of infancy with survival to adult life. Pediatr Cardiol 5: 119-122, 1984.
10. Dremsek PA, Grindl K, Voitl P, et al: Renal pyelectasis in fetuses and neonates: Diagnostic value of renal pelvis diameter in pre-and postnatal sonographic screening. AJR 168: 1017, 1997.
11. Kleiner B. Callen PW. Filly RA. Sonographic analysis of the fetus with ureteropelvic junction obstruction. AJR. 148: 359-363, 1987.
12. Gilday DL, Special clinical problems in pediatrics. In Maisey MN, Britton KE, Gilday DL (eds.): Clinical Nuclear Medicine, London, Chapman and Hall, 331- 3643, 1983.
13. Mc Donald P, Tarar R, Gilday DL et al. Some rediologic observations in renal vein thrombosis. Am J Roentgenol 120: 368, 1974.
14. Homsy YL, Williot P, Danais S. Transitional neonatal hydronephrosis: fact or fantasy. J Urol 136: 339-341, 1986.
15. Koff SA, Campbell K. Nonoperative management of unilateral neonatal hydronephrosis. J Urol 148: 525-531, 1992.
16. Gordon I, Dhillon HK, Gatanash H, Peters AM. Antenatal diagnosis of pelvic hydronephrosis: assessment of renal function and drainage as a guide to management. J Nucl Med 32: 1649-1654, 1991.
17. Grignon A, Filiatrault D, Homsy Y et al. Ureteropelvic junction sterosis: Antenatal Ultrasonographic diagnosis. Postnatal investigation and follow-up. Radiology 160:649, 1986.
18. Lebowitz RL, Griscomb NT: Neonatal hydronephrosis-146 cases. Radiol Clin North Am 15:49, 1971.
19. Herndon CD, Ferrer FA, Freedman A, McKenna PH. Consensus on the prenatal management of antenatally detected urological abnormalities. J Urol, 164: 1052-1056, 2000.

CHOLESCINTIGRAPHY IN THE DIAGNOSIS AND FOLLOW UP OF HEPATOBILIARY INJURY

CHOTIPANICH Chanisa,[1] STATES Lisa[2]

Cholescintigraphy is used as a diagnostic procedure in children with suspected biliary trauma. It is a simple and reliable way to detect a liver injury accompanied by biliary leakage and is well suited to assess the effectiveness of treatment and to follow recovery. A case of nonpenetrating bicycle handlebar injury emphasizes these points.

Key Words: Cholescintigraphy, Bicycle handlebar, Hepatobiliary Injury

Cholescintigraphy with Tc-99m iminodiacetic acid analog (Tc-99m IDA) is a well-established hepatobiliary imaging method. It is a non-invasive technique, capable of identifying function and morphologic abnormalities of the liver and biliary tract. Currently, its principal role is evaluating adults with suspected acute cholecystitis. There are only a few references to its diagnosis capabilities in children[1-3] with injuries to the liver and biliary tract.[4-7] This report will discuss the role of cholescintigraphy and CT in treating a patient with hepatobiliary tract injury following blunt trauma.

CASE REPORT

A 12-year-old boy was admitted to the hospital as an emergency patient after he fell from his bicycle and fell on the handlebar. He complained of chest pain and vomiting. On admission, his vital signs were stable. Physical examination showed tenderness of the upper right abdomen. His hemoglobin and hematocrit were 13.9 g/dl and 41.1%. Liver enzymes were abnormal (Fig 1); however, chest x-rays were normal. Computed Tomography (CT) revealed a laceration of the liver (Grade III) adjacent to the falciform ligament with free fluid surrounding the liver (Figure 3). Therefore, cholescintigraphy with Tc-99m IDA was performed to evaluate the possibility of bile leakage (figure 2). Serial images demonstrated an area of radioactive retention at the site of laceration in the right lobe of the liver, previously noted on the CT scan. This finding was thought to represent bile leakage caused by the hepatic laceration. The patient was treated with octreotide injection. On the seventh post octreotide injection day, cholescintigraphy was epeated to evaluate effectiveness of treatment and to follow recovery. There was no further leak (figure 4), so the patient was discharged.

[1] Division of Nuclear Medicine, Department of Radiology, Faculty of Medicine, Ramathibodi Hospital, Mahidol University, Thailand
[2] The Children's Hospital of Philadelphia, University of Pennsylvania, Pennsylvania, United States of America

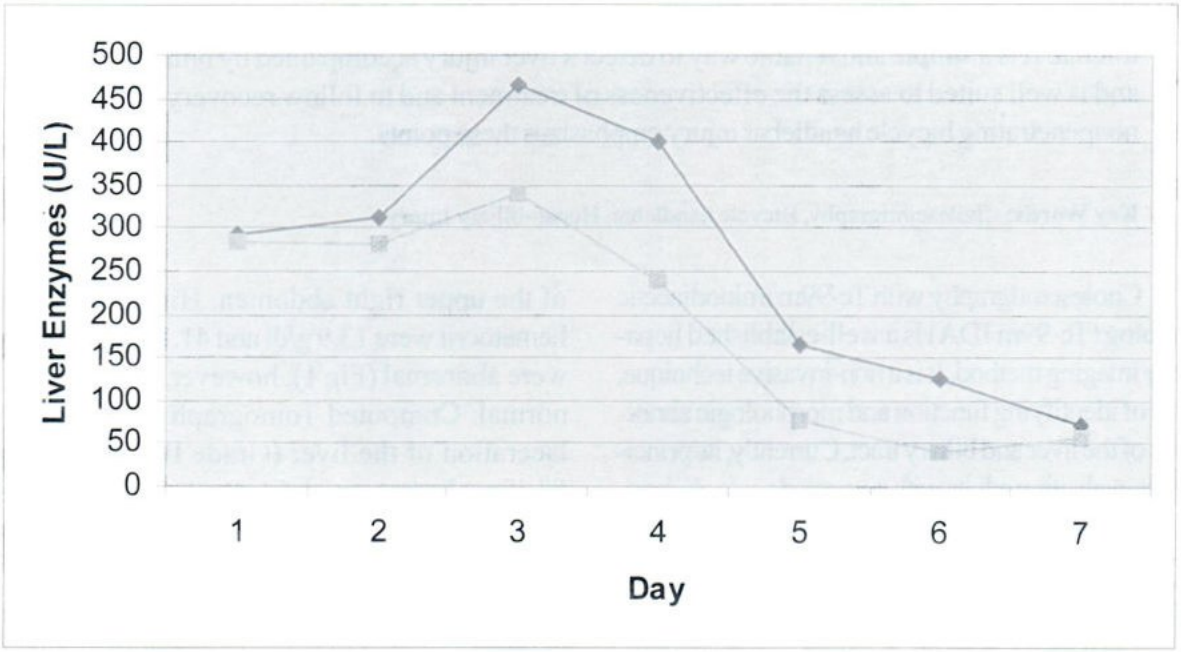

Figure 1. Biochemical findings in the patient during liver injury and its subsequent octreotide injection. (Black line is alanine aminotrasferase (ALT); White line is aspartate aminotransferase(AST); first day, after trauma; seventh day, post octreotide injection since 7 day and repeated cholescintigraphy)

A. 5 min B. 15 min C. 25 min

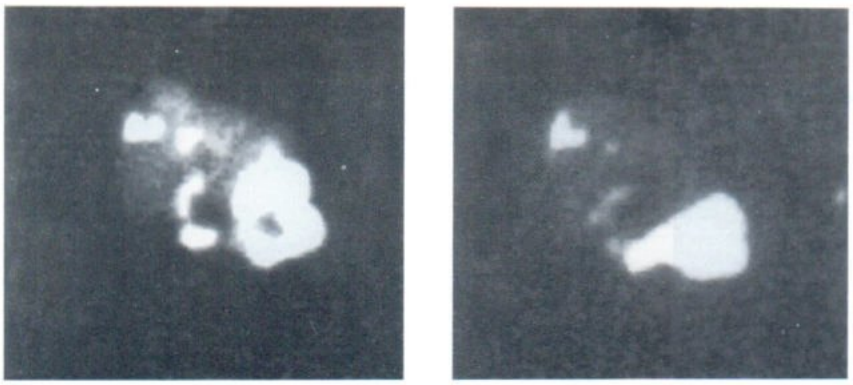

D. 30 min E. 60 min

Fig 2. Cholescintigraphy after trauma showed bile leakage located (arrow) at the site of the right lobe of liver.

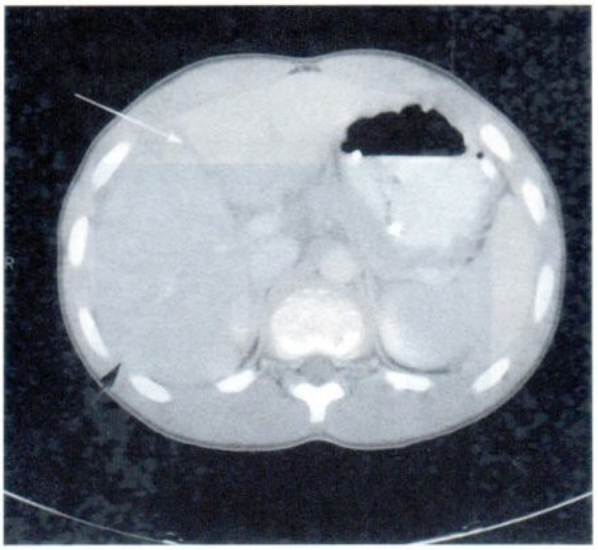

Fig 3. Computed tomography (CT) of the patient after trauma showed liver laceration adjacent to the falciform ligament (white arrow) and hemoperitoneum (thin layer surrounding the liver, black arrow)

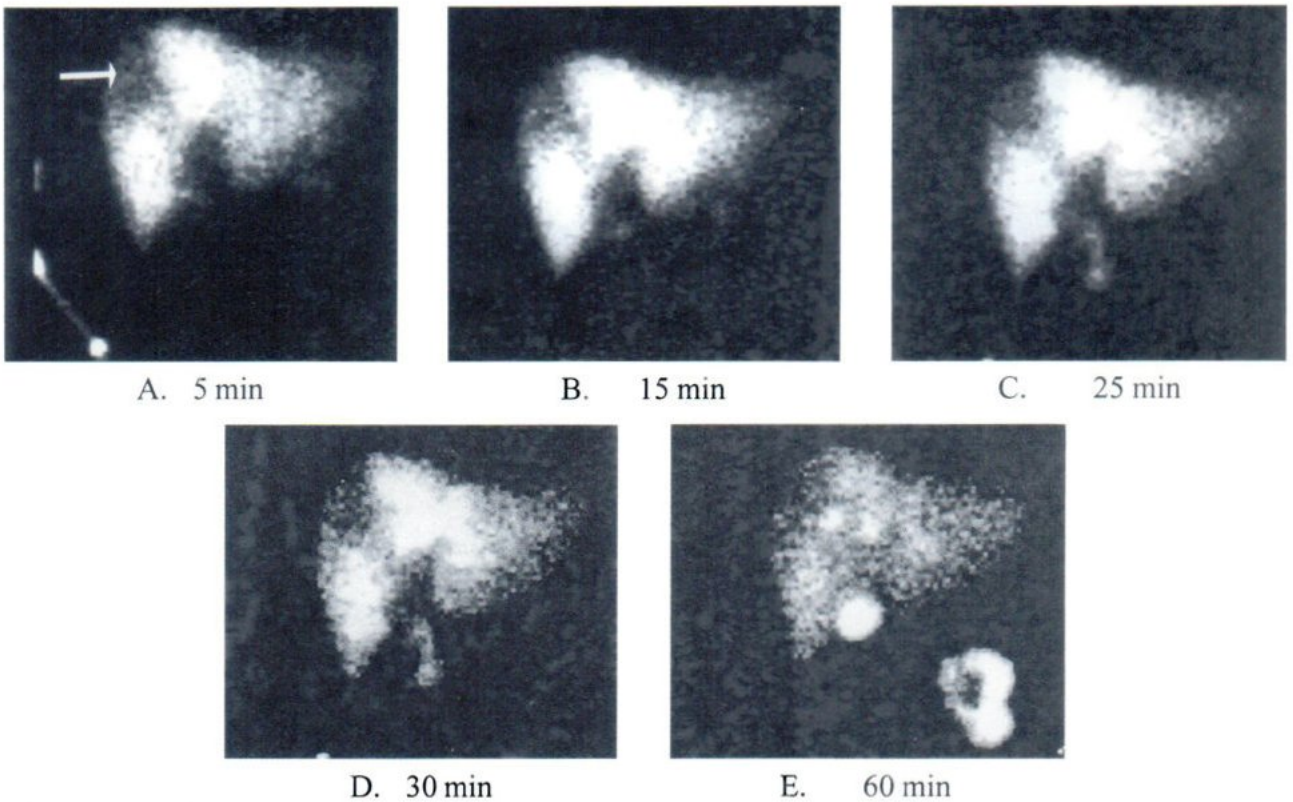

Figure 4. Cholescintigraphy done on the seventh day after octreotide injection: There is resolution of bile leakage. Large photon-deficiency area (arrow) is noted in the area of the known liver laceration of the right lobe of the liver, possibly due to parenchymal loss secondary to infarction or fibrosis. The value of serum liver enzymes decreased at this time.

DISCUSSION

An accurate evaluation of the injury has become increasingly important. The liver is the most commonly injured solid abdomen organ and now non -operative management in hemodynamically stable children has become the standard.[8-14]

In most cases, documenting the presence and the extent of the bile leakage is difficult in a child. The use of radiographic contrast media to identify this abnormality is usually hampered by overlying gas and ribs[15] and the inability of the child to cooperate.[16] Due to these limitations, a variety of imaging techniques have been employed to evaluate biliary trauma. Computed tomography (CT) and ultrasonography (US) are clinically useful procedures to evaluate hepatic injuries. The major advantage with these high-resolution modalities is that sensitivity methods of detecting intraabdominal fluid collection and other abdominal viscera and the retroperitoneum can be assessed simultaneously. Their main limitation, however, is that they are not able to demonstrate an active bile leak.[17] By comparison, cholescintigraphy yields information physiologically and characterizes the fluid as active bile. Furthermore, the Tc-99m IDA scan can provide information regarding the status of the hepatic capsule. If the integrity of the capsule is preserved, the bile leak will be confined. Disruption shows leakage of the bile into the peritoneal activity. It is important to realize that a bile leak is not an indication for surgery, since small leaks frequently clear spontaneously.

The presented case confirms the diagnostic value of cholescintigraphy in bile leakage and adds a new dimension to the ability to assess effectiveness of treatment and follow up the recovery of the patient. The rise in the blood level of the liver enzymes was clearly relative to the acute injury of the liver cells (Figure1). By the seventh post octreotide injection day, the value of serum alanine aminotransferase and aspartate aminotransferase decreased from 292 U/L to 72 U/L and 285 U/L to 56 U/L respectively and the scan showed no further leakage (Fig 4).

In conclusion, Tc-99m IDA cholescintigraphy has proved to be one of the most sensitive and highly specified tests that are available for the detection, the presence or absence of biliary leakage in the post traumatic setting. The simplicity and ease of performing cholescintigraphy as well as the relatively low radiation exposure and lack of morbidity, making radionuclide imaging ideally suited for the performance of serial studies, as the patient's clinical condition deems necessary. Therefore, IDA scan should be in cluded in the management protocol of all patients with the initial CT scan to confirm liver trauma graded as " major".[18]

ACKNOWLEDGEMENT

The authors would like to thanks the International Atomic Energy Agency (IAEA), as providing the fellow scholarship at the University of Pennsylvania Medical Center.

REFERENCES

1. Miller JH, Sinatra FR, Thomas DW. Biliary excretion disorders in infants: evaluation using 99mTc-PIPIDA. AJR 1980; 135: 47-52.
2. Majd M, Reba RC, Altman RP. Hepatobiliary Scintigraphy with 99m Tc - PIPIDA in the evaluation of neonatal jaundice. Pediatrics 1981; 67:140-5.
3. Sty JR, Babbitt DP, Boedecker RA, et al. (1979) 99m Tc-PIPIDA biliary imaging in children. Clin Nucl Med 1979; 4: 315-24.
4. Caride VJ, Gibson DW. Noninvasive evaluation of bile leakage. Surg Gynecol Obstet 1982; 154: 517-20.
5. Lecklitner ML, Dittman W. Postoperative evaluation of penetrating hepatic trauma and complications. J Nucl Med 1984; 25: 982-3.

6. Mc Pherson GAD, Collier NA, Lavender JP, Blumget LH. The role of HIDA scanning in the assessment of external biliary fistulae. Surg Gastroenterol 1984; 3: 77-80.
7. La Manna MM, Korsrik HE, Parker JA. Subcapsular bile leak following percutaneous drainage. Clin Nucl Med 1984; 9: 588-9.
8. Stone HH, Ansley JD. Management of liver trauma in children. J Pedia Surg 1977; 12: 3 10.
9. Grison ER, Gauderer MWL, Ferron J, et al. Nonoperative management of liver injuries following blunt abdominal trauma in child. J Pedia Surg 1984; 19: 515-8.
10. Learp MP, Looner DR, Prosga, et al. The nonoperative management of pediatric hepatic trauma. J Pedia Surg 1983; 18: 512-8.
11. Losty PD, Okoye BO, Walter DP, et al. Management of blunt liver trauma in children. Br J Surg 1987; 84: 1006-8.
12. Giacomantonio M, Filler RM, Rich RH. Blunt hepatic trauma in children: Experience with operative and nonoperative management: J Pedia Surg 1984; 19: 519-22.
13. Galat JA, Grisoni ER, Gauderer MW. Pediatric blunt liver injury: Establish of criteria for appropriate managements. J Pedia Surg 1990; 25: 1162-5.
14. Rossi D, de Ville de Goyet J, Clemet de Cletys, et al. Management of Intra-abdominal organ injury following blunt abdominal trauma in children. Int Care Med 1993; 19.
15. Henzel JH, Blessing WD, Deweese MS. Intrahepatic biliary disruption, report of two cases occuring during use of balloon-tipped biliary catheters. Arch Surg 1971; 102: 218-20.
16. Eikman EA, Cameron JL, Colman, et al. A test for potency of the cystic duct in acute cholecystitis. Ann Intern Med 1975; 82: 318.
17. Weissman HS, Chin KJ, Frank M, et al. Demonstration of traumatic bile leakage with cholescintigraphy and ultrasonography. AJR 1979; 133: 843-7.
18. Sharif K., Pimpalwar A.P., John P., Johnson K., Donnell S., and de ville de Goyet. Benefits of Early Diagnosis and Presumptive treatment of Biliary tract complications after Major Blunt Liver trauma in children. J Pedia Surg 2002; 37: 1287-92.

COMMUNICATIONS:

1. HALF-FILLED BLADDER FOR PELVIC SONOGRAMS

Dr. M. A. Taher

Since 1981, we are performing pelvic sonograms, but we never used enema or frusemide tablet or injection to fill the urinary bladder, however, we encouraged the patients to drink water prior to pelvic sonogram and in many occasions, we perform pelvic sonograms before and after micturition to avoid confusions regarding any cyst or placenta previa. Therefore, we do agree with Benacerraf,[1,2] however, many of our centres do not have transvaginal sonography or Doppler imaging. Benacerraf et al. studied 206 patients undergoing pelvic sonography and found that transvaginal scans alone were sufficient to visualize all findings in 172 patients (83.5%). An additional transabdominal component through an empty bladder was necessary to fully evaluate another 31 patients (15.1%). The full-bladder technique was beneficial to only 3 patients (1.5%). However, whether these 3 patients benefited from the full bladder scan was debatable, because the only additional finding was a normal ovary. Their study showed that the transabdominal scan with the empty bladder was indeed important particularly for evaluating enlarged uteri and masses high in the pelvis. These organs were easily visualized by a transabdominal approach with mild pressure applied by the sonographer or sonologist. Tessler et al. also showed that in patients undergoing transvaginal scans, the transabdominal full-bladder technique only resulted in the identification of normal ovaries, thus not altering patient outcome.[3] Hill and Breckle [4]suggested that the postvoid transabdominal scan of the pelvis is helpful in visualizing a high-riding ovary, which may have been pushed out of view by the full bladder. Wayne Persutte and Roger Lenke wrote an article on filling of the bladder for pelvic sonograms and it was presented at the Society of Perinatal Obstetricians meeting in 1988. Their original study was performed after a questionnaire showed that compared with having amniocenthesis, most patients said that the full bladder was more uncomfortable.[5] Lenke of Indiana Center for Prenatal Diagnosis (USA) reviewed a case in which the full bladder approach resulted in the death of both the mother and her fetus. The patient was admitted with undiagnosed severe preeclampsia, ultrasonography was ordered, she was given several glasses of water and her intravenous line was opened. Because she was in renal shutdown her bladder would not be filled, but pulmonary edema developed, and both she and the fetus died. Lenke now tells patients going to other offices to not fill their bladder but, rather than argue with the sonographers, they should just tell them that their bladder is full.[6]

For prostate exam we like to have sonograms both before and after micturition to know post-void residue.

Director, Centre for Nuclear Medicine & Ultrasound, Post Box No.-16, Rangpur-5400, Bangladesh.

COMMUNICATIONS:

2. WATER IN DIAGNOSIS AND TREATMENT

Dr. M.A. Taher

From the time of immemorial, water had been used externally to reduce the temperature in fever and/or waking up the patient from sudden unconsciousness, and internally as a carrier of various drugs, the discovery of the specific water-channel protein aquaporin 1 (AQP1), and the subsequent identification in mammals of nine other members of the aquaporin family, have suggested that, in many cases water movement across membranes is facilitated by water channels.[1,2] A few members of the family can transport ions. Some, like AQP1 are expressed in various tissues, whereas others, like AQP2, seem to be confined to a single site. Most aquaporin seem to be constitutively expressed, but the expression of some can be regulated, e.g. in the kidney high concentrations of vasopressin increase concentrations of AQP2 and AQP3. Recently we have shown that water diuresis renography is useful in obstructive uropathy,[3] and side-effects of frusemide and mannitol can be avoided.

Jens Jordan and colleagues reported that oral water has substantial pressor effects[4] and observed a volume-dependent pressor response in patients with autonomic failure with 240 ml of water, the rise was about 15 mm Hg less than with 480ml,[5] they speculated that gastric distension may have been the stimulus that activated sympathetic reflexes, as previously described in normal people whose stomach had been distended with a barostat and whose sympathetic nerve activity had been directly measured with micro neurography.[6] In 1978, Kossoff and colleagues showed that the ultrasonic examination of upper abdomen is facilitated through the liquid-filled stomach[7] and recently we showed that water is a good echo-contrast in gastric emptying studies.[8] However, the precise mechanisms causing the pressor response to oral water, especially in patients with sympathetic denervation still remain to be determined.[9] To avoid urinary retention secondary to impacted pelvic mass, one should limit fluid intake before sleep.[10] King et al. studied two unrelated women with a deficiency of aquaporin-1and found that they had impaired urinary concentrating ability, suggesting that aquaporin-1 has a physiologic role in renal function. They performed renal and bladder ultrasonography and measured the glomerular filtration rate (GFR)) with Tc-99m DTPA (technetium-99 metastable diethylenetriamine penta acetic acid) by nuclear medicine techniques.[11] The pathophysiology associated with the aquaporin family of water-channel proteins includes mutations in some patients with nephrogenic diabetes insipidus (AQP2) and cataracts (AQP0) and abnormal transport of aquaporin-5 in patients with Sjogren's syndrome. Aquaporin-1 is essential for maximal urinary concentrating ability.

REFERENCES

1. Preston GM, Carroll TP, Guggino WB, Agre P. Appearance of water channels in Xenopus oocytes expressing red cell CHIP 28 protein, Science 1992; 256: 385-87
2. Marples D. Water channels: who needs them anyway? Lancet 2000; 355: 1571-2
3. Taher MA. Water diuresis renography. Indian J Nucl Med 2001; 16(2): 62-64

Director, Centre for Nuclear Medicine & Ultrasound, Post Box No.-16, Rangpur-5400, Bangladesh.

4. Jordan J, Shannon SR, Grogan E, Biaggioni I, Robertson D. A potent pressor response elicited by drinking water. Lancet 1999; 353:723
5. Jordan J, Shannon SR, Black BK et al. The pressor response to water drinking in humans. A sympathetic reflex? Circulation 2000; 101: 504-09
6. Rossi P, Andriesse G1, Oey PL. Wieneke GH, Roelofa JM, Akkermans LMA. Stomach distension increases efferent muscle sympathetic nerve activity and blood pressure in healthy humans. J Neurol Sci 1998; 161: 148-55
7. Kossoff G, Warren P, Garrett W. The examination of upper abdomen through the liquid filled stomach. 3 rd European Congress of Ultrasonics in Medicine, 1-5 Oct. 1987, Bologna, Italy, abstracts 17-18
8. Taher MA. Water as an echo-contrast for gastric emptying studies. Bangladesh J Ultrasonography f2001;8 (2) 109-11
9. Mathias CJ. A 21 st century water cure. Lancet 2000; 356:1046-47
10. Yang J-M, Hung W-C. Sonographic findings of acute urinary retention secondary to an impacted pelvic mass. J Ultrasound Med 2002; 21: 1165- 1169
11. King LS, Choi M, Frenandez PC, Cartron J-P, Agre P.Defective urinary concentrating ability due to a complete deficiency of aquaporin-1 Engl J Med 2001; 345: 175-179

COMMUNICATIONS:

3. CASE REPORT: TWO HEALTHY DAUGHTERS BORN TO A CRETIN

Dr. Muhammad Abu Taher

INTRODUCTION

Thyroxine replacement therapy can cure congenital hypothyroidism (cretinism) if institued early in life. We like to report a case of healthy daughter born to a congenitally hypothyroid woman considering its rarity.

CASE REPORT

A girl aged 11 months was put on thyroxine therapy in 1971 by the renowned pediatrician Professor M R Khan who diagnosed her to be congenitally hypothyroid. The initial dose was 12.5 microgram (mcg) daily and gradually it was increased to 150 mcg/day in adult life. She was highly educated (Master of Science) and was married on 18 August/ 2000 and got pregnant in 2001 when she took 175 mcg/day of thyroxine and her daughter was born on 03 January/ 2002 by Cesarean section due to transverse lie. Cord blood hormones were assayed: T_3 = 0.76 nmol/L (normal range 0.8-3.16), T_4 = 113 nmol/L (normal range 64-175), TSH = 6 mIU/L (normal range 0.4-5), However, she was euthyroid clinically on 13.03.2002. On 9 Feb. 2004, she had another sister born on 22 Dec. 2003 whose TSH is 9.5 mIU/L and she is also euthyroid clinically and all three (mother and both daughters) are on long-term follow-ups.

DISCUSSION

Permanent primary congenital hypothyroidism affects about one newborn in 3500. Eighty to ninety percent of the cases are due to developmetal defects of the thyroid gland (thyroid dysgenesis), such as arrested migration of the embryonic thyroid (ectopic thyroid) or a complete absence of thyroid tissue (athyreosis). Most cases of thyroid dysgenesis are sporadic and result from as yet unknown mechanisms. The remaining 10-20% have functional defects in one of the steps involved in thyroid hormone biosynthesis (thyroid dyshormonogenesis)-defects transmitted by an autosomal recessive mode of inheritance.[1] The pathogenesis of thyroid dysgenesis is not known.[2] Healthy baby born to a hypothyroid mother is a rare phenomenon, however, early treatment and regular monitoring of hormone levels may lead to an absolutely normal life. In 1989, a starting dose of 10-15 mcg./kg per day of thyroxine was proposed[3] and has been widely used since then, however, a recent systematic review dose not support clinical recommendation of high or standard starting doses of levothyroxine.[4] The upper range of normal values for plasma free thyroxine in normal infants is much higher than that for older children or adults.[5] Premature fusion of the fontanelles, a recognised complication of perinatal hyperthyroidism (such as seen in children born to mothers with Graves' disease), had never been reported in infants with congenital hypothyroidism treated with 10-15 mcg/ kg per day of levothyroxine.[1] During pregnancy and

Director, Centre for Nuclear Medicine and Ultrasound, Rangpur

estrogen therapy the need for thyroxine is increased.[6] Screening of neonates for congenital hypothyroidism is being done in many countries, but screening of pregnant woman for hypothyroidism is not yet universal.[8] Haddow et al. and Utiger encouraged adequate iodine intake and it should be increased during pregnancy.[9,10] In North America, screening programs usually initially measure T_4 and for those with low T_4 levels, TSH is then measured on the initial sample. In Europe and Japan, screening programs often use TSH elevation as the initial screening test, but this approach does not detect pituitary insufficiency. Transient neonatal hypothyroidism may also occur in infants of mothers with autoimmune thyroid disease and is due to maternal antibodies, particularly TSH -binding inhibitory antibody. A thyroid with normal morphology and normal or decreased uptake may be seen with transient hypothyroidism, and this can be evaluated by discontinuing thyroid replacement. Such a trial is usually not performed until 3 years of age so that the child is not subjected to thyroid insufficiency while the thyroid is needed for neurologic development.[11]

REFERENCES

1. Van Vliet G. Treatment of congenital hypothyroidism. Lancet 2001; 358: 86-87.
2. Castanet M, Lyonnet S, Bonaiti-Pellie C et al. Familial forms of thyroid dysgenesis among infants with congenital hypothyroidism. N Engl J Med. 2000;343:441-44
3. Fisher DA, Foley BL, Early treatment of congenital hypothyroidism. Pediatrics 1989; 83:785-89.
4. Hrytstuck I, Gilbert R, Logan S, Pindoria S, Brook CGD. Starting dose of levothyroxine for the treatment of congenital hypothyroidism. A systematic review. Arch Pediatr Adolesc Med 2002; 156:485-491.
5. Zurakowski D, Di Canzio J, Majzoub JA. Pediatric reference intervals for serum thyroxine, triiodothyronine, thyrotropin, and free thyroxine. Clin Chem. 1999; 45:1087-91.
6. Arafah BM. Increased need for thyroxine in women with hypothyroidism during estrogen therapy. N Engl J Med 2001; 344:1743-9.
7. Taher MA. Follow-ups of congenital hypothyroidism. ASEAN J Radiol 2001; VII (ii): 121-3.
8. Pop VJ, Van Baar AL, Vulsma T. Should all pregnant women be screened for hypothyroidism? Lancet 1999; 354:1224-5.
9. Haddow JE, Plaomaki GE, Allan WC, et al. Maternal thyroid deficiency during pregnancy and subsequent neuropsychological development of the child. N Eng J Med 1999; 342: 549-55.
10. Utiger RD. Maternal hypothyroidism and fetal development. N Engl J Med 1999; 341:601-02.
11. Shore RM. Pediatrics. In Wilson MA (ed.): Text book of Nuclear Medicine,1998, Lippincott-Raven, Philadelphia pp. 259-277.

COMMUNICATIONS:

4. CASE SERIES: SUB-FERTILITY AND MILD HYPOTHYROIDISM

Dr. M. Murshed Ali,[1] Dr. M. A. Taher[2]

ABSTRACT

Mild degree of hypothyroidism may be associated with reduced fertility as depicted by two cases reported below.

CASE 1

A lady of age 23 years came with the complain of obesity, had a technetium thyroid scan on 8 July 2001 which revealed mild degree of hypothyroidism. She had a past history of ovarian cyst, which was operated on 19 years of age. She started thyroxine 50 micrograms (mcg) per day and checked her T^3, T^4, & TSH levels at few-monthly intervals (Table-1), but she had two abortions in Dec.'02 & May '03 likely due to inadequate and irregular thyroxine ingestion, e.g., sometimes she takes 25 mcg/ day.

CASE 2

A lady of age 30 years came to CNMU Rangpur with the complaints of anorexia, constipation, cold intolerance, voice changes, irregular menstruation and secondary infertility. Her only child is a daughter of 6 years. Her past history includes thyroidectomy for multinodular goitre in May 1999 followed by inadequate supplementation therapy-she is taking only 50 micrograms of thyroxine daily. She had only one thyrotropin (TSH, thyroid stimulating hormone) estimation elsewhere in 2001 which was 1.11 μU/ml (normal range: 0.23-4), and as it was normal, no estimations of thyroid hormones (T_3 & T_4) were done there. We have done her thyroid function tests (Table 2) and found her to be mildly hypothyroid and advised to increase her daily thyroxine dose to 100 micrograms.

Table 1 Hormones levels of Case 1

22 Oct. 03	May 03	Oct.02	11 Aug. 02	17-01-02
T_3 = 0.23	2.4	2.15	4.1	2.8
T_4 = 108	152	108	243	142
TSH=2.85	8.21	5.75	8.58	13.5

Normal ranges: T_3 = 0.8 – 3.16 nmol/L T4 = 64-175 nmol/L TSH= 0.4-5 mIU/L

[1] Medical Officer,
[2] Director, Centre for Nuclear Medicine & Ultrasound (CNMU), Rangpur.

Table 2 Thyroid function tests of case 2

Date	Test	Values
7 July 2003	Radiommuno assay (RIA)	T_3 = 0.2 nmol/L T_4 = 106 ,, TSH = 2 mIU/L
10 Sept. 2003 Radioiodine uptake test		Normal ranges
2 hours uptake	3.5%	(5 – 15%)
24 hours uptake	22.3%	(16 - 40%)

DISCUSSIONS

The introduction of radioimmunoassay (RIA) by Yalow and Berson in 1959 provided superior measures for serum T_3, T_4 and TSH.[1] Clinical features of hypothyroidism depend on the duration and severity of the condition. A consequence of prolonged hypothyroidism is the infiltration of many body tissues by the mucopolysaccharides, hyaluronic acid and chondroitin sulphate, resulting in a low-pitched hoarse voice, poor hearing, slurred speech due to a large tongue and compression of the median nerve at the wrist,[2] menorrhagia, amenorrhea, infertility, galactorrhea, impotence, cold intolerance, constipation, goitre, tiredness and somnolence. T_3 concentrations may not discriminate reliably between euthyroid and hypothyroid patients, but in our case 1 it was the only hormone, which was low. Subclinical hypothyroidism is most often encountered after radioiodine (I-131) therapy or thyroidectomy and may persist for many years. With pituitary hypothyroidism, since serum TSH is not elevated, serum T_4 estimations are used to monitor the dose of thyroid replacement, which is increased until the serum T_4 concentration is within the upper normal range.[3,4] The subtle presence of hypothyroidism, which may be associated with elevated prolactin levels, demands screening of anovulatory and amenorrheic women with a TSH level,[5] although it seems rather extravagant to measure TSH in such a large number of patients for such a small return, because treatment for hypothyroidism is so simple and is rewarded by such a prompt return of ovulatory cycles, and, if galactorrhea is present, by a disappearance of the breast secretions (a slower process that can take several months). Effect of thyrotoxicosis and its treatment by methimazole and radioiodine (I-131) on gonads is well-evidenced,[6-7] however, that of mild hypothyroidism seems yet to be elucidated fully. Thyroid hormones are essential for mammalian life as they regulate many key biochemical reaction, especially protein synthesis and enzymatic activity. They also play a determining role in the process of early growth and development of fetal and first 2-3 years of postnatal life.[8] Brain damage to the developing child is entirely preventable by correction of iodine deficiency of the mother. During pregnancy and estrogen therapy, the need for thyroxine is increased.[9] Screening of neonates for congenital hypothyroidism is being done in many countries,[10] but screening of pregnant woman for hypothyroidism is not yet universal.[11] Haddow et al. and Utiger encouraged adequate iodine intake and it should be increased during pregnancy.[12,13] When the iodine supply to the thyroid gland is limited, the gland produces relatively more T_3 than T_4. When T_4 levels are low, target tissues also convert T_4 to T_3 However, the brain can only take up T_4 but not T_3, so brain function is affected when T_4 levels are low even though there may be sufficient T_4 and T_3 to carry out the function of thyroid hormones in other organs/ tissues. This is particularly important for the fetus in the first half of pregnancy. If maternal T_4 levels are low, the

fetal brain will be exposed to low T_4 levels, and this will result in brain damage.[14]

REFERENCES

1. Yalow RS, Berson SA. Immunoassay of endogenous plasma insulin in man. J Clin Invest 1960; 39:1157- 1175.
2. Edwards CRW, Baird JD, Frier BM, Shepherd J, Toft AD. Endocrine and metabolic diseases. In Edwards CRW, Bouchier IAD, Haslett C, Chilvers ED (editors): Davidson's Principles and practice of Medicine 17 th ed. 1995 Edinburgh, Churchill Livingstone, pp. 669-774.
3. Maisey MN. Thyroid. In Maisey MN, Britton KE, Collier BD, Siraj QH (editors). Clinical Nuclear Medicine 3 rd ed. London. Chapman & Hall, pp. 331-356.
4. Safrit HF. Thyroid disorders. In Fitzgerald PA (ed): Handbook of Clinical Endocrinology, Jones Med. Pub. California 1986; pp.122 -169.
5. Speroff L, Glass RH, Kase NG. Clinical Gynecologic Endocrinology and Infertility 5 th ed. 1994, Williams & Wilkins, Baltimore.
6. Taher MA. Effect of radioiodine (I-131) therapy on gonads. ASEAN J Radiol 2001: VII: 47-49.
7. Krassas GE. A prospective controlled study of the impact of hyperthyroidism on reproductive function in males. Sept. 2003, the 4 th Royan International Research Award p. 31.
8. Delange FM. Iodine deficiency disorders in mothers and infants. In Delange FM, West KP Jr. (eds.): Micronutrient Deficiencies in the first months of life. Pp. 89-102, Karger/ Nestec, Switzerland 2003.
9. Arafah BM. Increased need for thyroxine in women with hypothyroidism during estrogen therapy. N Engl. J Med 2001; 344: 1743-9.
10. Taher MA. Follow-ups of congenital hypothyroidism. ASEAN J Radiol 2001; VII (ii): 121-3.
11. Pop VJ, Van Baar AL, Vulsma. T. Should all pregnant women be screened for hypothyroidism? Lancet 1999; 354; 1224-5.
12. Haddow JE, Plaomaki GE, Allan WC, et al. Maternal thyroid deficiency during pregnancy and subsequent neuropsychological development of the child. N Engl. J Med 1999; 342: 549-55.
13. Utiger RD. Maternal hypothyroidism and fetal development. N Engl. J Med 1999; 341: 601-02.
14. Verhoef H, West CE, Bleichrodt N, Dekker PH, Born MP. Effects of micronutrients during pregnancy and early infancy on mental and psychomotor development. pp. 327-357. In Delange FM. West KP Jr. (eds.) ibid. 2003

COMMUNICATIONS:

5. URINARY TRACT TUBERCULOSIS: CASE SERIES

Dr. M.A. Taher

ABSTRACT

Urinary tract tuberculosis is a rare disease and therefore, we like to report the following cases.

Key words Radionuclide renogram, ultrasonogram, tuberculosis.

INTRODUCTION

World Health Organization (WHO) estimates there are 10 million new cases of all forms of tuberculosis (TB.) in the world yearly, particularly in developing countries. Extrapulmonary TB. accounts for 33% of the cases, and the genitourinary type, CNS and tuberculous meningitis are the next most frequent, respectively. The doubling time of mycobacterium is 20 to 24 hours (E. coli doubling time is 20 minutes), therefore renal tuberculosis is often silent and the non invasive imaging tests ultra-sonogram (USG) and nuclear medicine scan may help in the management as depicted by the cases reported here.

CASE 1

A male, aged 60 years, complained of painless hematuria, cough and general weakness. Chest X-ray showed bilateral infiltrations in mid-zones of both lungs. Urinalysis revealed sterile pyuria and microscopic hematuria. Abdominal ultrasonography showed multiple cysts and irregular echotexture in left kidney and mild calyceal dilation in right kidney. Nuclear medicine renal scan (Technetium 99 metastable diethylene triamine pentaacetic acid, Tc-99m DTPA) confirmed non-visualized left kidney and compensatory hypertrophy of right kidney and dilated upper right ureter. Antibiotic therapy with cephalosporin did not improve the symptoms of the patient. Tuberculin test was positive and a combination of antituberculous drugs made the patient symptom-free.

CASE 2

A man of 35 years came with the complaints of urgency and frequency of micturition for four months. His past history includes having appendicectomy 1 year ago and a course of anti-tuberculous drugs 2 years ago. DTPA renogram showed poorly functioning right kidney (Fig. 1) and normally functioning left kidney. USG showed small (4 cm dia.) right renal cyst and thickened urinary bladder mucosa. Vesical biopsy revealed features suggesting tuberculosis. Anti-tuberculous drugs make him symptom-free.

DISCUSSION

In renal tuberculosis, follow-up radionuclide renograms are recommended initially at about 1 mo. and then at 3-6 mo. intervals, depending on the site of tuberculosis in the renal tract.[1] Das et al.[2,4] found bilateral renal disease in 30% cases, but Premkumar and colleagues[3] could not show contralateral disease with either CT or sonography. In our case 1, compen-

Director, Centre for Nuclear Medicine & Ultrasound, Rangpur, Bangladesh.

satory hypertrophy of the contralateral kidney was noted in the nuclear scan and in our Case 2, although USG showed a small cyst in right kidney, but DTPA renogram showed poorly functioning right kidney. The multi-imaging approach, radioimmunoassay (RIA) and polymerase chain reaction (PCR) may clarify the diagnosis within 24 hours.[5] Only 30% of patients with urinary tract tuberculosis (TB.) have an abnormal chest radiograph and only 50% have a history of tuberculous infection.[6-9] The ultrasound appearance of urinary TB., may be (1) calycectasis, pyelocalyectasis or ureterectasis (depending on the side of scarring /obstruciton); (2) papillary or medullary cavitation; (3) cortical scarring; (4) generalized parenchymal thinning (advanced disease), (5) calcification (strong reflections with acoustic shadowing); and (6) a thick-walled, contracted bladder (from scarring). Obviously, these findings are diverse and nonspecific, but Tb should be a particular consideration when hydronephrosis and papillary or medullary cavitation are confined to one or a few major calyces (due to infundibular scarring), or when the calyces are diffusely dilated but the renal pelvis is not seen (due to scarring). Uncommonly, the granulomatous reaction replaces the renal parenchyma, generating a nonfunctioning 'putty' kidney that may appear relatively normal sonographically. Urinary Tb. may present as a hypoechoic 'mass' identical to focal bacterial nephritis or a small benign or malignant tumor.[10] Ultrasound guided skinny needle aspiration of collecting system (or a mass, if present) is of value in patients in whom standard urine cultures are negative for acid-fast bacilli.[4] Tuberculosis in a horse-shoe kidney may mimic a malignant tumor.[11] Tuberculosis of the glans penis is a rare disease and may simulate carcinoma.[12]

REFERENCES

1. Sweny P, Farrington K, Moorhead JF. The kidney and its disorders 1989, Blackwell, Oxford.
2. Das. KM, Indudhara R, Vaidynathan S. Sonographic features of genitourinary tuberculosis. Am J Roentgnol (AJR) 1992; 158: 327-329.
3. Premkumar A, Lattimer J, Newhouse, JH. CT and sonography of advanced urinary tract tuberculosis. AJR. 1989; 148:65-69.
4. Das KM, Vaidyanathan S, Rajwanshi A et al. Renal tuberculosis: diagnosis with sonographically guided aspiration cytology. AJR. 1992; 158: 571-573.
5. Lopez de Mesa BE. Arevalo AC, Cusnir PG, Revelo HAC. Imaging in Tuberculosis of the Genitourinary Tract. Ultrasound Quarterly. 15 (4): 201-205, 1999.
6. Zwiebel WJ. Urinary tract infection and calculi. In Zwiebel WJ, Sohaey R. introduction to Ultrasound. Saunders, Philadelphia, 1998,pp. 226-235.
7. Kenney PJ: Imaging of chronic renal infections, AJR Am Jroentgenol 155: 485-494, 1990.
8. Goldman SM, Fishman EK: Upper urinary tract infection: The current role of CT, ultrasound and MRI. Semin Ultrasound CT MR 12: 335-361, 1991.
9. Scott F, Engelbrecht HE: Ultrasonography of the advanced tuberculous kidney. S Afr Med J 75: 371-372, 1989.
10. Schaffer R, Becker JA, Goodman J. Sonography of tuberculous kidney. Urology 22: 209-211, 1983.
11. Elangovan S, Bhubaneswari V, Kannan RR, Dorairajan L N. An interesting case of tuberculosis in a horse-shoe kidney mimicking malignant tumor. Ind J Radiol Imag 12: 4: 513-514, 2002.
12. Islam M N, Quyum M A. Shaha A C, Ali O, Khan L A, Nag M N. tuberculosis of the glans penis- a review with a case report. North Med J 2002; 11(1): 54-56.

COMMUNICATIONS:

6. UNILATERAL BREAST ENLARGEMENT IN A 7 YEARS GIRL : CASE REPORT

Dr. M.A. Taher

Recently we found a girl of 7 years who came with her parents for ultrasonography (USG) of the enlarged left breast. No other problem was found in hepatobiliary, urogenital and adrenal regions. Mammary echotexture was fairly uniform, highly reflective pattern typically seen in the young breast tissue. Only a small layer of subcutaneous fat and no significant retromammary fat was identified. The pectoral muscles stood out clearly in contrast to the strongly reflective breast tissue plate.

Long term follow up was advised. We like to report it as a rare case of isolated thelarche (IT). Cases of isolated thelarche are usually self-limiting, although 10% may progress to central precocious puberty (CPP).[1] In IT, breast development may be unilateral or bilateral and is not associated with development of the areola.[2] It usually occurs before 2 years of age. Before the gonadotropin-estradiol negative feedback mechanism becomes sensitive. No other sign of pubertal progression e.g. height velocity, bone age acceleration and progressive development or appearance of other secondary sex characteristics, are observed. In girls with IT, uterine and ovarian volumes are similar to those of prepubertal girls.[3-6] Ovarian macrocysts (follicles measuring 10-20 mm in diameter) may be found in patients with IT.[6-8] Breast development may regress after several months, as happened in our case.

Unlike CPP, isolated thelarche is not associated with maturation of the hypothalamic-pituitary -gonadal axis.[9]

Timmerman believes that the best way forward in gynecologic sonography is to produce a list of recommended terms, procedures and definitions of end-points.[10]

REFERENCES

1. Root AW. Precocious puberty. Pediatr Rev 2000; 21: 10-19.
2. O'Dea LSL, Siegel SF, Lee PA. Pubertal disorders: precocious and delayed puberty. In: Sanfilippo JSS, Muram D, Lee PA, Dewhurst J (eds). Pediatric and Adolescent Gynecology. Philadelphia, PA: WB Saunders Co; 1994: 53-76.
3. Griffin IJ, Cole TJ, Duncan KA, Hollman AS, Donaldson MDC. Pelvic ultrasound findings in different forms of sexual precocity. Acta Paediatr 1995; 84: 544-549.
4. Haber HP, Wollman HA, Ranke MB. Pelvic ultrasonography: early differentiation between isolated premature thelarche and central precocious puberty. Eur J Pediatr 1995; 154: 182-186.
5. Blogowska A. significance of ultrasonographic examinations in diagnostics of premature and normal puberty in girls. Ann Acad Med Stetin 1997; 43: 161-180.
6. Buzi F, Pilotta A, Dordoni D, Lombardi A, Zaglio S, Adlard P. Pelvic ultrasonography in normal girls and in girls with pubertal precocity. Acta Pediatr 1998; 87: 1138-1145.

Director, Nuclear Medicine Centre, Rangpur.

7. Stanhope R, Abdulwahid NA, Adams J Brook CGD. Studies of gonadotropin pulsatility and pelvic ultrasound examinations distinguish between isolated premature thelarche and central precocious puberty. Eur J Pediatr 1986; 145: 190-194.
8. King LR, Siegel MJ, Solomon AL. Usefulness of ovarian volume and cysts in female isosexual precocious puberty. J Ultrasound Med 1993; 12: 577-581.
9. Herter LD, Golendziner E, Flores JAM, Moretto M, Di Domenico K, Becker E Jr., Spritzer PM. Ovarian and uterine findings in pelvic sonography. Comparision between prepubertal girls. Girls with isolated thelarche, and girls with central precocious puberty. J Ultrasound Med 2002; 21: 1237-1246.
10. Timmerman D. Lack of standardization in gynecological ultrasonography. Ultrasound Obstet Gynecol 2000; 16: 395-398.

COMMUNICATIONS:

7. SPONTANEOUS RESOLUTION OF CHOLECYSTO -ENTERIC FISTULA

Dr. M.A. Taher

Gall bladder perforation following acute cholecystitis is a rare phenomenon[1] and often follow a vague and insidious cilinical course. We report a case of gall bladder perforation resulting in cholecysto-enteric fistula as confirmed by ultrasonography (USG) and resolved spontaneously.

CASE REPORT

A 46 year-old woman with acute abdominal pain was referred for USG. The sonogram showed irregular thickening of the gall bladder wall with associated complex pericholecystic together with perihepatic fluid and communication with adjacent bowel loop. Focal loss of reflectivity of the gall bladder was also noted consistent with gall bladder wall disruption. The patient was managed conservatively and was scheduled for cholecystectomy. She was lost to follow-up.

DISCUSSION

Gallbladder perforation (also referred to as lacerations or ruptures) occur secondary to acute cholecystitis, infection, trauma or malignancy. Sonography, cholescintigraphy (hepatobiliary scan), and computed tomography along with a high index of suggestion are useful for early diagnosis of gall bladder perforation. Sonographic findings, including a complex echogenic pericholecystic fluid collection, a thickened hypoechoic edematous gall bladder wall, a collapsed gall bladder lumen despite a prolonged fasting and disruption of the gall bladder wall with focal loss of its reflectivity were reported.[2, 3] The treatment of choice for gall bladder perforation is cholecystectomy. Alternative treatments including biliary stent placement and conservative treatment were also recommended.

REFERENCES

1. Kao EY, Desser TS; Jeffrey RB Sonographic diagnosis of traumatic gall bladder rupture. J Ultrasound Med 2002; 21:1295-1297
2. Kim PN, Lee KS, Kim IY, Bae WK Lee BH. Gall bladder perforation: comparison of US finding with CT. Abdom Imaging 1994; 19: 239-242
3. Siskind BN, Hawkins HB, Cinti DC, Zeman RK, Burrell MI, Gall bladder perforation: an imaging analysis. J Clin Gastroenterol 1987; 9: 670-678

Director, Centre for Nuclear Medicine and Ultrasound, Rangpur-5400, Bangladesh.

DIFFUSION WEIGHTED IMAGE (DWI) AND MAGNETIC RESONANCE SPECTROSCOPY (MRS) OF MASS LIKE LESIONS IN THE BRAIN AS CORRELATED TO HISTOPATHOLOGY.

Pichest METARUGCHEEP,[1] Suchart PHUDHICHAROENRAT,[2] Nitat KIATHIRANNON,[1] Somsak CHANYAWATTIWONGES[1]

ABSTRACT

Bachground and purpose:

DWI and MRS have been used for the differentiation and grading of the brain tumors for more than 10 yrs. We attempted to study the diagnostic efficacy of these two techniques in MR imaging as correlated to the histopathology.

METHODS

Seventy patients with mass like lesions diagnosed by conventional MRI and pathologically or clinically proved (11 low grade astrocytomas and 10 high grade astrocytomas, 7 metastases,3 lymphomas, 2 germinomas,1 medulloblastoma, and 1 neuroblastoma, as well as 17 meningiomas, 5 schwannomas and 13 non tumors) and 20 normal controls were prospectively evaluated with conventional MRI, MRS (Press TR1500 and TE135) and DWI(b=0,500and 1000 s/mm2)

RESULTS

MRS shows diagnostic efficacy in differentiate tumor from non-tumor($p<0.5$), benign from malignant ($p<0.5$) and intraaxial from extraaxial tumor. Cho/CR more than 1.3 is the key value for differentiate of tumor from non-tumor and increase frequency in lactate or lipid may be used for differentiate of malignant from benign tumor. The Cho mono peak is the characteristic of extraaxial tumor.The present of the alanin is the feature of meningioma. ADC values were not effective for grading tumor or to differentiate malignant from benign and tumor from non-tumor. Only restricted diffusion (low ADC value) were noticed in 2 brain abscesses but the number of case is too small.

INTRODUCTION

Conventional MRI is the most useful technique in the diagnosis and evaluation of mass like lesion in the brain. For some instances, it is ineffective. MRS have been used for detection of brain abnormality with nearly 100% sensitivity and differentiate of tumor types by characterization of metabolic changes.[2-24] DWI and ADC (apparent diffusion coefficients) have been used to distinguish normal white matter from necrosis, cyst formation, edema and solid enhancing tumor.[24-33] DWI were also very effective in grading

ADC = Apparent Diffusion Coefficient, **DWI** = Diffusion Weighted Image, **MRS** = Magnetic Resonance Spectoscopy, **CHO** = Choline, **CR** = Creatine, **b** = diffusion Strength, **s** = second

[1] From the Department of neuroradiology,Prasat neurological institute,Bangkok,Thailand.
[2] From the Department of neuropathology,Prasat neurological institute, Bangkok,Thailand. Address reprint requests to Pichest Metarugcheep MD, Department of neuroradiology,Prasat neurological institute,Bangkok, Thailand.

tumor and in the demarcation of tumor by directional dependence of molecular diffusion.[25,28,29,34-38] In this study we attempted to evaluate the effectiveness of MRS and DWI for the differential diagnosis of mass like lesion in the brain. The main purposes were as follows: 1) to differentiate tumor from non-tumor. 2) to differentiate malignant from benign. 3) to do the grading of the tumor and 4) to distinguish pathologic subtypes by correlation of the MRS and ADC parameters with histopathologic findings.

METHODS

Study population:

70 patients comprising 40 men and 30 women ranging from 15 to 75 years of age (means age 45 yrs) with mass like lesion of the brain on conventional MRI were prospectively evaluated with DWI and MRS. 57 cases were pathological proved to be tumor and 13 were non-tumor. 20 normal control study were also done.

MRI evaluation:

All patients were examined by 1.5-Tesla MR imager (Magnetom vision plus, Seimens, Erlangen, Germany) with a standard head coil and protocol axial T1W(TR/TE=650/14 ms), T2WFSE(2000/80 ms) and Flair (TR/TE/TI=9000/2500/110 ms), 5 mms slice thickness, 210 mms FOV and 160x256 matrix size. DWI were done at tumor and peritumoral area and MRS at only tumor area (solid part) as well as other normal looking part.

MRS evaluation:

MRS were obtained by single voxel, PRESS sequence (TR/TE=1500/135 ms) with one-pulse water suppression and avoiding contamination from scalp fat, 256 acquisitions and automatic shimming. Spectroscopic data is from cubic volumes of 1.5x1.5x1.5 cms and acquisition time about 6.30 minutes.

MR diffusion imaging:

DWI were obtained by using axial echo-planar SE sequence (TR/TE=5700/139 ms), 5 mms slice thickness, 96x128 matrix size, FOV 240 mms in 22 seconds. The DWI were acquired by using b values of 0, 500, 1000 s/mm^2 applied in the X,Y, Z directions. Post processing of the ADC maps was performed by using software on a workstation and standard mean ADC values calculated automatically and expressed in 103 mm^2/s.

Histopathologic classification:

Total resection or multiple biopsy specimens were obtained from each patient. The tumor type and grading was according to WHO classification of nervous system tumors. For statistic analysis, lesions were classified as tumor or non-tumor, benign or malignant and high or low grade tumor.

Statistic analysis:

The mean and standard deviation (SD) of all MRS and ADC values were calculated with SPSS. Data were analyzed with independent sample T-test to compare mean of tumor versus non-tumor, benign versus malignant and high versus low grade tumor. The mean different was significant at the level of $p<.05$.

RESULTS

Seventy patients were screwed to the inclusion criteria comprising of 40 men and 30 women,age ranging from 15 to 75 yrs (mean age 45

ADC = Apparent Diffusion Coefficient, **DWI** = Diffusion Weighted Image, **MRS** = Magnetic Resonance Spectoscopy, **FOV** = Field of view, **b values** = Diffusion Strength, **PRESS** = Point Resolved Spectroscopy, **NAA** = N- Acitylaspartate **shimming** = Processes to make the magnetic field not variable, **SPSS** = Computer program for calculating different parameters in statistics such as, means, standard deviations, etc.

years). Fifty seven patients (81%) were tumors and thirteen patients(19%) non-tumors. Base on the histopathologic classification, 24/57(42%) were malignant (10 high grade astrocytomas, 7 metastases, 3 lymphomas, 1 medulloblastoma, 1 neuroblastoma and 2 germinomas) and 33/57 (58%) were benign (11 low grade astrocytomas, 17 menigiomas, 5 schwannomas). The 13 non-tumors were cerebral infarct 6, cysticercosis 3, abscess 2 and multiple sclerosis 2. The MRS showed that it is beneficial for differentiating tumor from non-tumor, malignant from benign, and extraaxial from intraaxial tumor. The most significant parameters were the Cho/Cr value with cut point at 1.3 and the presence of lactate or lipid, Cho/Cr more than 1.3 favored tumor and less than 1.3 favored non-tumor. Malignant tumor showed more frequent lactate and lipid. The character of choline mono peak was found only in extraaxial tumor which helped to differentiate from intraaxial tumor.The Alanin was present only in meningioma. The ADC values were not useful in the differentiating tumor from non-tumor, malignant from benign, or in the grading of the tumor. However, restricted diffusion with low ADC value was noted in both of the brain abscesses and MS.(Table 1)

MR spectroscopic findings:

MRS shows benefit to differentiate the tumor from non-tumor, malignant from benign tumor ($p<.05$). (Table 3&4). The most significant parameter to differentiate tumor from non-tumor is the Cho/Cr value with cut point at 1.3. Malignant tumor shows more Cho/Cr value but less NAA/Cr ratio. In grading of the tumor in the same type such as glioma, the MRS parameter shows no efficacy to differentiate(Table 5). The more frequency of lactate or lipid in malignant tumor (Table 7) is the parameter to differentiate malignant from benign tumor. The present of Alanin in only meningioma can used to be the character of this tumor (Table 6) as well as the Cho mono peak which was seen in other extraaxial tumnor such as Schwannoma as well.

Table 1: Summary of histopathologic diagnosis

Tumor group	Histodiagnosis	No of patients (n=70)
Malignant or high grade(n=24)	Astrocytoma grade 3,4 or GBM	10
	Germinoma	2
	Lymphoma	3
	Medulloblastoma	1
	Metastasis	7
	Neuroblstoma	1
Low grade(n=11)	Low grade astrocytoma	11
Benign(n=22)	Meningioma	17
	Schwannoma	5
Non-tumor(n=13)	Abscess	2
	Cysticercosis	3
	MS	2
	Cerebral infarct	6

Table 2: Normal control subjects

	N=20	N=20
Parameter	Mean	SD
NAA/Cr	1.90	0.46
Cho/Cr	0.85	0.13
ADC/Cr	88.00	5.00

Table 3: Differentiattion of tumor versus non tumor

	Tumors(n-57)		Non-tumor(n=13)			
Parameter	**Mean**	**SD**	**Mean**	**SD**	***P* value**	
NAA/Cr	0.91	0.59	1.35	0.56	0.02	Significant
Cho/Cr	2.03	1.16	1.00	0.21	0.002	Significant
Lactate/Cr	0.88	0.45	2.08	3.28		
Lipid/Cr	1.00	2.31	3.50	-		
Alanin/Cr	0.51	0.15	-	-		
ADCT	130.0	49.0	141.0	37.0	0.44	NS
ADCPT	157.0	38.0	158.0	46.0	0.97	NS

Note: ADCT indicates calculated ADC values from tumoral area. ADCPT, calculated ADC values from peritumoral area. NS = no significant different. P values were obtained by using independent Sample T-Test.

Table 4 :Differentiation of tumor as benign versus malignant

	Malignant(n=24)		Benign(n=33)			
Parameter	**Mean**	**SD**	**Mean**	**SD**	***P* values**	
NAA/Cr	1.16	0.65	1.15	0.47	0.41	NS
Cho/Cr	2.35	1.47	1.76	0.78	0.05	Significant
Lactate/Cr	1.01	0.49	-			
Lipid/Cr	1.71	2.62	0.93	0.30		
Alanin/Cr	-		0.51	0.15		
ADCT	126.0	41.0	135.0	53.0	0.51	NS
ADCPT	147.0	30.0	164.0	41.0	0.07	NS

Note: ADCT indicates calculated ADC values from tumoral area. ADCPT, calculated ADC values from peritumoral area. **NS** = no significant different. P values were obtained by using independent Sample T-Test.

Table 5: Differentation of tumor as low versus high grade

	High grade(n=10)		Low grade(n=11)			
Parameter	**Mean**	**SD**	**Mean**	**SD**	***P* values**	
NAA/Cr	1.35	0.78	0.93	0.49	0.15	NS
Cho/Cr	2.80	1.91	2.10	1.05	0.30	NS
Lactate/Cr	1.24	0.50	0.49	0.30		
Lipid/Cr	1.05	0.69	0.53	0.53		
Alanin/Cr	-		-			
ADCT	145.0	45.0	178.0	46.0	0.12	NS
ADCPT	147.0	27.0	151.0	31.0	0.79	NS

Note: ADCT indicates calculated ADC values from tumoral area. ADCPT is calculated ADC values from peritumoral area. **NS** = no significant different. P values were obtained by using independent Sample T-Test.

Table 6: Differentiation of histopathologic tumor types

	HGA (n=10)		Metastasis (n=7)		LGA (N=11)		Schwannoma (n=5)		MNG (N=17)	
Parameter	**Mean**	**SD**	**Mean**	**SD**	**Mean**	**SD**	**Mean**	**SD**	**Mean**	**SD**
NAA/Cr	1.35	0.78	1.39	0.46	0.93	0.49	0.84	0.60	0.61	0.40
Cho/CR	2.89	1.91	2.07	1.33	2.10	1.05	1.47	0.19	1.63	0.64
Lactate/Cr	1.24	0.50	0.99	0.47	0.40	0.30	-		1.00	-
Lipid/Cr	1.05	0.69	2.60	0.43	0.53	0.10	0.90	0.42	-	
Alanin/Cr	-		-		-		-		0.51	0.15
ADCT	145.0	45.0	126.0	25.0	176.0	46.0	153.0	74.0	103.0	25.0
ADCPT	147.0	27.0	153.0	32.0	154.0	31.0	213.0	63.0	157.0	31.0

Note: ADCT indicates calculated ADC values from tumoral area. ADCPT is calculated ADC values from peritumoral area. **NS** = no significant different. P values were obtained by using independent Sample T-Test.

Table 7: Frequency of lactate or lipid in malignant and benign tumor

	Malignant tumor(N=24)	Benign tumor(N=33)
Frequency	n (%)	n (%)
Lactate	5 (20%)	3 (9%)
Lipid	10 (41%)	3 (9%)

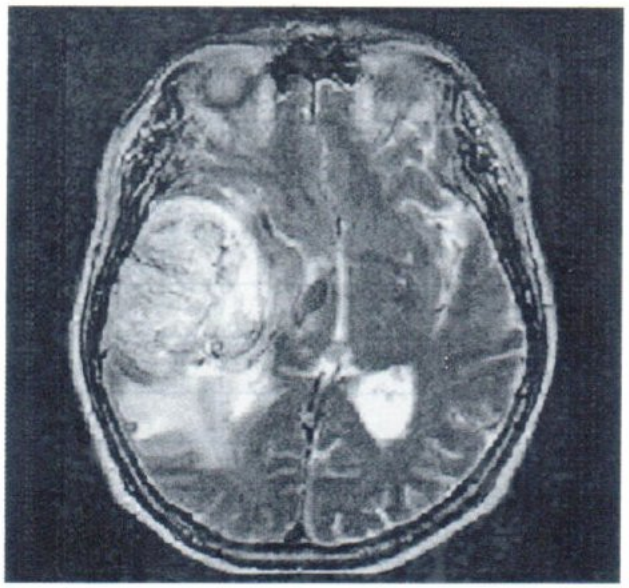

Fig. 1A

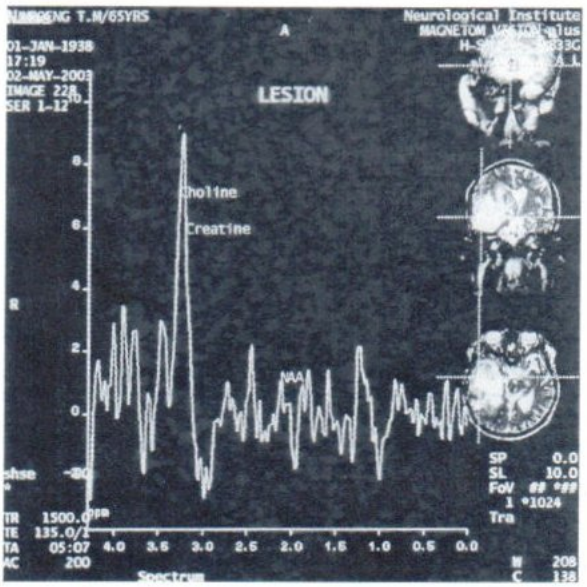

Fig. 1B

Fig.1 65-year-old man with meningioma at right sphenoid wing.

A: T2-weighted image shows a well demarcated slightly hyper SI with mild perifocal edema and mass effect.

B: MR spectrum reveals Cho mono peak with marked decrease of the NAA and presenting of the alanin(arrow).

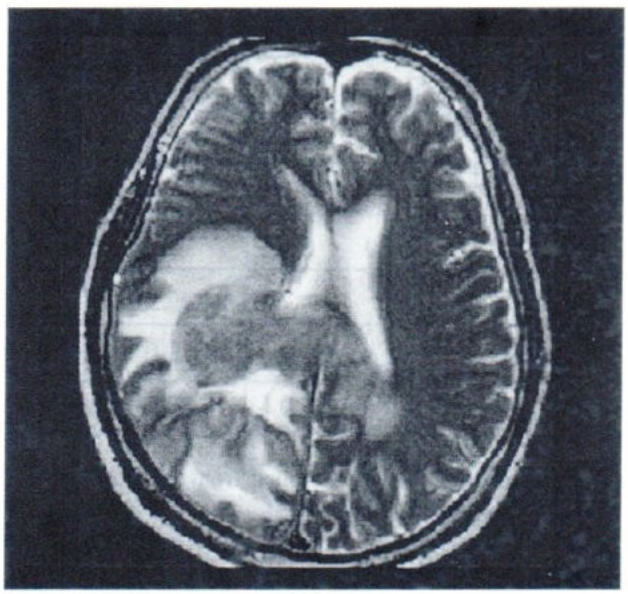

Fig. 2A

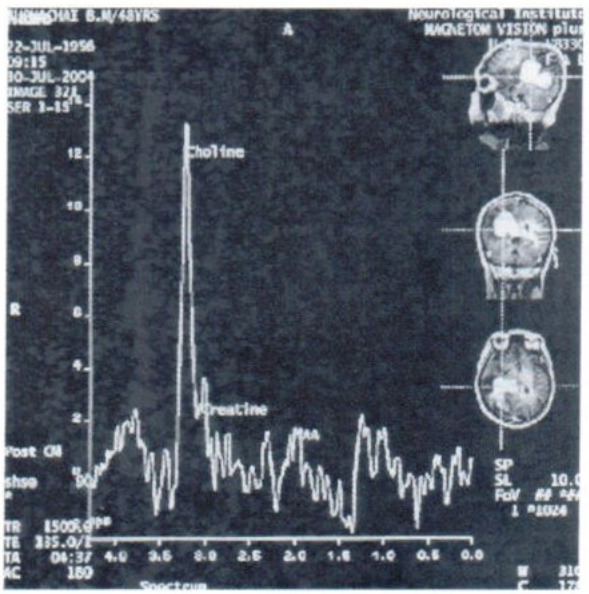

Fig. 2B

Fig 2 48-year-man with brain lymphoma at the splenium of right corpus callosum.

A: T2-weighted image shows slightly hyper SI mass at the splenium of right corpus callosum with moderated perifocal edema and mass effect.

B: MR spectrum of the tumor reveals marked increase level of Cho(CHO/Cr=2.6) and decrease NAA (NAA/Cr=0.6)

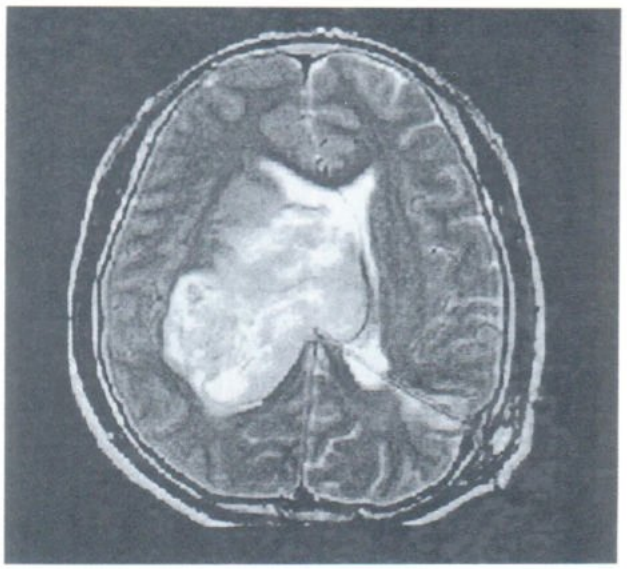

Fig. 3A

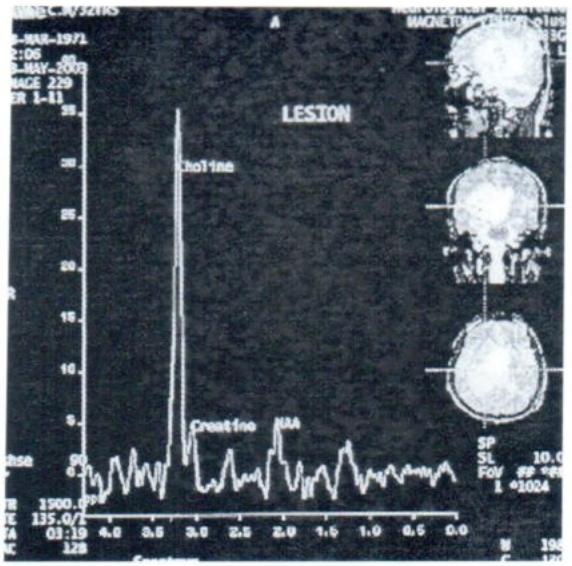

Fig. 3B

Fig. 3 32-year-man with Glioblastoma multiforme at right corona radiata

A: T2-weighted image shows a hyper SI mass at right corona radiata with moderated perifocal edema and mass effect.

B: MR spectrum reveals marked increase level of the Cho (Cho/Cr =4.00) and decrease NAA (NAA/Cr =1.00)

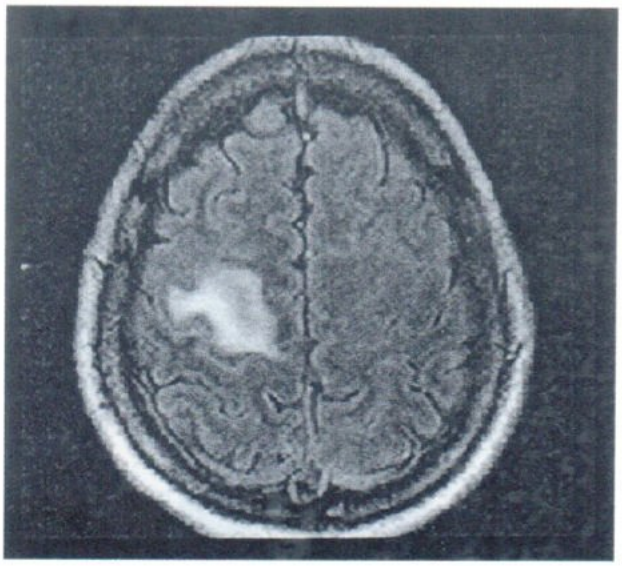

Fig. 4A

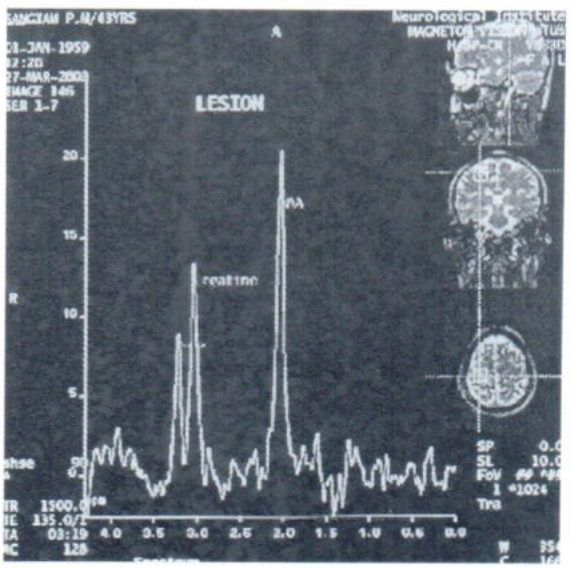

Fig. 4B

Fig. 4 43 year-man with brain cysticercosis in the right frontal lobe.

A; Flair image shows hyper SI lesion at right frontal lobe with mild perifocal edema and mass effect.

B: MR spectrum reveals mild decrease level of the NAA(NAA/Cr =1.4), unremarkable otherwise.

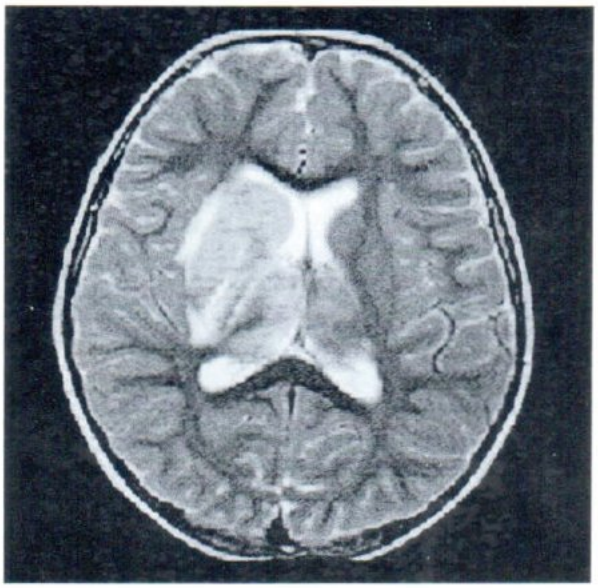

Fig. 5A

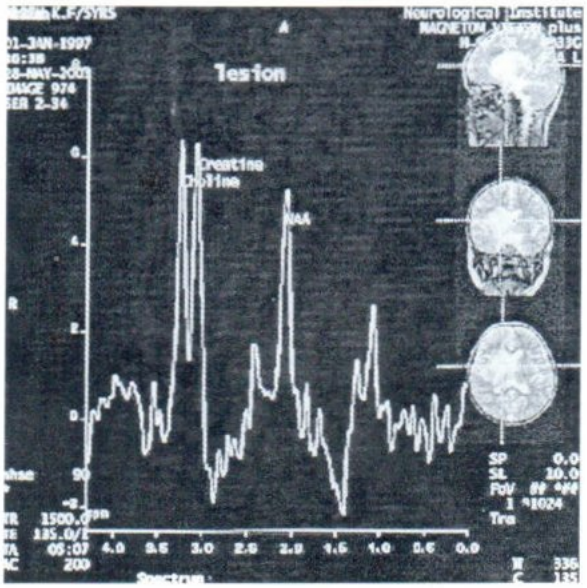

Fig. 5B

Fig. 5 5-year-female with cerebral infarct at right BSG and caudate neucleus.

A; T2-weighted image shows slightly hyper SI lesion at right BSG and caudate neucleus with mild perifocal edema and mass effect.

B: MR spectrum reveals decrease level of NAA(NAA/Cr=0.8) and presenting of lactate.

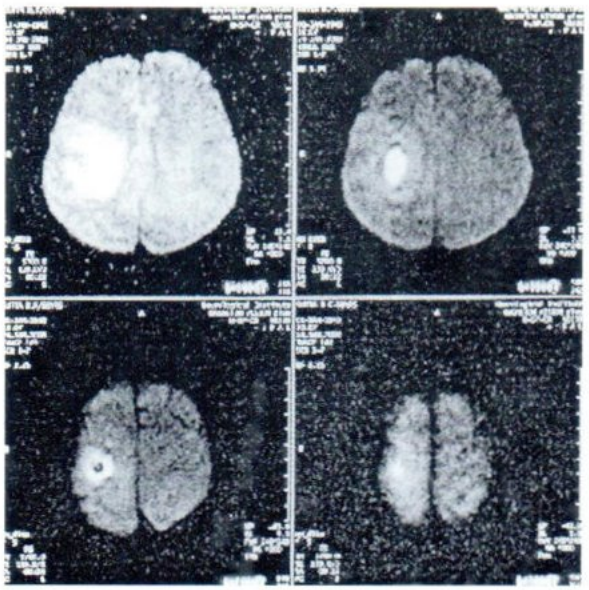

Fig. 6A

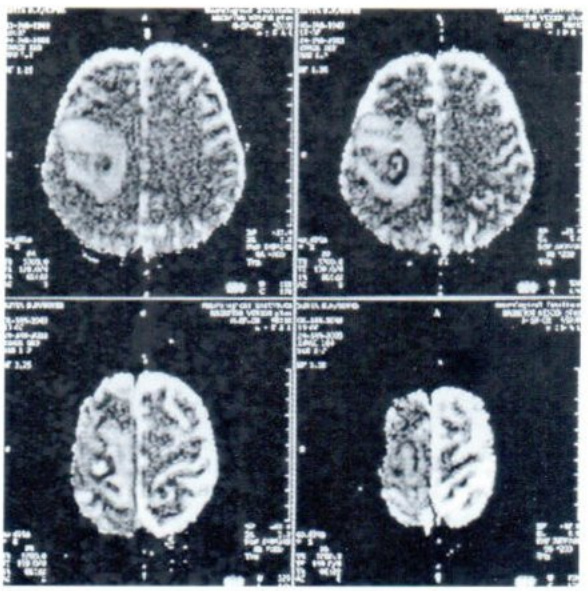

Fig. 6B

Fig. 6 60-year-female with brain abscess at centrum semioavale of right frontal lobe.

A: Diffusion weighted image (b=1000s/mm2) shows hyper SI lesion at right frontal lobe with moderated perifocal edema .

B: ADC map reveals the hyper SI lesion on DWI to be marked hypo SI and the calculated ADC value is 73 (Mean of ADC value of normal control= 88 ,SD=5 from table 2) ,consistent with restricted diffusion.

DWI and calculated ADC values

The ADC values in both tumor and peri tumor area were not useful in the differentiation tumor from non tumor, malignant from benign or in grading of the tumor(Table 2,3,4). Between subtypes of the tumor they also shows no efficacy, as shown in table 5. Only 2 restricted diffusion were noted in the brain abscesses, but the number of cases are too small.

DISCUSSION

DWI and MRS have been used in the evaluation of brain tumor for more than 10 years. Lower ADC values were accepted as a marker of high tumor grades.[24-39] NAA as marker of neuronal integrity, increase in Cho involved in increased cell membrane and myelin turn over as well as Cr represent cellular energetic and osmotic balance were reported. [2,3,6,8,12,17,18,22,40] Presence of the lactate and lipid were compatible with aggressiveness of the tumor, reflecting increase anaerobic metabolism and cellular necrosis, respectively. [2,3,6,7,9,12,17,18,22,40] The diagnostic accuracy of MRS in differentiate patients from control subjects was 0.96, and neoplasm from non-neoplasm was 0.96 and 0.83 in non blinded and blinded study, respectively.[41]

In our study ,the MRS could differentiate tumor from non-tumor and malignant from benign tumor but not effective in grading tumor. This is along with study by Nail et al.[1] The Decrease in NAA/Cr and incresse Cho/CR is the parameter for differentiate tumor from non-tumor. More malignant tumor shows more increase in Cho/Cr consistent with previous reports.[2,4,10,18,20,23] The increase Cho/Cr was mainly due to increase membrane turn over and liberation of unbound Cho-containing compound caused by destruction of neurons during malignant process, rather than decrease of the Cr level, which is rather constant in many conditions.[2,3,7,12] We also noticed more frequency of lactate or lipid in malignant tumor than benign tumor. This is also consistent with many reports.[7,10,12,23] Presence of lactate the indicator of non functional normal oxidative respiratory and increase anaerobic glycolysis[18] and it represented a loss of normal brain parenchyma and necrosis on MR image.[3] An increase in lipid level has been reported as the indicator of necrosis and usually prominent in non astrocytic tumors and metastasis.[7-9,13,22,23] We detected alanin in 12 of 17 meningioma close to the findings of Nail et al.[1] This could be the specific findings of meningioma. The alanin /Cr ratio in meningeal cells were three to four time higher in that found in astrocytes, neuron and oligodendrocytes.[12]

Krabbe et al[25] found that ADC of contrast enhancing areas and edema surrounding cerebral metastasis were significant higher than those of high grade astrocytoma and Kono et al[32] demonstrated a good correlation between ADC and cellularity in glioma, but in our study shows no different of the ADC in the tumor or peri tumor between malignant and benign as well as high and low grade tumor. Only restricted diffusion with marked low ADC was noticed in two brain abscesses compatible with the study by Noguchi et al.[30] Cho mono peak were found in nearly all extra axial tumor (Meningioma and Schwannoma) and this feature could be used to differentiate extraaxial from intraaxial tumor.

CONCLUSION

MRS showed diagnostic efficacy in differentiating tumor from non-tumor ($p<0.5$), benign from malignant tumors ($p<0.5$) and intraaxial from extraaxial tumors. Cho/CR more than 1.3 was the key value for the differentiation of tumor from non-tumor. The increased frequency in lactate or lipid might be used for differentiation of malignant from benign tumors. The Choline mono peak was the characteristic of extraaxial tumor. The presence of the alanin was the feature of meningioma. ADC values were not effective for grading tumor or differentiating malignant from benign tumor, and tumor from non-tumor, but restricted

diffusion (low ADC value) was noticed in brain abscess.

REFERENCES

1. Nail B, Murat K, Fatih O, Cem T , Taner U. Combination of single-voxel proton MR spectroscopy and apparent diffusion coefficient calculation in the evaluation of common brain tumors. AJNR Am J Neuroradiol 2003; 24: 225-233(Abstract/Free Full Text)
2. Bruhn H,Frahm J,Gyngell ML,et al. Noninvasive differentiation of tumors with use of localized H-1 MR spectroscopy in vivo:initial experience in patients with cerebral tumor. Radiology1989;172:541-548(Abstract)
3. Segebarth CM,Baleriaux DF,Luyten PR,den Hollander JA.Detection of metabolic heterogeneity of human intracranial tumor in vivo by H-1 NMR spectroscopic imaging.Magn Reson Medl 1991;62-76(Medline)
4. Fulham MJ,Bizzi A,Dietz MJ,et al. Mapping of brain tumor metabolites with proton MR spectroscopic imaging: clinical revevance. Radiology1992;185:675-686(Abstract)
5. Baker PB,Glikson JD,Brayn RN.In vivo magnetic resonance spectroscopcy of human brain tumorsTop Magn Reson Imaging 1993; 5:32-45(Medline)
6. Poptani H,Gupta RK,Roy R,Pandey R, Jain VK,Chhabra DK.Chracterization of intracranial mass lesions with in vivo proton MR spectroscopy.AJNR AM J Neuroradiol 1995;16:1593-1603(Abstract)
7. Castillo M,Kwock L,.Clinical application of MR spectroscopy.AJNR AM J neuroradiol 1996;17:1-15(Free full text)
8. Krouwer HGJ,Kim TA,Rand SD,et al .,Single -voxel proton MR spectroscopy of nonenoplastic brain lesions suggestive of a neoplasm. AJNR Am J Neuroradiol1998;19:1695-1703(Abstract)
9. Castillo M,Kwock L.Proton MR spectroscopy of common brain tumors.Neuroimaging Cli North Am1998;8:733-752
10. Meyeland ME, Pipas JM, Mamourian A, Tosteson TD, Dunn JF.Classification of biopsy-confirmed brain tumors using single -voxel MR spectroscopy.AJNR Am J Neuroradiol1999;20:117-123(Abstract/Free Full Text)
11. Nelson SJ,Vignerron DB,Dillon WP.Serial evaluation of patients with brain tumors using volume MRI and 3D 1-H MRSI. NMR Biomed1999;12:123-128 (Medline)
12. Castillo M,Kwock L.Clinical applications of proton magnetic resonance spectroscopy in the evaluation of common intracranial tumors.Top magn Reson Imaging 1999; 10: 104-113(Medline)
13. Grand S,Passaro G,Ziegler A,et al. Necrotic tumor versus brain abscess : importance of amino acids detected at 1-H MR spectroscopy-initial results.Radiology1999;213:785-793(Abstract/Free Full Text)
14. Burtscher IM, Skagerberg G, Geijer B, Englund E,StahbergF,Holtas S.Proton MR spectroscopy and preoperative diagnostic accuracy: an evulation of intracranial mass lesions characterized by stereotactic biopsy findings.AJNR Am J Neuradiol2000;21:84-93(Abstract/FreeFull Text)
15. Shimizu H,Kumbe T,Shirane R,Yoshimoto T. Correlation between choline level measured by proton MR spectroscopy and Ki-67 labeling index in gliomas.AJNR Am J Neuroradiol2000;21:659-665(Abstract/Free Full Text)
16. Bendszus M, Warmuth-Metz M, Klein R, et al. MR spectroscopy in gliomatosis cerebri. AJNR Am J Neuroradiol2000;21:375-28 -380(Abstract/Free Full Text)
17. Butzen J, Prost R, Chetty V, et al. Discrimination between neoplastic and nonneoplastic brain lesions by use of proton MR spectroscopy: the limits of accuracy with logical regression model. AJNR Am J Neuroradiol 2000; 21: 1213-1219 (Abstract/Free Full Text)

18. Kimura T, Sako K, Gotoh T, Tanaka K, Tanaka T, Invivo single-voxel proton MR spectroscopy in brain lesions with ring-like enhancement.NMR Biomed 2001; 14: 339 349 (Medline)
19. Dowling C, Bollen AW, Noworolski SM, et al. Preoperative proton MR spectroscopic imaging of brain tumors: correlate to histopathologic analysis and resection. AJNR Am J Neuroradiol; 22: 604-612 (Abstract/Free Full Text)
20. Schlmmer HP, Bachert P, Herfarth KK, Zunna I, Debus J, van Kaick G. Proton MR spectroscopic evaluation of suspicious brain lesions after stereotactic radiotherapy.AJNR Am J Neuroradiol;22:1316-1324(Abstract/ Free Full Text)
21. Tzika aa, Cheng, LL, Goumnerova L, et al. Biochemical characterization of pediatric brain tumors by using ex vivo magnetic resonance spectroscopy. J Neurosurg 2002; 96: 1023-1031(Abstract/Free Full Text)
22. Tzika AA, Zarifi MK, Goumnerova L, et al. Neiroimaging in pediatric brain tumors: Gd-DTPA-enhanced,hemodynamic,and diffusion MR imaging compared with MR spectroscopic imaging. AJNR Am J Neuroradiol 2002; 23: 322-333 (Abstract/Free Full Text)
23. Moller-Hartmann W, Herminghaus S, Krings T, et al. Clinial application of proton magnetic resonance spectroscopy in dianosis of intracranial mass lesions. Neuroradiology 2002; 44: 371-381(Medline)
24. Sener RN. Longstanding tectal tumor: proton MR spectroscopy and diffusion MRI findings. Comput Med Imaging Graph 2002; 26: 25-31(Medline)
25. Krabbe K, Gideon P, Wang P, Hansen U, Thomsen C, Madsen F. MR diffusion imaging ofhuman intracranial tumors.Neuroradiology 1997; 39: 483-489
26. Le Bihan D, Breton E, Lallemand D, Grenier P, Cabanis E, Laval-Jeantet M. MR imaging of intravoxel incoherent motions: application to diffusion and perfusion in neurologic disorders. Radilogy 1986; 161: 401-407(Abstract)
27. Remy C, Grand S, Lai ES, et al.1H MRS of human brain abscess in vivo and in vitro.Magn Reson Med1995;34:508-514
28. Tien RD, Felberg GJ, Frieman H, Brown M, MacFall J. MR imaging of high-grade cerebral gliomas: value of diffusion-weighted echoplanar pulse sequence AJR Am J Roentgenol1994;162: 671-677(Abstract)
29. Brunberg JA, Chenevert TL, McKeever PE, et al. In vivo MR determination of water diffusion coefficients and diffusion anisotropy: correlation with structural alteration in gliomas of the cerebral hemispheres. AJNR Am J Neuroradiol1995;16:361-371(Abstrat)
30. Noguchi K, Watanabe N, Nagayoshi T,et al. Role of diffusion-weighted echo planar MRI in distinguishing between brain abscess and tumor: a primary report. Neuroradiology 1999; 41:171-174(Medline)
31. Stadnik TW, Chakis C, Michotte A, et al. Diffusion-weighted imaging of intracerebral masses: comparison with conventional MR imaging and histologic findings. AJNR Am J Neuroradiol2001;22969-976(Abstract/Free full Text)
32. Kono K, Inoue Y, Nakayama K, et al. The role of diffusion-weighted image in patients with brain tumors. AJNR Am J Neuroradiol 2001;221081-1088(Abstract/Free Full Text)
33. Filippi CG, Edgar MA, Ulu AM, Prowda JC, Heir LA, Zimmerman RD. Appearance of meningioma on diffusion-weighted images: Correlating diffusion constants with histopathologic findings. AJNR Am J Neuroradiol 2001; 22: 65-72 (Abstract/Free Full Text)

34. Le Bihan D, Douek P, Argyropoulou M, Turner R, Patronas N, Fulham M. Diffusion and perfusion magnetic resonance imaging in brain tumors. Top Magn Reson Imaging 1993; 5:25-31(Medline)
35. Eis M, Els T, Hoehn-BerlageM, Hossman KA. Quantitative diffusion MR imaging of cerebral tumor and edema. ActaNeurochirSuppl (Wien) 1994; 60: 344-346 (Medline)
36. Castillo M, Smith JK, Kwock L, Wilber K. Apparent diffusion coefficients in the evaluation of high-grade cerebral gliomas. AJNR Am J Neuradiol2001;22:60-64(Abstract/ Free Full Text)
37. Maier SE, Bogner P, Bajzik G, et al. Normal brain and brain tumor: multi component apparent diffusion coefficient line scan imaging Radiology 2001;219: 842-849 (Abstract/Free Full Text)
38. Sinha S, Bastin ME, Whittle IR, Wardlaw JM. Diffusion tensor MR imaging of high-grade cerebral gliomas. AJNR Am J Neuroradiol 2002; 23: 520-527(Abstract/Free Full Text)
39. Law M, Cha S, Knopp EA, Johnson G, Arnett J, Litt AW. High-grade gliomas and solitary metastases: differentiation by using perfusion and proton spectroscopic MR imaging. Radiology 2002; 222: 715-72 (Abstract /Free Full Text)
40. Tedeschi G, Lundbom N, Raman R, et al. Increased choline signal coinciding with malignant degeneration of cerebral gliomas: a serial proton magnetic resonance spectroscopy imaging study. J Neurosurg 1997; 87: 516-527(Medline)
41. Rand SD, Prost R, Haughton V, et al. Accuracy of single-voxel proton MR spectroscopy in distinguishing neoplastic from non -neoplastic brain lesions. AJNR Am J Neuroradiol 1997; 18: 1695-1704 (Abstract)

TUBERCULOUS ADRENAL ABSCESS ASSOCIATED WITH TUBERCULOSIS OF THE LUNGS AND BRAIN: A CASE REPORT

Phuvitoo SUNGTONG, M.D.[1]

ABSTRACT

Tuberculous adrenal abscess was diagnosed in a 46-year-old man who presented with fever, abdominal pain, and weight loss. Ultrasonography revealed a well-marginated right suprarenal mass with internal hypoechoic areas. By CT scan, it showed thin rim enhancement with multiple septal enhancement and central hypodense areas. Tuberculous adrenal abscess was diagnosed by isolation of tuberculous bacilli from the lesion under CT guidance. He also had evidence of miliary pulmonary tuberculosis from chest radiograph and intracranial tuberculosis from CT scan of the brain.

INTRODUCTION

Tuberculosis is an infectious disease caused by microorganism Mycobacterium tuberculosis. It is on the rise and revisiting both the developed and developing world and is increasing prevalence in both immunocompetent and immunocompromised individuals. It is a chronic, contagious bacterial infection, which can affect several organs of the human body, including the brain, bone, gastrointestinal tract, kidneys, adrenal glands, lymph node, but most commonly it affects the lungs. A case of disseminated tuberculosis which are composed of miliary tuberculosis of the lungs, intracranial tuberculosis, and tuberculous abscess of the adrenal glands is present in the emphasis of radiological findings and differential diagnosis with a review of the current literatures.

CASE REPORT

A 46-year-old man presented with fever, progressive increasing right upper quadrant pain and weight loss 9 kg in approximately 3 months. There was neither cough nor hemoptysis. His past medical history was unremarkable and he had no past history of tuberculosis. There was neither past history of intravenous drug used nor risk factors for human immunodeficiency virus (HIV) infection.

The initial physical examination revealed an obviously unwell patient. He was cachectic, mild pale, and no jaundice. The body temperature was 38 °C, BP 100/70 mmHg, pulse 70 beats/min, and respiratory rate 22 breaths/min. The heart and lungs appear normal. The abdominal examination revealed soft on palpation without point of maximum tenderness. A questionable abdominal mass was palpable on the right side of abdomen. It is deeply located. The rest of physical examination including neurological examination was within normal limits.

Chest radiograph revealed innumerable, 1-3 mm, noncalcified nodules scattering through out both lungs. No cavitary lesion was observed. There was no evidence of mediastinal mass. Minimal right pleural effusion was also noted. (Figure 1A, 1B). Miliary tuberculosis was the most likely diagnosis. However, repeated acid fast smears of the sputum were negative.

[1] Division of Radiology Hatyai Hospital Songkhla Thailand 90110.
E-mail addresses : **phuvitoo@hotmail.com, Phuvitoo@yahoo.com**

Fig. 1 Chest radiograph.

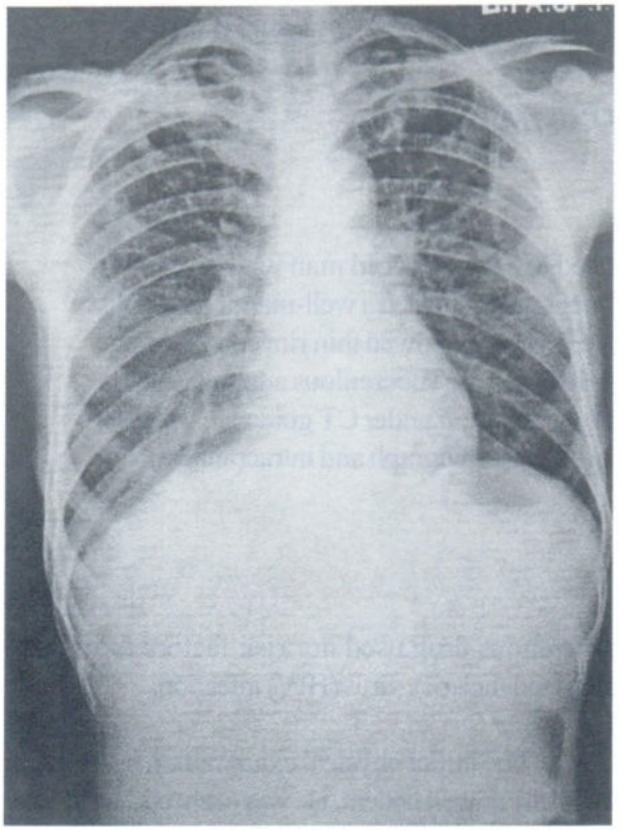

Fig. 1A Posteroanterior chest radiograph revealed diffuse miliary shadows through out both lungs. Small amount of right pleural effusion was evident.

Fig. 1B Close-up right basal lung clearly demonstrated miliary pulmonary infiltrations.

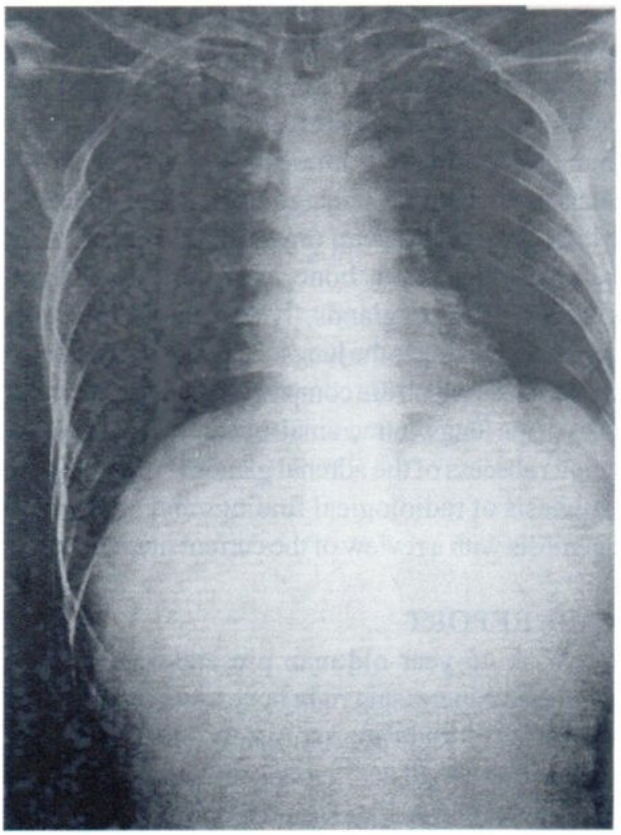

Fig. 1C Follow-up chest radiograph after six weeks of antituberculous treatment showed disappearance of pulmonary infiltrations.

Owning to abdominal pain and a palpable mass, ultrasonography of the abdomen was requested. The abdominal ultrasonography revealed a well -marginated right-sided suprarenal mass with multiple internal hypoechoic areas (Figure 2A, 2B). There was no obvious suprarenal mass on the contralateral side. The liver, gallbladder, pancreas, spleen, and kidneys were normal. There was neither enlarged lymph node nor ascites. Small amount of right pleural effusion was observed.

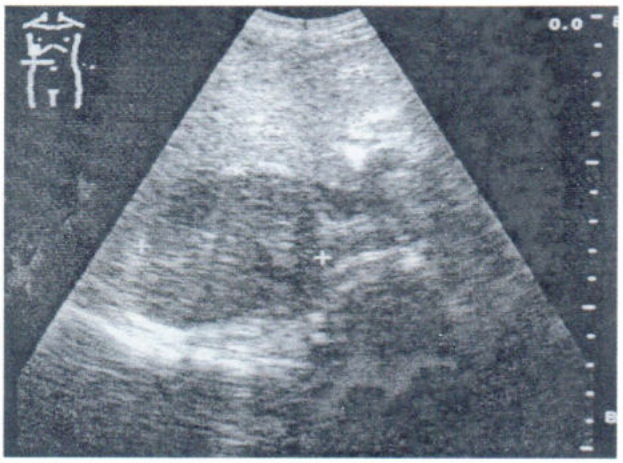

Fig. 2A

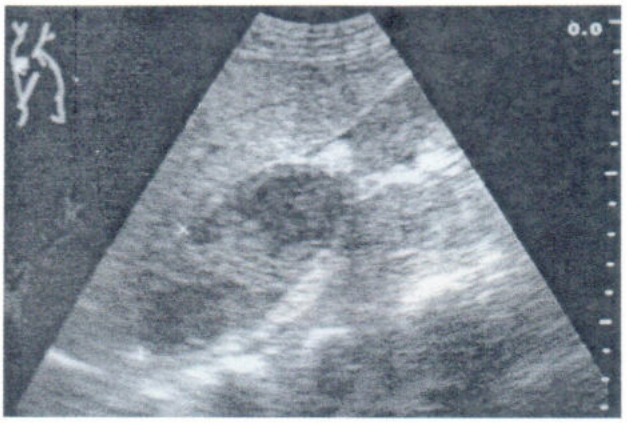

Fig. 2B

Fig. 2 Ultrasonography of the right adrenal gland. Transverse (Figure 2A) and longitudinal (Figure 2B) ultrasonographic images showed a large right suprarenal mass with internal hypoechoic areas.

Computed tomography scan of the abdomen showed a mass originating from the right adrenal gland. On precontrast scan it was inhomogeneous hypodensity and had an attenuation of approximately 27 HU. Neither calcification nor fat density was noted (Figure 3A). Following IV contrast, the mass showed thin rim enhancement with multiple septal enhancement. The internal hypodense areas were not enhanced. Its size was approximately 4x5x6 cm. The left adrenal gland was slightly enlarged and showed rim enhancement with central hypodensity (Figure 3B, 3C). Neither enlarged lymph node nor ascites was noted.

CT-guided aspiration was performed for the correct diagnosis of the right adrenal pathologic condition. It was done by placing the patient in the prone position and using a 20G spinal needle (Figure 3D). Pus was obtained, approximately 20 cc. It was sent for gram stain and AFB stain. Acid fast stain showed organisms as slender red rods. Gram stain showed many WBC and few RBC but no organism. Antituberculous drugs (INH, Rifampicin, PZA, and Ethambutal) were started after the report of adrenal abscess aspiration. The patient was discharged after gradual getting well in 2 weeks.

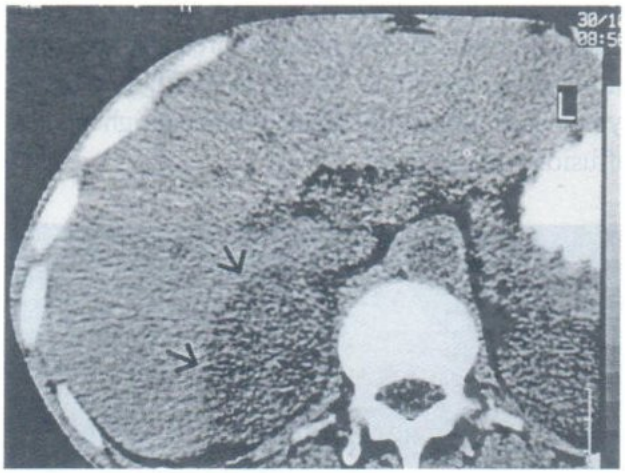

Fig. 3A

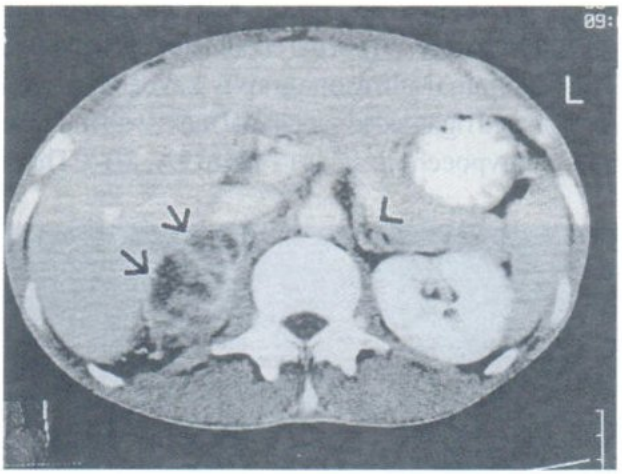

Fig. 3B

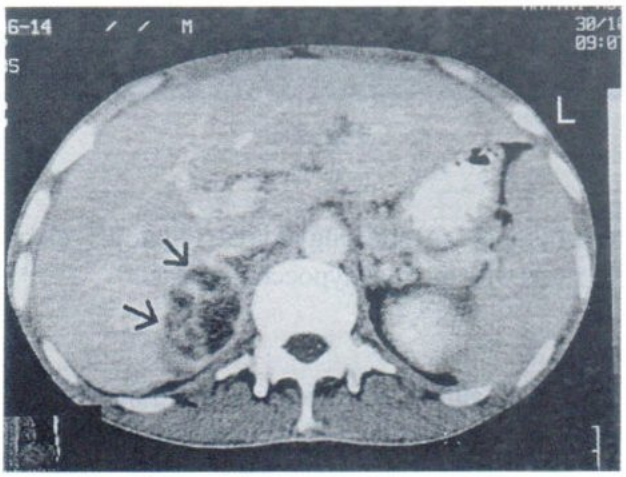

Fig. 3C

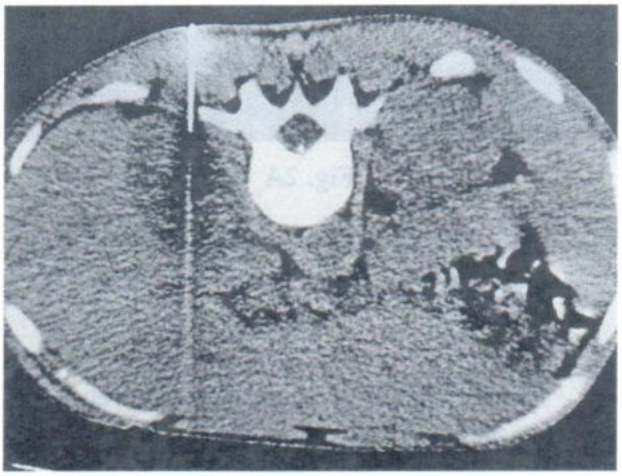

Fig. 3D

Fig. 3 CT scan of the adrenal glands.

Fig. 3A CT scan obtained before I.V. contrast administration showed a large right suprarenal mass with heterogeneous hypodensity (arrows).

Fig. 3B and **3C** Contrast-enhanced CT scan showed rim and septal enhancement of the right adrenal mass with internal hypodense areas (arrows). The left adrenal gland is slightly enlarged with rim enhancement and central hypodensity (arrow head).

Fig. 3D CT-guided aspiration of right adrenal abscess was performed on prone position.

One month later, he was admitted with progressive headache, and drowsiness. The physical examination revealed decreased visual field, papilledema, and impaired cerebellar functions. The body temperature was 36.8 °C, BP 110/70 mmHg, pulse 80 beats/min, and respiratory rate 22 breaths/min.

CT scan of the brain was performed. Multiple, various-sized nodular and ring enhancing lesions with associated brain edema were observed in the cerebrum and cerebellum. They measured less than 1 cm in size. Many miliary tubercles were also noted (Figure 4A, 4B).

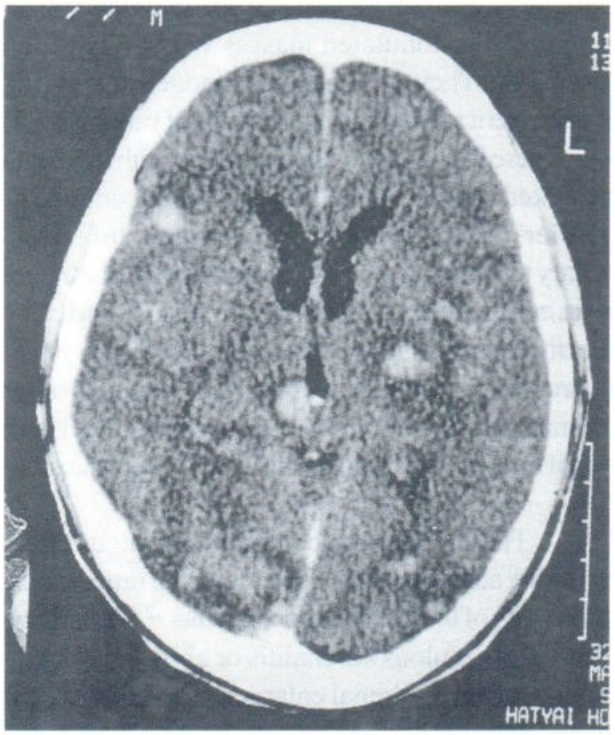

Fig. 4A

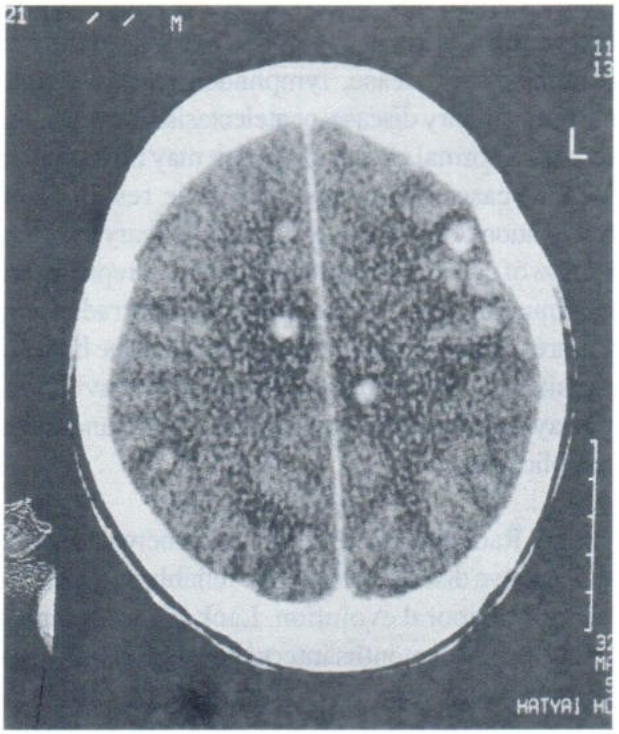

Fig. 4B

Fig. 4 CT scan of the brain.
Fig. 4A and **4B** CT scan of the brain post I.V. contrast showed multiple small nodular and ring enhancing lesions scattered in the brain with associated brain edema.

Chest radiograph of this admission showed disappearance of miliary infiltrations in both lungs. No pleural effusion was noted (Figure 1 C).

The follow up ultrasonography revealed persistence of a large right suprarenal mass. Its size and echogenicity were similar to the previous examination. Right pleural effusion disappeared. No additional abnormal finding of abdominal ultrasonography was observed.

According to persistence of right adrenal abscess after medical treatment, surgical exploration with right adrenalectomy was performed. Large amount of pus inside the bisected adrenal gland was noted. The specimen was submitted for pathological examination and revealed caseous granulomatous inflammation.

After operation, multiple medical problems occurred. The patient got worsen with cardiac arrest and died with disseminated tuberculosis 3 weeks after the operation.

DISCUSSION

Tuberculosis is most commonly limited to the chest but it can affect virtually any organ system in the body and can be devastating if left untreated. Because tuberculosis demonstrates a variety of clinical and radiologic findings and has a known propensity for dissemination from its primary site, it can mimic numerous other disease entities.[1]

Pulmonary tuberculosis is classically divided into primary and postprimary (reactivation) tuberculosis. There is considerable overlap in the radiologic

manifestations between these two entities. Primary tuberculosis typically manifests radiologically as parenchymal disease, lymphadenopathy, pleural effusion, miliary disease, or atelectasis. However, the results of normal chest radiograph may be normal in 15% of cases. Postprimary disease results from reactivation of a previously dormant primary infection in 90% of cases; in a minority of cases, it represents a continuation of the primary disease. The radiologic features of postprimary tuberculosis can be broadly classified as parenchymal disease with cavitation, airway involvement, pleural extension, and other complications.[1,2,3]

Radiographic differentiation between active and inactive disease can only be reliably made on the basis of temporal evolution. Lack of radiographic change in a 4-6 months interval generally indicates inactive disease.[4,5]

Dissemination of tuberculosis may occur during either primary or post primary stages of disease. It results when a focal collection of tubercle bacilli discharges into a blood or lymph vessel, releasing a large number of viable bacilli that embolize to capillary beds in multiple organs.[2,6]

A chest radiographic finding of profuse, tiny, well-defined nodules 1-4 mm in size is termed miliary shadowing. It comes from "mellet seed" (a popular birdseed), and the areas of increased opacity are said to resemble mellet seeds in size and shape.[7] Miliary shadowing is highly suggestive of disseminated tuberculosis in the appropriate clinical setting. However, it may also indicate varicella pneumonia, histoplasmosis, metastases (particularly from thyroid tumor, melanoma, and choriocarcinoma), pneumoconiosis, hemosiderosis, eosinophilic granuloma, or sarcoidosis.[1,7,8]

Central nervous system tuberculosis may take a variety of forms, including meningitis, tuberculoma, abscess, cerebritis, and miliary tuberculosis. Parenchymal disease can occur with or without meningitis and most commonly manifests as either solitary or multiple tuberculomas. At CT, tuberculomas appear as rounded or lobulated masses with low or high attenuation. They demonstrate homogeneous or ring enhancement and have irregular walls of varying thickness. These lesions are often associated with moderate to marked edema, but calcification is uncommon.[1,9] Smaller lesions were termed miliary tubercles. Miliary tubercles appear as numerous round, homogeneous enhancing lesions, less than 2 mm in diameter.[10,11] The differential diagnosis for central nervous system tuberculomas and miliary tubercles includes other granulomatous infections (e.g. cysticercosis), and fungal infections as well as metastatic neoplasms.[1]

The CT appearance of granulomatous infection of the adrenal glands depends on the time, course and activity of the inflammatory process.[12] CT findings of early tuberculous adrenalitis or abscess typically include bilateral adrenal enlargement with a central necrotic area of hypoattenuation and a peripheral enhanced rim but unilateral involvement can occur.[12,13,14,15] Adrenal abscess caused by nontuberculous bacterial infection is uncommon in an adult but occurs more frequently in neonates.[16,17] Neonatal adrenal abscesses can be unilateral or bilateral and are caused by either hematogenous bacterial seeding of normal adrenal glands or seeding of a neonatal adrenal hemorrhage with subsequent abscess formation.[17]

The differential diagnosis of bilateral adrenal enlargement must include other granulomatous infections such as histoplasmosis, cryptococcosis, and blastomycosis. Other diseases that may produce a similar appearance include lymphoma, bilateral adrenal metastases, bilateral hemorrhage, and bilateral primary adrenal tumors.[15]

In the healing stage of adrenal tuberculosis, the adrenal glands become calcified and atrophy. However, its CT appearance is indistinguishable from that of other long-standing granulomatous infections, previous hemorrhage, and idiopathic adrenal calcifications.[12,13,14,15]

Bilateral adrenal involvement occasionally results in adrenal insufficiency or Addison's disease. The disease was first described by Dr. Thomas Addison in 1849. The problem may be due to a disorder of the adrenal glands themselves (primary adrenal insufficiency) or to inadequate secretion of ACTH by the pituitary gland (secondary adrenal insufficiency). Primary adrenal insufficiency is a severe or total deficiency of the hormones made in the adrenal cortex, caused by a destruction of the adrenal cortex. Tuberculosis accounts for about 20% of cases of primary adrenal insufficiency in developed countries. The disease is characterized by weight loss, muscle weakness, fatique, low blood pressure, and sometime darkening of the skin in exposed and nonexposed parts of the body. A definitive diagnosis of Addison's disease requires definitive tests that be carried out. These tests measure the amount of cortisol and aldosterone in blood and urine, and document a lack of the normal increase in the levels of these two hormones after administration of ACTH given by injection. An elevated blood level of ACTH should also be found in Addison's disease.[18,19]

Disseminated tuberculosis of this reported case was composed of miliary pulmonary tuberculosis, intracranial tuberculomas and miliary tubercles, and tuberculous abscess of the bilateral adrenal glands. The diagnosis was made by isolation of tuberculous bacilli from the right adrenal abscess under CT guidance. Miliary pulmonary tuberculosis was strongly evident by miliary shadowing on the intitial chest radiograph which disappeared after six weeks of antituberculous drug treatment. Intracranial tuberculosis were concluded by typical CT findings together with evidence of the disease in previously mentioned organs. Bilateral adrenal involvement in this patient could result in Addison's disease but there was no biochemical investigation for confirming the diagnosis.

CONCLUSION

Tuberculosis of the lungs and brain are common and have been well described radiologically in the literature. Adrenal tuberculosis is not uncommon and is mostly bilateral involvement and may be the cause of adrenal insufficiency. Tuberculous adrenal abscess appears as rim enhancing mass with central hypodensity by CT scan. Old adrenal tuberculosis, the glands may atrophy and calcify.

REFERENCES

1. Harisinghani MG, Mclound TC, Shepard JO, Ko JP, Shroff MM, Mueller PR. Scientific exhibit Tuberculosis from head to toe. Radiographics 2002; 20 :449-470.
2. Leung AN. Pulmonary tuberculosis: The essential. Radiology 1999; 210: 307-322.
3. Kim HY, Song KS, Goo JM, Lee JS, Lee KS, Lim TH. Education exhibit The Thoracic sequelae and complications of tuberculosis. Radiographics 2001; 21 : 839-858.
4. Bass JR, Farer LS, Hopewell PC, Jacobs RF, Snider DE. Diagnostic standards and classification of tubeerculosis. Am Rev Respi dis 1990; 142 : 725-735.
5. Miller WT, MacGregor RR. Tuberculosis: frequency of unusual radiographic findings. AJR 1978; 130 : 867-875.
6. Geppert EF, Leff A. The pathogenesis of pulmonary and miliary tuberculosis. Arch Intern Med 1979; 139 : 1381-1383.
7. Roche CJ, O'Keeffe DP, Duddalwar VA, Torreggiani WC. Selections from the Bufflet of food signs in Radiology. Radiographics 2002; 22 : 1369-1384.
8. Reed JC. Chest radiology Plain films patterns and differential diagnoses. 3rd ed. St Louis, MO: Mosby-Year book. 1991.
9. Engin G, Acunas B, Acunas G, Tunaci M. Scientific exhibit Imaging of extrapulmonary tuberculosis. Radiographics 2000; 20: 471-488.

10. Gee GT, Bazan C, Jinkins R. Miliary tuberculosis involving the brain: MR findings. AJR Am J Roentgenol 1992; 159 : 1075-1076.
11. Jinkins JR, Gupta R, Chang KH, Rodriguez -Carbajal J. MR imaging of central nervous system tuberculosis. Radiol Clin North Am 1995; 33 : 771-786.
12. Kawashima A, Sandler CM, Fishman EK, Charnsangavej C, Yasumori K, Honda H, et al. Spectrum of CT findings in nonmalignant diseases of the adrenal gland. Radiographics 1998; 18 : 393-412.
13. Mayo-Smith WW, Boland GW, Noto RB, Lee M. Satate-of-the-art adrenal imaging. Radiographics 2001; 21 : 995-1012.
14. Wilms GE, Baert AL, Kint EJ, Pringot JH, Gooddeeris PG. Computed tomographic findings in bilateral adrenal tuberculosis. Radiology 1983; 146 : 729-730.
15. Wilson DA, Muchmore HG, Tisdal RG, Fahmy A, Pitha JV. Histoplasmosis of the adrenal glands studies by CT. Radiology 1984; 150 : 779-783.
16. O' Brien WM, Choyke PL, Copeland J, Klappenbach RS, Lynch JH. Computed tomography of adrenal abscess. J Comput Assist Tomogr 1987; 11 : 550-551.
17. Atkinson GO, Kodroff MB, Gay BB, Rickette RR. Adrenal abscess in the neonate. Radiology 1985; 155 : 101-104.
18. Williams GH, Dluhy RC. Disorders of the adrenal cortex. In : Braunwald E, ed. Harrison's principles of internal medicine. 15th ed. New York. MacGraw-Hill Profesional; 2001: 2084-2105.
19. Ten S, New M, Maclaren N. Clinical Review 130: Addison's disease 2001. Journal of Clinical Endocrinology & Metabolism 2001; 86(7): 2909-2922.